Charles University

Faculty of Science

Study programme: Biology

Branch of study: Biology

Bc. Michal Bogdan

Tissue-specific knockout of starch synthesis in columella cells of *Arabidopsis thaliana* and gravitropic response

Tkáňově specifický knockout syntézy škrobu v buňkách kolumely *Arabidopsis thaliana* a gravitropická odpověď

Diploma thesis

Supervisor: Matyáš Fendrych, Ph.D.

Consultant: Mgr. Eliška Kobercová

Prague, 2022

Acknowledgement

I have many people to thank from who I have received a great deal of support and assistance throughout my studies and the writing of this thesis.

First of all, I would like to express my deepest thanks to my supervisor, Dr Matyáš Fendrych, whose guidance in methodology, scientific writing and research was invaluable. I would also like to thank my consultant Mgr. Eliška Kobercová for providing me with the necessary tools and knowledge to be successful with the CRISPR/Cas9 system.

My gratitude goes out to my colleagues Dr Eva Medvecká, Dr Pruthvi Vittal, Dr Denisa Oulehlová, Dr Nelson B.C. Serre, Mgr. Shiv Mani Dubey, Mgr. Monika Kubalová and MSc. Lorena Meusel for their assistance and insight during my studies.

In addition, I would like to thank my parents for their sympathetic ears and support. Finally, I would like to thank Bc. Martin Kuchař, Bc. Patrik Hohoš and Mgr. Pavel Krupař who supported me and provided distractions in times of need when rest was in order.

Declaration

I declare that I carried out this diploma thesis independently, and only with the cited sources, literature, and other professional sources. I declare that this thesis has not been used to gain any other academic title.

Prague, 01.01.2022

Bc. Michal Bogdan

Abstract:

Since the studies of plant gravitropism by Charles Darwin, the identity of specific sensors of gravity in plants has been uncertain. To this date, statoliths – starch granules in the root tips – are considered to play a key role in gravity sensing. The role of statoliths as organelles that mediate the gravity sensing ability of plant roots is based on research that uses plants which have severely impaired ability to synthesize starch in general or have their cells that contain statoliths removed or damaged. This represents methodical imperfections that give rise to alternative explanations, like disturbed auxin flow due to heavy damage to the root tip or unknown involvement of starch from other parts of the plant in gravity perception. Thanks to advances in the field of CRISPR/Cas9 technology, we are now able to produce tissue-specific mutants that might help with clarification of whether starch granules in the root tip are involved in sensing gravity and if so, how significant is this involvement. This diploma thesis aimed to answer these questions by adapting the tissue-specific CRISPR/Cas9 system and using it for the creation of mutants that are starchless specifically in the columella cells. Using this approach, we generated one tissue non-specific mutant line and three tissue-specific mutant lines, two of which have targets in genes responsible for starch synthesis. The observations made by fluorescence imaging and genotyping proved that this adapted gene-knockout system works both for non-specific and tissue-specific applications. However, the generated tissue-specific starchless mutants proved to have varying degrees of root tip starch content and differing response degrees to the vector of gravity. Due to this variability, we did not achieve any significant results. We anticipate that achieving plants that are homozygous from the perspective of our insert and selecting them according to the strength of mCherry protein fluorescence might help answer the question of how big of a role the root tip starch granules play in gravity perception. Furthermore, optimization of the adapted CRISPR/Cas9 system could aid the research of tissue-specific mutants.

Keywords: *Arabidopsis thaliana*, gravitropism, root, PIN, statolith, starch, CRISPR/Cas9, PGM, ADG1

Abstrakt:

Od studií gravitropismu rostlin Charlesem Darwinem je identita specifických senzorů gravitace v rostlinách nejistá. K dnešnímu dni jsou statolity – škrobové granule v kořenových čepičkách – považovány za klíčové při percepci gravitace. Úloha statolitů jako organel zprostředkujících schopnost vnímat gravitaci v kořenech rostlin je obecně založena na výzkumech, jejichž subjekty mají vážně narušenou schopnost syntetizovat škrob nebo mají buňky obsahující statolity odstraněny či poškozené. To představuje metodické nedokonalosti, které vedou k alternativním vysvětlením, jako je narušený tok auxinu v důsledku těžkého poškození kořenové čepičky nebo neznámé zapojení škrobu z jiných částí rostliny do vnímání gravitace. Díky pokroku v oblasti technologie CRISPR/Cas9 jsme nyní schopni vytvářet tkáňově specifické mutanty, které by mohly pomoci s objasněním, zdali se škrobová zrna v kořenové čepičce podílejí na vnímání gravitace, a pokud ano, jak významné je toto jejich zapojení. Tato diplomová práce se pokusila na tyto otázky odpovědět adaptací tkáňově specifického systému CRISPR/Cas9 a jeho využitím pro tvorbu mutantů, které jsou specificky v kolumele bez škrobu. Pomocí tohoto přístupu jsme vytvořili jednu obecnou mutantní linii a tři tkáňově specifické mutantní linie, z nichž dvě mají cíle v genech odpovědných za syntézu škrobu. Pozorování provedená fluorescenční mikroskopií a genotypováním prokázala, že tento adaptovaný gene-knockout systém funguje jak pro tkáňově nespecifické, tak pro tkáňově specifické aplikace. Ukázalo se však, že vytvořené tkáňově specifické mutanty mají různé stupně obsahu škrobu v kořenové čepičce a různé stupně odezvy na vektor gravitace. Kvůli této variabilitě jsme nedosáhli signifikantních výsledků. Očekáváme, že získání rostlin, které jsou homozygotní z pohledu našeho transgenu a jejich výběr podle síly fluorescence proteinu mCherry může pomoci odpovědět na otázku, jak velkou roli hrají zrna škrobu kořenové čepičky ve vnímání gravitace. Kromě této selekce by optimalizace adaptovaného systému CRISPR/Cas9 mohla pomoci při výzkumu tkáňově specifických mutantů.

Klíčová slova: *Arabidopsis thaliana*, gravitropismus, kořen, PIN, statolit, škrob, CRISPR/Cas9, PGM, ADG1

List of contents

1. List of used abbreviations

ARG1	ALTERED RESPONSE TO GRAVITY 1
ABCB	ATP-binding Cassette B
ADG1	small unit of AGPase
ADPGlc	ADP-glucose
AGPase	ADP-glucose pyrophosphorylase
ARF	auxin response factor
AUX1/LAX	AUXIN RESISTANT 1/LIKE AUX1
CNGC14	Cyclic Nucleotide-Gated Channel 14
CRISPR	clustered regularly interspaced short palindromic repeats
CRISPR-TSKO	CRISPR-tissue-specific knock-out
crRNA	CRISPR RNA
DMSO	dimethyl sulfoxide
EC1.2	Egg-cell specific
GB	GoldenBraid
GFP	Green Fluorescent Protein
gRNA	guide RNA
IAA	Indole-3-acetic acid
L-Kyn	l-kynurenine
LZY	LAZY
MAR	matrix attachment region
MDR	Multidrug resistance
NAA	1-Naphtaleneacetic acid
NGR	NEGATIVE GRAVITROPIC RESPONSE OF ROOTS
PAM	protospacer adjacent motif
PGM	phosphoglucomutase
PGP	P-Glycoprotein
PIN	PIN-FORMED protein
RFP	Red Fluorescent Protein
RLD	RCC1-like domain
SCF	SKP1-Cullin-F-box
sgRNA	single guide RNA
SMB	Sombrero
SS	Starch synthase
tracrRNA	crRNA-trans activating RNA
tRNA	transfer RNA
wt	wild-type
X-gal	5-Bromo-4chloro-3-indoxyl-beta-D-galactopyranoside

2. Introduction

Even after 150 years of research, the molecular workings of plant root gravitropism are still not entirely clear. The gravity sensing phase of the phenomenon lacks clarity. This phase is thought to be carried out by statoliths – starch-filled plastids in the columella. However, recently there have been indications by (Edelmann, 2018) that this might not be the case, as maize de-capped roots could still sense gravity.

The techniques used to study the need for statoliths for gravity sensing were either based on the removal/death of the cells containing statoliths or mutants that are considered starchless, as they only contain about 1-2% of starch, compared to wild-type plants. This thesis considers the first method imperfect because this approach disturbs the flow of auxin by transporter protein disruption. The other method cannot rule out the involvement of starch granules located in other tissues of the plant. Given the limitations of the techniques used to study the role of statoliths in gravity perception, we have decided to approach the problem differently.

The goal of this thesis is to shed some light on the importance of columellar amyloplasts in gravity sensing by creating tissue-specific gene knockouts, using an adapted CRISPR/Cas9 system.

The thesis is divided into four main parts: Literature overview, Methods and materials, Results, and Discussion. Alongside these parts, there are a few supplementary parts – Abstract and Keywords, List of contents, List of used abbreviations, Introduction, Conclusion, Future perspectives, Bibliography and Supplement. The theoretical part of the thesis is divided into two parts – the first part focused on plant gravitropism while the second part is focused on CRISPR/Cas9 gene editing. Similarly, the results are divided into two main parts – the adaptation of the modular CRISPR/Cas9 system with polycistronic sgRNA and the results of using this system in *Arabidopsis thaliana*.

3. Hypothesis and aims

Hypothesis:

- "The amyloplasts of the columella are the gravity sensing organs responsible for the gravitropism of the root and they act as statoliths, the sedimentation of which conveys the direction of the gravity vector."

My diploma thesis aims to create novel experimental material that will allow testing this hypothesis by:

- Adopting a modular CRISPR-Cas9 system to support the use of multiple gRNAs and creation of tissue-specific and tissue non-specific mutant plants
- Further adapting the CRISPR-Cas9 system to be usable with GoldenBraid Cloning system
- Creating tissue-specific knockout mutants in the PGM and ADG1 genes
- Answering the question – does lowering the amount of starch in the columella significantly affect the gravitropism of *Arabidopsis* roots?

4. Literature overview

4.1 Gravitropism in plants

The sessile lifestyle of plants is one of their defining features. Despite this, plants do move and react to the world around them. Their orientational growth in response to an external stimulus is called tropism. Gravity, as a stimulus, controls a portion of this directional growth response (Knight, 1806). This phenomenon is referred to as gravitropism. We can generalize that while the shoot grows in a direction antiparallel with the gravity vector, the roots display growth that is parallel with gravity.

Gravitropism was studied as early as the second half of the 19th century by Charles Darwin and his son who laid the foundations of these movement studies alongside other tropisms (Darwin, 2014), (Darwin and Darwin, 2009). Gravitropism requires differential growth of root sides to produce root curvature (Barlow and Rathfelder, 1985). The phases of gravitropic responses are as follows – signal perception, signal transduction and gravitropic response (Toyota and Gilroy, 2013), (Sato *et al.*, 2015). At present, the phenomenon is still being studied as its specific molecular mechanisms are unclear. From this part onward, the thesis focuses exclusively on the gravitropism of roots.

4.2. Signal perception

Early experiments showed that by surgically removing the root cap, plant roots become agravitropic (Shachar, 1967; Barlow, 1974). This implies that the root cap is the primary sensor of the gravity vector in the roots. The root cap itself is made of two distinct cell groups – cells of the central columella and lateral root cap cells – both developing from two sets of stem cells – central 'columella initials' and a surrounding ring of cells respectively (Dolan *et al.*, 1993). These two clonally unrelated cell types must undergo cell division in synchronization, otherwise, the structural integrity of the root cap would be damaged. The columella was labelled as responsible for gravity sensing because its cells contain amyloplasts which sediment according to the vector of gravity. Experimentally, through methods like laser ablation (Blancaflor, Fasano and Gilroy, 1998), genetic ablation (Tsugeki and Fedoroff, 1999) and heavy-ion micro beam usage (Tanaka *et al.*, 2002), columella cells were confirmed to be the primary gravity sensing tissue of roots. Typically, there are four vertical layers of columella cells in *A. thaliana*, labelled as S1-S4 – See Figure 1.

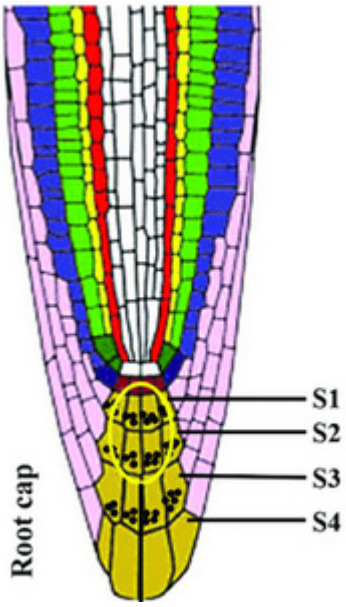

Figure 1 - Root cap layers of *A.thaliana*
*A*dapted from (Singh, Gupta, and Laxmi 2017).

The previously mentioned laser ablation experiments also showed that the layers S1 and S2 of the columella seem to be the most important layers for responses to the vector of gravity (Blancaflor, Fasano and Gilroy, 1998). The main hypothesis of how roots sense gravity is the starch-statolith hypothesis (Němec, 1900; Haberlandt, 1902) which assumes that the amyloplasts of the columella are the gravity sensing organelles responsible for the gravitropism of the root and they act as statoliths, the sedimentation of which conveys the direction of the gravity vector.

On the other hand, the model of protoplast pressure hypothesis suggests that due to the gravitational vector, there is pressure on the lower plasma membrane created by the weight of cytoplasm which changes according to the changes of the gravitational vector, creating a differential of pressure between the perceived top and bottom of the cell (Wayne, Staves and Leopold, 1990; Staves, 1997). The protoplast pressure hypothesis was introduced as early as 1966 by (Pickard and Thimann, 1966). However, this theory is not without a counterargument. The protoplast pressure hypothesis is unreasonable in the view of (Björkman, 1992) as the turgor pressure greatly exceeds the theoretical difference of pressures between the top and bottom of the cells. In addition to this, turgor pressure varies in time.

According to (Perbal, 1999), both of these hypotheses may be valid at the same time as they require a hypothetical stimulation of receptors on the plasma membrane, the only differences being in the area and amount of pressure exerted.

Changes in pH are associated with gravistimulation. Upon changing the orientation of the *Arabidopsis* roots (Fasano *et al.*, 2001) found a rapid (2 min after stimulus) acidification of the columella apoplast from pH 5.5 to 4.2. At the same time, the pH of the columella cell cytoplasm rose from pH 7.2 to 7.6. The mentioned pH changes took place before the detection of pH changes in the elongation zone of the root. Starchless *pgm* mutants (Fasano *et al.*, 2001) and agravitropic *arg1* (altered response to gravity) mutants (Boonsirichai *et al.*, 2003) are flawed in these pH changes. Moreover, it has been found that blocking the pH change of columella cytoplasm, reduces lateral auxin gradient, thus affecting gravitropism processes downstream of perception (Hou *et al.*, 2004).

There are multiple views on how the physical signal of statolith sedimentation is converted into a physiological one. These hypotheses include protein interaction between amyloplasts and other organelles such as the plasma membrane or the endoplasmic reticulum. Research by (Limbach *et al.*, 2005) carried out on *Chara* suggests that the contact of statoliths (in the case of *Chara* crystals of barium sulphite) with the plasma membrane is required. This is based on experiments, where they inverted rhizoids 31 times from 90° to 270° in 120 minutes. This resulted in significant curvature reduction $P < 0.01$ - See Figure 2.

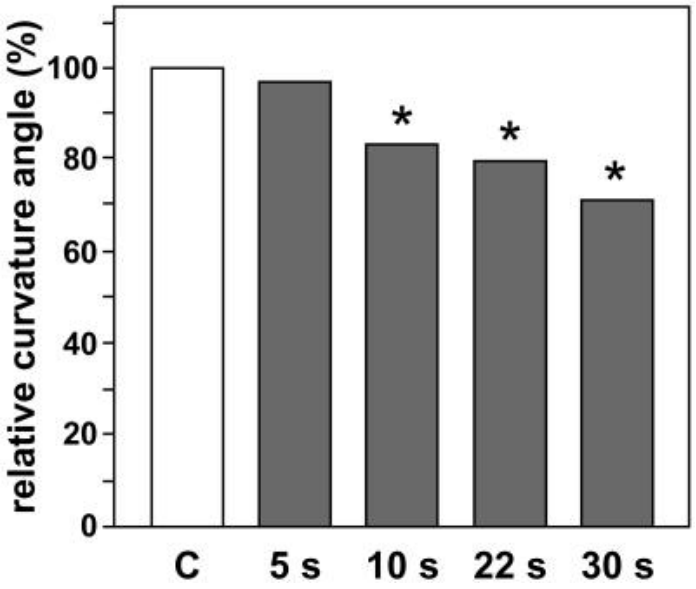

Figure 2 - Mean curvature angles of *Chara* rhizoids, inverted 31 times to 270° for 5s, 10s, 22s and 30s respectively. *= P< 0.01, Students *t-test* Adapted from (Limbach et al. 2005).

Based on this, (Braun and Limbach, 2006) in their review proposed an interaction of statolith surface components with receptors localized at the plasma membrane. Vascular plants might have similar statolith-membrane interactions. The experiments of (Fitzelle and Kiss, 2001)

show that agravitropic, starchless plants can gain a gravitropic phenotype by introducing them into hypergravitational conditions. At 5g the starchless plants have visibly improved gravitropic growth and at 10g, the mutant plants had a similar response to gravity as their wild-type counterparts - See Figure 3.

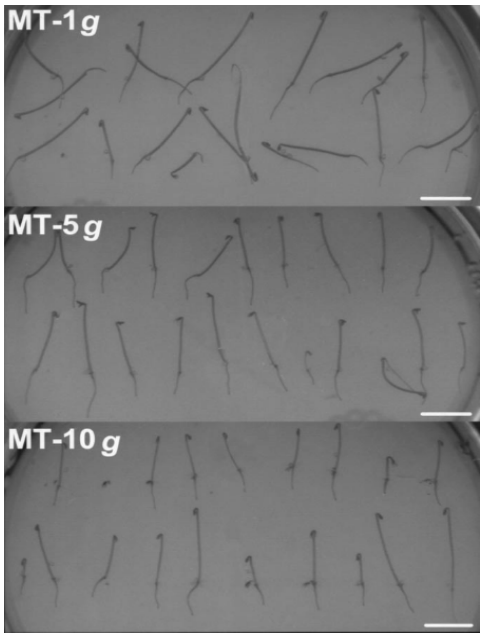

Figure 3- Etiolated *Arabidopsis ACG 21* (starchless mutant) grown under 1, 5 and 10 g accelerations. Bar = 0.5 cm Adapted from (Fitzelle and Kiss 2001).

More recent works like (Richter, Strauch and Lebert, 2019) imply that amyloplasts should not be considered the organelles responsible for gravity sensing in plants. Experiments of (Edelmann, 2018) on maize demonstrated that the removal of the root cap (which also removes PIN (PIN-Formed) proteins of the root cap which redistribute auxin) results in the halting of response to the gravity vector. However, this does not mean that the roots do not still perceive gravity as latrunculin application makes the de-capped roots respond by a growth that is opposite to the gravity vector (Edelmann, 2018). The fact alone implies that there is something inherent to the root itself that perceives gravity. Data from the work (Firn and Digby, 1977) suggest that epidermal tissues also perceive gravity, as, by their removal, gravitropic growth is lost. Experiments with a microscope with a rotational platform carrying a petri dish and a motor used for automatic rotation –a system called ROTATO – were carried out by the team of (Wolverton, Ishikawa and Evans, 2002). ROTATO could be set to maintain the root tip at a specific angle from the vertical, resulting in platform rotation as it was trying to maintain the root tip at the specified angle. However, if a subapical region was selected for monitoring, the rotation should end when the root reached the vertical as the curvature would also end at that time. What happened was that

the platform continued to rotate and so that the elongation zone (4-5 mm from the tip) remained at a 60° angle, suggesting, that there is probably a sensor of gravity within that region. When the target region to be fixed at the specified angle was further back (5-6 mm from the tip) the rotation of ROTATO stopped when the tip of the root reached the vertical. (Edelmann, 2018) criticizes the lack of amyloplast addressing when talking about PIN proteins and claims that in the light of recent studies (reviewed by Sato et al. 2015), amyloplasts are redundant as PIN protein redistribution is per se dependent on gravity.

4.1.2 Signal Transduction

4.1.2.1 AUX1/LAX and PIN mediated auxin transport

After the gravity vector has been perceived, a directional signal must be transduced for the differential growth of the root to occur (Blancaflor and Masson, 2003). The phytohormone auxin (major form as Indole 3-Acetic Acid or IAA) is a small molecule derived from the amino acid tryptophan and produced by multiple pathways (Müller, Hillebrand and Weiler, 1998; Brumos, Alonso and Stepanova, 2014). This molecule along with its transport and biosynthesis is responsible for the polarity of plant cells and tissues, affecting plant development and growth (Boutté, Ikeda and Grebe, 2007; Robert and Offringa, 2008; Vanneste and Friml, 2009). Auxin signal transduction is in agreement with the Cholodny-Went theory that states that after gravity perception, a signal is transduced from the statocytes to the cells of the elongation zone of the root, resulting in response (Went, 1926; Cholodny, 1927). First of all, auxin must be carried from its sources into the root cap, as it has been shown that auxin is transporters from the lateral cells of the root cap into the cells of the elongation zone (Swarup *et al.*, 2005). Auxin transport is mediated via auxin influx carriers from the AUX1/LAX (AUXIN RESISTANT 1/LIKE AUX1) family, efflux carriers called PIN-FORMED (PIN) proteins and PGP/MDR/ABCB (P-Glycoprotein/Multidrug resistance/ATP-Binding Cassette B) proteins (Marchant *et al.*, 1999; Noh, Murphy and Spalding, 2001; Friml *et al.*, 2003).

Although all of these proteins are involved in the auxin transport it seems that the PIN proteins are the ones that can direct the flow of auxin via their polar localization (Petrášek *et al.*, 2006; Wisniewska *et al.*, 2006). The transport of auxin to the root tip is mediated by AUX1/LAX proteins as well as PIN1 (Okada *et al.*, 1991; Gälweiler *et al.*, 1998; Swarup *et al.*, 2001). Along with these two proteins, AtPIN4, expressed in the quiescent centre, was shown to maintain the auxin gradient, feeding auxin into the columella (Jiří Friml *et al.*, 2002). The PIN proteins endocycle between their endosomal compartments and plasma membrane by clathrin-mediated

endocytosis, affecting their distribution (Geldner *et al.*, 2001; Dhonukshe *et al.*, 2007). During gravitropism, PIN3 accumulates asymmetrically, predominantly at the lateral cell surface of the new bottom, while when not gravistimulated, it is non-polar (Jlří Friml *et al.*, 2002; Kleine-Vehn *et al.*, 2010). This accumulation affects auxin redistribution, affecting root gravitropism due to its changed lateral gradient (Band *et al.*, 2012). The closest homolog of the PIN3 protein is PIN7. PIN7 seems to act in a compensatory way to PIN3, as upon gravistimulation, both move and localize in overlapping regions of the columella. Gravitropism of *pin3* mutants is a bit weaker than that of the wild-type and according to data, PIN7 expands into the PIN3 expression zone, indicating compensation. The *pin3 pin7* double mutant has lesser gravitropic responses compared to both *wt* (wild-type) and *pin3* seedlings (Kleine-Vehn *et al.*, 2010). To sum up, the transport of auxin from the shoot to the roots is mediated by AUX1/LAX, PIN proteins (namely PIN1) and PGP/MDR/ABCB proteins. After the auxin reaches the tip of the root, PIN4 proteins along with PIN1 maintain auxin transport into the columella cells, where PIN3 and PIN7 proteins transport auxin to the lateral root regions according to their localization. The symmetry of this distribution depends on the gravity sensing step of gravitropism. Figure 4 shows the localization of PIN proteins and auxin transport in the root.

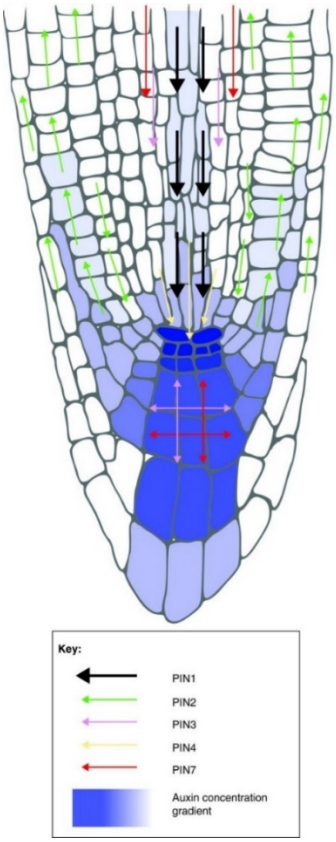

Figure 4 - Auxin transport in the root by PIN proteins. Adapted from (Krecek et al. 2009).

4.1.2.2 Auxin flow to lateral root cap cells

As mentioned before, PIN3 and PIN7 proteins transport auxin from the columella cells to the bottom side of the gravistimulated root depending on their localization asymmetry. This asymmetry is then reflected on the auxin levels of the lateral root cap cells. For auxin to reach the epidermal tissues of the elongation zone, it must be at first basipetally transported from the root tip. This transport is mediated by the PIN2 protein (Utsuno *et al.*, 1998). The localization of the PIN2 protein was studied by immunohistochemistry and fluorescence, was found to correspond with the transporter responsible for this auxin flow (Müller *et al.*, 1998) – See Figure 5. This role was further confirmed by the agravitropic phenotype of *pin2* (called also *eir1*) alongside auxin distribution which compared to the wild-type plants was restricted to the root tip, confirmed by *AtIAA2::GUS* experiments (Luschnig *et al.*, 1998). As auxin asymmetry of *pin2* mutants does not reach into the elongation zone of the root, the result is an agravitropic phenotype. The role of PIN2 was further confirmed by the experiments of (Wisniewska *et al.*, 2006). PIN1 expressed under the PIN2 promoter of the *pin2* mutant did not rescue the phenotype as PIN1 localised mainly on the basal side of root epidermis cells, resulting in the inability to transport auxin in a basipetal direction. Despite this, a PIN1 protein with GFP (Green fluorescent protein) insertion expressed under the PIN2 promoter was able to rescue the agravitropic phenotype as it localized more apically, yielding an auxin flux toward shoots.

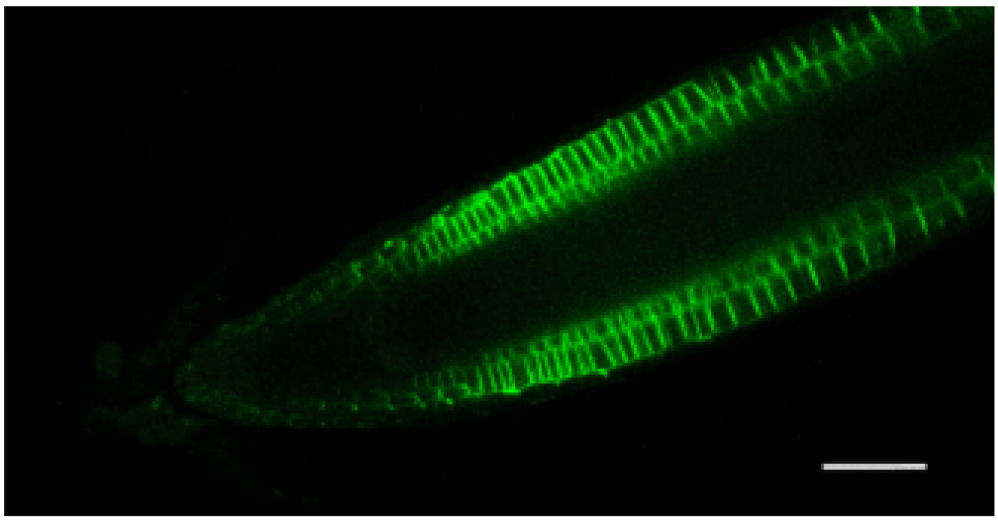

Figure 5 - PIN2 (PIN2-GFP) localization in *Arabidopsis* roots imaged by a confocal microscope. Adapted from (Jiang et al., 2016).

Recent studies have shown that PIN2 distribution is affected by brassinolide. Upon gravistimulation, roots that were pre-treated with brassinolide did not establish a PIN2 gradient similar to the wild-type plants. This seems to be controlled by brassinolide-dependent intracellular

distribution and sorting of PIN2. However, this disruption in the asymmetrical localization of PIN2 resulted in gravitropic root bending and differential auxin signalling. The simulations in this study have shown that the localization gradient of PIN2 is not a requirement for root curvature formation, but it lessens the asymmetry of the auxin flow and signalling. A plausible explanation has been proposed – the concentration gradient created in the columella and root caps might be enough for the establishment of asymmetrical elongation zone auxin concentration on the sides of the root, as long as PIN2 is expressed and functional (Retzer *et al.*, 2019).

4.1.2.3 Anti-gravitropic phenotype – NGR proteins

In 2016 a protein called NGR (NEGATIVE GRAVITROPIC RESPONSE OF ROOTS) that consists of 262 amino acids has been discovered in *Medicago truncatula* through a forward genetic screen. It was found to be a protein from the LAZY family (Yoshihara, Spalding and Iino, 2013). The "lazy" name originates from maize and rice gravitational indifferent plants that form prostrate growth in maize and spreading tillers in rice (Overbeek, 1936; Jones and Adair, 1938). Both in *Arabidopsis thaliana* and *Medicago truncatula*, the loss-of-function mutation of the NGR proteins in *ngr1,2,3* mutants results in plants with reversed gravitropism of roots, making them grow upward (Ge and Chen, 2016). The NGR protein is localized on the plasma membrane as confirmed by the MtNGR-GFP fusion protein, plasmolysis analysis and hydrophobicity analysis (Ge and Chen, 2019). The analysis of cell-sorted microarray data (Birnbaum *et al.*, 2003; Nawy *et al.*, 2005; Brady *et al.*, 2007) and the expression of GFP under the promoters AtNGR1 (AtLZY2), AtNGR2 (AtLZY4) and AtNGR3 (AtLZY3) suggest that NGRs are specifically expressed in root columella cells as well as lateral root cap cells where they act as a part of the root gravitropism response (Ge and Chen, 2019). Further analysis of *atngr1,2,3* triple mutant, *atngr1,2,3;pin3,4,7* sextuple mutant and *atngr1,2,3;agr1(pin2)* quadruple mutant was conducted. The results of this analysis show that PIN-2 mediated auxin transport is required for the negative gravitropic response as well as auxin sensitivity in the *atngr1,2,3* mutant is not altered. As intriguing it may seem, amyloplast sedimentation was not affected in the *atngr1,2,3* mutant after gravistimulation but the PIN3 was reversed. This was found to be the cause of reversed auxin flow from lateral root cap cells after gravistimulation. Experiments on the sextuple mutant *atngr1,2,3;pin3,4,7* confirm that PIN3, PIN4 and PIN7 are required for the negative response to gravity of the *atngr1,2,3* mutant (Ge and Chen, 2019).

The C terminus located V domain of NGR (LZY) proteins contains an EAR-like motif, conserved in the LZY family (Yoshihara, Spalding and Iino, 2013; Taniguchi *et al.*, 2017; Ashraf

et al., 2019). RCC1-like domain proteins (RLD) contain a BREVIS RADIX (BRX) domain (Briggs, Mouchel and Hardtke, 2006). The EAR-like motif interacts with the BRX domains of the RLD proteins, resulting in the binding and recruitment of RLDs from the cytosol to the plasma membrane in the direction of gravity. After gravistimulation, NGR (LZY) proteins polarize in the direction of gravity to the bottom side of the plasma membrane. This appears to regulate the polar transport of auxin as NGR recruited RLDs seem to regulate the expression and localization of PINs (Furutani *et al.*, 2020).

4.1.3 The reaction of root cells to auxin

The transported auxin that reaches the bottom side of the gravistimulated root acts in the area by activating auxin-responsive gene transcription. This activation happens because auxin acts as molecular glue, binding together its coreceptors TIR1/AFB F-box proteins and Aux/IAA proteins (Gray *et al.*, 2001; Tan *et al.*, 2007). TIR1/AFB F-box proteins are parts of the SKP1-Cullin-F-box (SCF)- E3 ubiquitin ligase complex (Skowyra *et al.*, 1997; Ruegger *et al.*, 1998). The interaction of auxin, TIR1/AFBs and Aux/IAAs result in the release of auxin response factors (ARFs) which were heterodimerized with the Aux/IAAs because of the degradation of Aux/IAAs (Dharmasiri, Dharmasiri and Estelle, 2005; Kepinski and Leyser, 2005). These ARFs are then responsible for auxin-responsive transcription (Weijers *et al.*, 2005). For a visual representation see Figure 6.

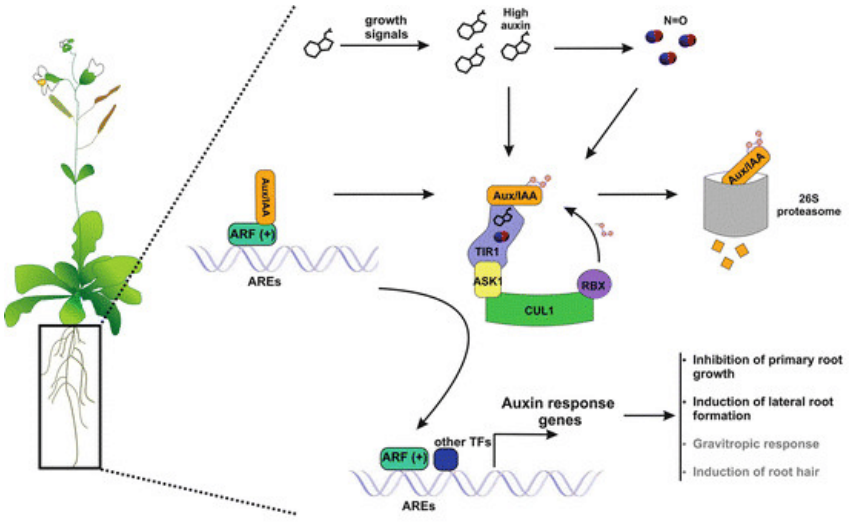

Figure 6 - Visualisation of the effect of high auxin levels on auxin-responsive transcription - interaction of Aux/IAA and TIR1/AFB and the following Aux/IAA degradation followed by the activation of auxin response genes. Adapted from (Correa-Aragunde et al., 2016).

Except for these transcriptional changes when reacting to auxin, the cell is thought to show responses that are too rapid to be transcriptional. With the median length of *A. thaliana* proteins (from 206 to 446 amino acids, depending on their Gene Ontology category “cellular component”

according to GO Slim terms) (Ramírez-Sánchez *et al.*, 2016) and the eukaryotic transcription rate of around 1,4 kbp/minute and translation rate around 5 amino acids per second (Milo *et al.*, 2009), at least 2 minutes are needed for these processes if the length of all other related events is disregarded. Auxin response related events, like proton secretion (Senn and Goldsmith, 1988) and TIR1-dependent protein synthesis (Fendrych *et al.*, 2018) take around 7-15 minutes respectably to be detected. Responses that occur quicker than this can be referred to as rapid responses and of a non-transcriptional character (review by Dubey et al. 2021).

The AUX1/LAX mentioned in the chapter "AUX1/LAX and PIN mediated auxin transport" imports IAA^- with two H^+ (Sabater and Rubery, 1987). As of now, there are no reports of PIN protein facilitated auxin transport alongside H^+. Therefore, the influx of protons with auxin into the cell might be the case for the observed auxin-induced plasma membrane depolarisation of roots (Paponov *et al.*, 2019) and root hairs (Bates and Goldsmith, 1983; Dindas *et al.*, 2020). This hypothesis is however counterargued by the fact, that 1-NAA significantly depolarizes the cell (Felle, Peters and Palme, 1991), however, it is not a substrate of AUX1/LAX (Yang *et al.*, 2006). Instead, based on the data of (Hayashi *et al.*, 2012; Dindas *et al.*, 2018) it seems possible that instead of AUX1/LAX auxin import induced depolarization, the change might stem from TIR1/AFB as *tir1/afb2/3* shows a decreased response.

Imaging with pH and calcium-sensitive probes (Monshausen *et al.*, 2011) demonstrated quick alkalinization of the root cell surface upon auxin treatment alongside a calcium influx into the cytoplasm accompanied by a small decrease of pH inside cells. Lanthanum chloride application (Shih *et al.*, 2015; Dindas *et al.*, 2018) that results in the blockage of calcium channels diminished these pH and calcium responses. The Cyclic Nucleotide-Gated Channel 14 seems to be responsible for these reactions to auxin as *cngc14* mutants have compromised calcium signalling upon gravistimulation and no cytoplasmatic calcium concentration increase was measured. The *cngc14* mutants had also delayed pH changes which were significant after 9 minutes following tilting and delayed bending which became significant after 11.5 and 12.5 minutes for *cngc14-1* and *cngc14-2* mutants respectively (compared to wild-type = 4 mins after gravistimulation) (Shih *et al.*, 2015).

Gravitropism induced by the root growth inhibition of the lower side of the root by auxin is another rapid response. This was demonstrated by root growth inhibition after IAA application that occurred under 2 minutes (Fendrych *et al.*, 2018; Prigge *et al.*, 2020). Additionally, when cycloheximide, a translation inhibitor, was applied, IAA still inhibited the growth of the roots (Fendrych *et al.*, 2018). Not only the response to the presence of IAA is rapid, but it has a rapid

counterpart – when IAA is removed, even after an application that lasted 80 minutes, root growth was restored within 3 minutes after IAA removal.

Auxin must enter the cell, as *aux1* mutants do not respond to low IAA levels and grow as normal, however, when treated with NAA, a noticeable growth inhibition occurs (Fendrych *et al.*, 2018). This growth inhibition is initialized by the TIR1/AFB co-receptors, with AFB1, a paralogue of TIR1/AFB, being crucial (Fendrych *et al.*, 2018; Prigge *et al.*, 2020). Recently, it was shown that this growth inhibition correlates with auxin-induced membrane depolarization. Both of these events require the AFB1 auxin co-receptor, as AFB1 is vital for the rapid membrane depolarization gradient formation across gravistimulated roots (Serre *et al.*, 2021).

All the observations combined, it seems that some responses to auxin are non-transcriptional and require further research.

4.2 Statoliths and starch biosynthesis

The hypothesised gravity sensing organelle of *Arabidopsis thaliana* – amyloplasts are plastids containing starch. This starch is synthesized from sucrose produced in leaves. Sucrose is transported, unloaded and then converted into starch. About 30 – 50% of photoassimilates in *Arabidopsis* are converted into starch – polymers of α-1,4-linked and α -1,6-linked glucose assembled into granules with crystalline structure (Zeeman, Kossmann and Smith, 2010). Fructose 6-phosphate is converted into ADP-glucose (ADPGlc) which is the donor of glucosyl required for the biosynthesis of starch (Iglesias and Preiss, 1992). The first step of this enzymatic reaction is the conversion of fructose 6-phosphate into glucose 1-phosphate by phosphoglucoisomerase (PGI) and phosphoglucomutase (PGM). Then, the enzyme called ADP-glucose pyrophosphorylase (AGPase) uses Glucose 1-phosphate and ATP to generate ADP-glucose, while releasing an inorganic pyrophosphate. All of the mentioned steps are reversible, but if the inorganic pyrophosphate is hydrolysed, the last step becomes irreversible (reviewed in Stitt and Zeeman 2012). ADP-glucose is used to form α-1,4 glucan chains by starch synthases (SSs). Multiple SSs are involved in the glucan chain elongation, while starch branching enzymes introduce α -1,6 linkages into the chain. Starch debranching enzymes trim glucan chains that are irregularly arranged, ordering amylopectin and making the semi-crystalline structure formation possible (reviewed in Nazarian-Firouzabadi and Visser 2017). This pathway alongside an alternative pathway of cereal endosperm can be seen in Figure 7.

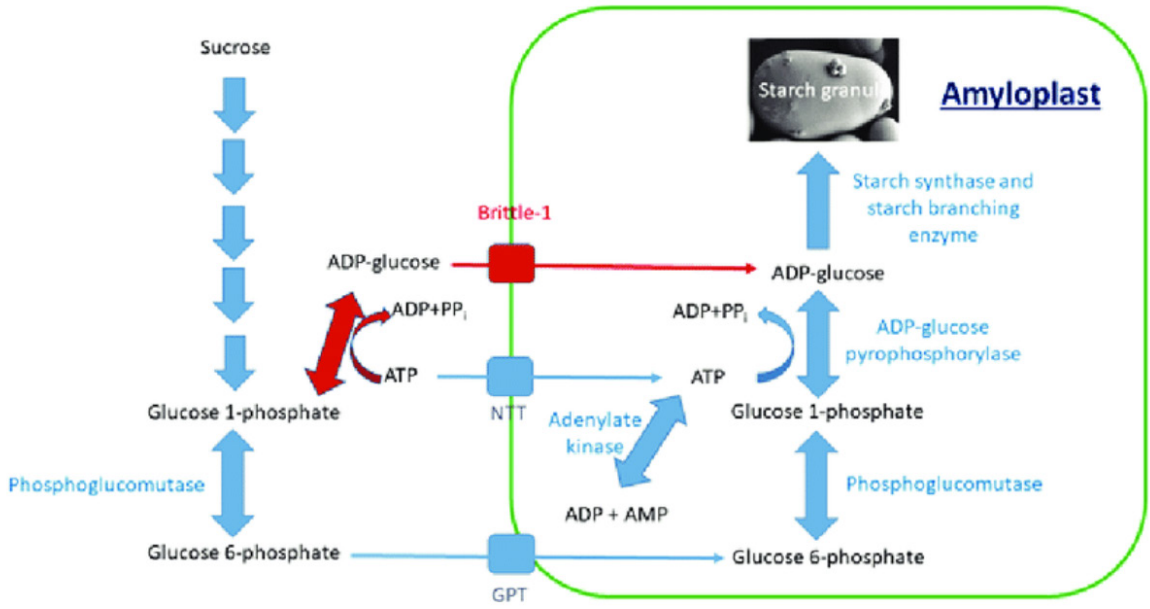

Figure 7 - There are two pathways of starch synthesis in vascular plants. One is shared in all plants (blue arrows), while the other is present only in cereal endosperm (red arrows). Sucrose is degraded to glucose 6-phosphate which is transported into amyloplasts.

There were hypotheses that amyloplasts in roots act as a force/acceleration sensor either by sensing the weight of statoliths (Leitz, Kang and Schoenwaelder, 2009) on the edges of the cells or via cytoskeleton interactions (Yoder *et al.*, 2001). These have been disproved by experiments as shoot gravitropism was observed to be indifferent between 0.1g to 3g (Chauvet *et al.*, 2016). This suggests that statoliths do not function as force sensors as thought before, rather, they act as an inclination/positional sensor (reviewed in Pouliquen et al. 2017). The problem with this type of sensor is that statoliths are expected to behave as granules, thus having a critical angle to be met before they re-position during inclination, called an avalanche angle (Courrech du Pont *et al.*, 2003). This angle is between 5° and 30°, depending on the properties of observed particles (Clavauda *et al.*, 2017). However, if this was the only factor in statolith sedimentation, it would make gravity sensing at small angles not possible, should the inclination/positional sensor hypothesis be true.

The team of (Bérut *et al.*, 2018) made a series of observations and made biomimetic models based upon said observations. They found that statoliths behave like an active granular liquid – a phenomenon that has two possible explanations – either this comes from Brownian motion or cytoskeletal activity. The latter was confirmed by them, as the biomimetic models showed, that statoliths flow about 10 000 times faster than they would be if their motion was purely Brownian.

This strongly suggests that the cytoskeleton of the cell plays a role in gravitropism, by enabling liquid-like motions of statoliths.

4.2.1 Mutations in PGM and ADG1

As we have established, PGM and AGPase are enzymes necessary for starch biosynthesis in roots. A nonsense mutation in the *At-PGM* gene results in a mutant called *pgm1* (Periappuram *et al.*, 2000). This results in plants that are lacking plastidial phosphoglucomutase and have nearly no starch - (Harrison, Hedley and Wang, 1998) reports 1% of the dry weight of *P. sativum* mutant compared to 60% in wild-type, and the quantitative analysis of *Arabidopsis pgm1* mutants grown in 12h light/ 12h darkness conditions showed barely detectable starch levels at all times and great accumulation of hexose sugars (Caspar, Huber and Somerville, 1985). *A. thaliana pgm1* mutants were found to not have any reduced photosynthetic activity per unit of fresh weight, but the respiration of their roots is highly elevated, resulting in retarded root growth (Brauner *et al.*, 2014).

The second mentioned plant enzyme, AGPase, is a tetramer of 2 subunits of different sizes (Preiss 1982 - book chapter). By analysis and complementation, (Wang *et al.*, 1998) found that *ADG1* encodes the small unit of AGPase. The presence of a functional small subunit was found to be required for the large subunit stability, as *adg1* mutants contain neither the large nor small subunit proteins. This phenotype could be rescued by complementation with the small subunit. In a similar fashion to *pgm1*, only low levels of starch were found in *adg1* mutants (less than 2% of wild-type values) (Lin *et al.*, 1988).

Additionally to missing starch, these mutants have been shown to possess reduced sensitivity to gravity. (Kiss, Wright and Caspar, 1996; Vitha, Zhao and Sack, 2000) found that when illuminated from above, *pgm1-1 Arabidopsis* mutants are about 12 times less sensitive than their wild-type counterpart. When testing without light, these mutants have shown even bigger differences in sensitivity – 36 times lesser than the sensitivity in wild-type plants. The starchless mutant *adg1-1* was reported to have similarly impaired sensitivity as *pgm1-1* mutants. (Vitha, Zhao and Sack, 2000) claims, that these effects are likely to be direct, as rates of growth were affected neither by genotype nor by the absence or presence of light. See Figure 8 for light/dark experiments.

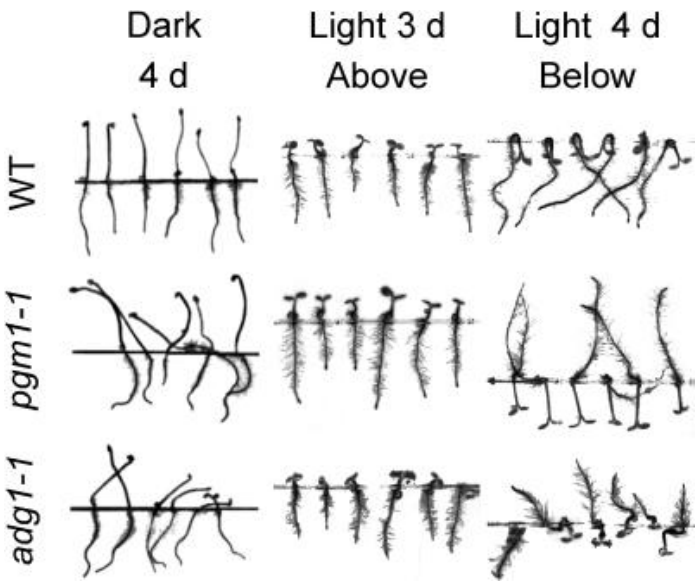

Figure 8 - *Arabidopsis* seedlings germinated and grown in different conditions - dark/light from above/ light from below. All 3 genotypes grew towards gravity while illuminated from above. Wild-type roots grown in darkness display less deviation from the vertical than the mutant genotypes. Light from below caused the greatest deviations from the vertical, as mutant genotypes grew away from the light source. The hypocotyls of all three genotypes grew towards the light, when available. Adapted from (Vitha, Zhao, and Sack 2000).

These "starchless" mutants have also been reported to have altered cell wall composition which results in less penetration-resistant plants which lead to an accelerated establishment of the hemibiotrophic fungus *Colletotrichum higginsianum* (Engelsdorf *et al.*, 2017). Leaves of these mutants contained significantly smaller amounts of arabinose and galactose, while xylose, mannose, fucose and rhamnose contents were significantly elevated compared with the wild-type plants. The cellulose contents along with galacturonic acid were not found to be affected. A previous report (Engelsdorf *et al.*, 2013) suggested that the reduced availability of carbohydrates might be the cause of lowered resistance to *C. higginsianum* in these "starchless" mutants.

4.2.2 Auxin and statoliths

The synthesis of starch granules seems to be also affected by auxin itself. Recent studies (Zhang *et al.*, 2019) have revealed different starch granule accumulation, depending on auxin levels. Application of l-kynurenine (L-Kyn), an inhibitor of auxin synthesis, resulted in lowered starch granule accumulation. Treatment with 1-naphthalene acetic acid (NAA) or N-1-Naphthylphthalamic acid (NPA) increased the formation of starch granules. If a root was treated both with L-Kyn and NAA, the granule accumulation was similar to NAA treatment alone. Mutants in *YUC* genes, which control auxin synthesis, showed reduced starch accumulation and downregulated expression of genes *ADG1, PGM* and *SS4*. Compared to wild-type plants,

the *pin3/4/7* triple mutant had slightly smaller starch granule accumulation as well as a lower *DR5::GFP* signal.

The results of these experiments indicate that auxin indirectly influences the ability to perceive gravity stimuli by impacting starch granule accumulation, see Figure 9 and Figure 10.

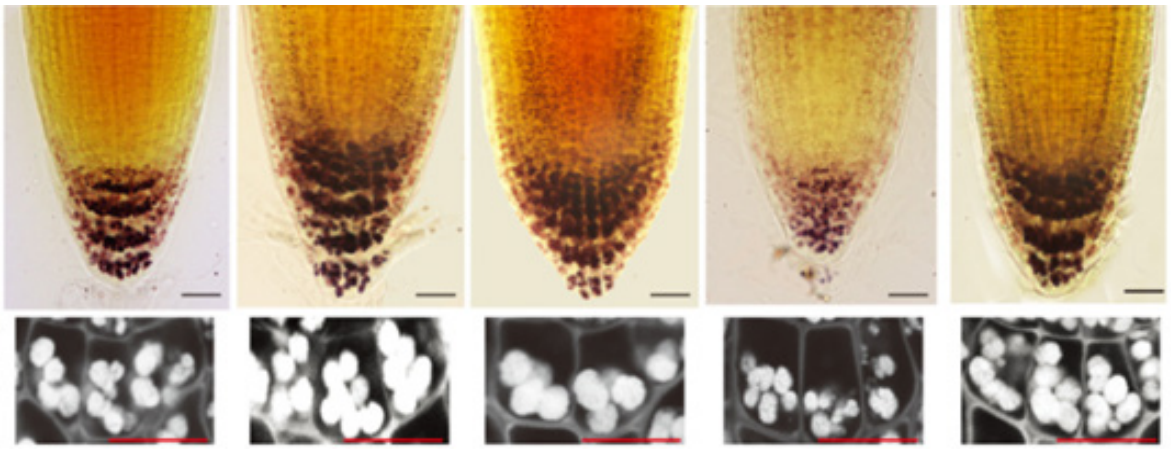

Figure 9 - Altered starch granule accumulation - 7 days old, Lugol treated *Arabidopsis*. From left to right: Treatment with dimethyl sulfoxide (DMSO) as control; treatment with 1 µM NAA for 48 h; treatment with 20 µM NPA for 48 h.; treatment with 25 µM L-Kyn for 48 h; treatment with both 25 µM L-Kyn and 1 µM NAA for 48 h. Bars, 20 µm Adapted from (Zhang et al. 2019).

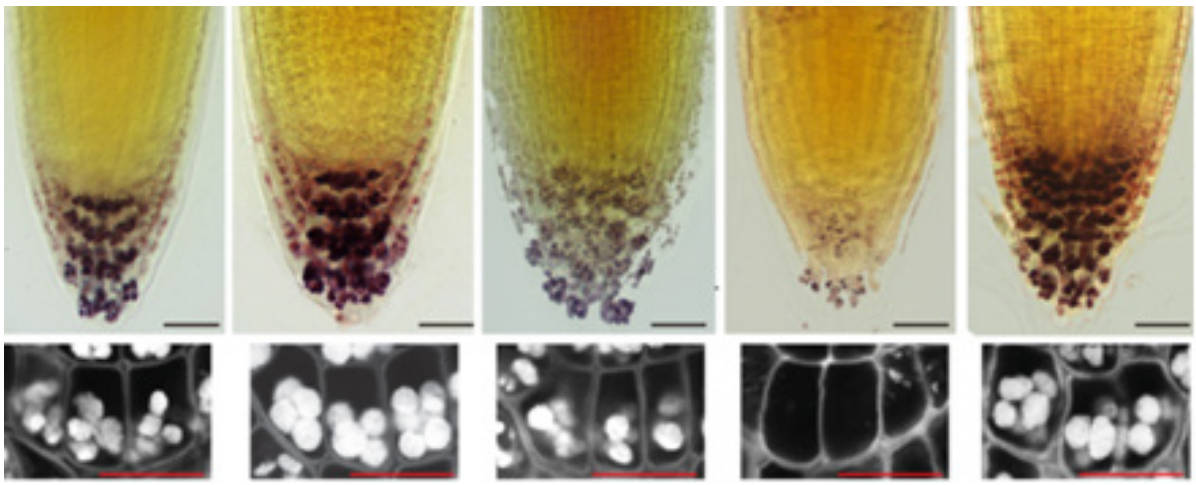

Figure 10 - Altered starch granule accumulation in *pin* mutants with altered auxin maxima - 7 days old, Lugol treated *Arabidopsis*. From left to right: wild-type (WT); *pin2* mutant; *pin3/4/7* triple mutant; *pin2* mutant treated with 25 µM L-kynurenine (L-Kyn) for 48 h; *pin3/4/7* triple mutant after treatment with 1 µM 1-naphthaleneacetic acid (NAA) for 48 h. Bars, 20 µm Adapted from (Zhang et al. 2019).

4.3 CRISPR/Cas9

With the improvements of genome sequencing techniques, scientists started to have an urgent need for tools to modify gene functions specifically. Targeted editing of the genome became a must. That is why DNA repair systems and nucleases were studied extensively. A novel genome-editing technique called CRISPR/Cas9 was developed in 2012 based on the studies of the tracrRNA molecules. These molecules are a part of the immune system of *Streptococcus pyogenes*. The discovery of these CRISPR/Cas9 ´molecular scissors´ was awarded in 2020 by a Nobel Prize in chemistry (The Nobel Prize, 2020).

In 1987 the team of (Ishino *et al.*, 1987) found 29 nucleotide long repeats that were interrupted by seemingly unrelated and non-repetitive sequences, called spacers, in *E. coli*. Later on, repeats like these were found in other microbes and prokaryotes, eventually getting named and referred to as clustered regularly interspaced short palindromic repeats (CRISPR) in 2002 (Jansen *et al.*, 2002). In the year 2005, two crucial discoveries were made, the first one being that CRISPR originates from foreign, extrachromosomal sources and the discovery of protospacer adjacent motif (PAM) (Bolotin *et al.*, 2005), along with an extensive sequencing of 4500 CRISPR sequences (Mojica *et al.*, 2005). The second one was an observation of the acquirement of new CRISPR sequences by *Yersinia pestis* from bacteriophage DNA (Pourcel, Salvignol and Vergnaud, 2005). Not much later, in 2007, the role of CRISPR sequences as a part of prokaryote immunity was first supported by experiments (Barrangou *et al.*, 2007) and later on confirmed by other experiments (Marraffini and Sontheimer, 2008; Garneau *et al.*, 2010).

In 2012 it was concluded that CRISPR can be used in genome editing and gene function research by the programming of Cas9 via CRISPR RNAs (crRNAs) and crRNA-trans activating RNAs (tracrRNAs) or by modifying the system to use only a single guide RNA (sgRNA) that is comprised of the crRNA sequence fused to the scaffold tracrRNA. (Jinek *et al.*, 2012).

There are multiple CRISPR systems. These can be divided into two distinct classes, class 1 and class 2. The main difference is in the target binding and target cleavage module. Class 1 systems comprise of multiple proteins in this module while class 2 systems use only one. These classes were further divided into types I-V, depending on what Cas proteins are used by each type (Makarova *et al.*, 2015; Ishino, Krupovic and Forterre, 2018). See Figure 11 for reference.

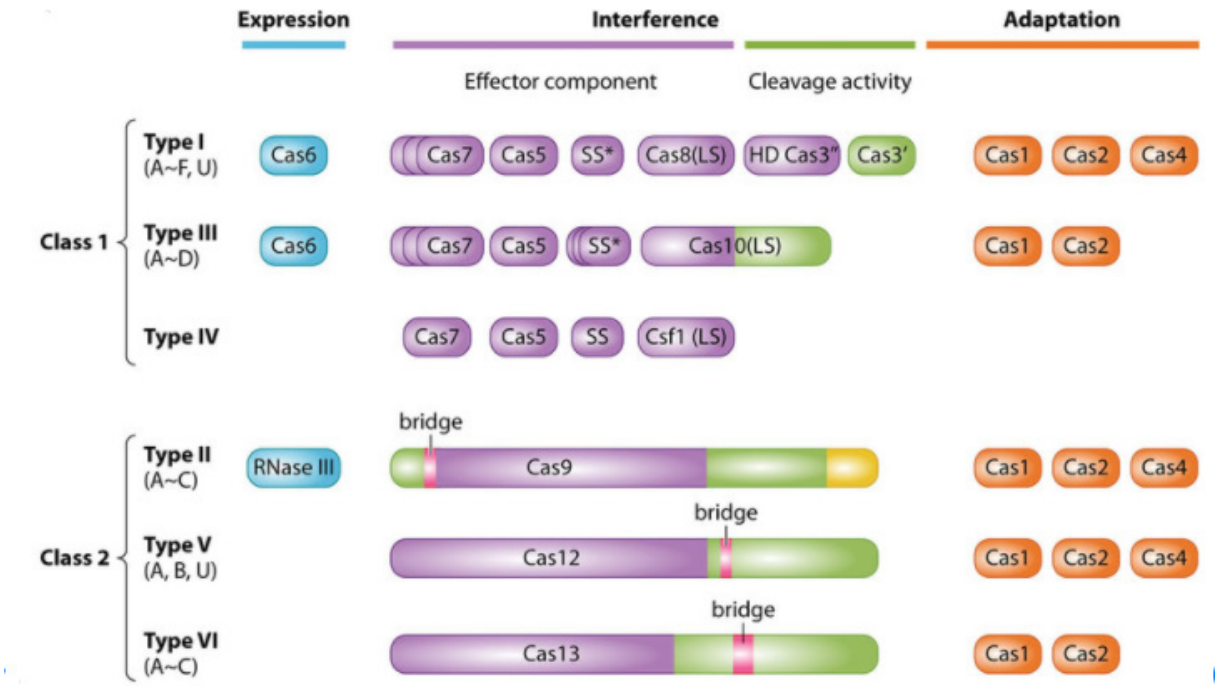

Figure 11 - CRISPR system classification by the number of interference related Cas proteins and Cas protein types Adapted from (Yoshizumi Ishino, Krupovic, and Forterre 2018).

4.3.1 Function and use of CRISPR/Cas9 in genome editing

Genome editing primarily uses the Type II CRISPR system, also called CRISPR/Cas9, that originates from *Streptococcus pyogenes*. By the introduction and expression of Cas9 and gRNA into an organism, targeted double-strand breaks are created. These double-strand breaks occur three base pairs upstream of the PAM sequence associated with the gRNA targeted region on the complementary DNA strand. The other, non-complementary, strand is cleaved one or multiple times 3-8 base pairs upstream of the associated PAM sequence. This cleavage is facilitated by HNH nuclease or RuvC-like nuclease domains of the Cas9 protein, with the HNH domain cleaving the complementary strand and the RuvC-like domain cleaving the non-complementary one (Jinek *et al.*, 2012). The highly conserved nuclease domains of Cas9 contain conserved motifs, specifically, the HNH nuclease domain has a ββα-metal fold motif while the RuvC-like nuclease is comprised of RuvC motifs (Nishimasu *et al.*, 2014).

Nowadays, as CRISPR/Cas9 systems use sgRNAs for targeting, the steps of the most used system can be broken down as follows. A sgRNA with a targeting sequence that is usually around 20 nucleotides long binds to Cas9, inducing a change in the conformation of Cas9 and its activation. The activated Cas9 searches and binds to the target DNA that matches the targeting sequence of the gRNA and also matches the PAM sequence of the Cas9. Once the activated Cas9

protein finds its target, it will melt bases immediately next to the PAM sequence and pair with the gRNA targeted region. If the pairing is successful, it induces a double-strand break of DNA described above (reviewed in Gupta et al. 2019). These double-strand breaks are later repaired by mechanisms of non-homologous end joining that might lead to frameshift mutations by the introduction of insertions or deletions in the target sire, or if a template is presented, it can be repaired by homology-directed repair that can be used for precise editing (reviewed in H. Zhang and McCarty 2017). See Figure 12 for visualisation.

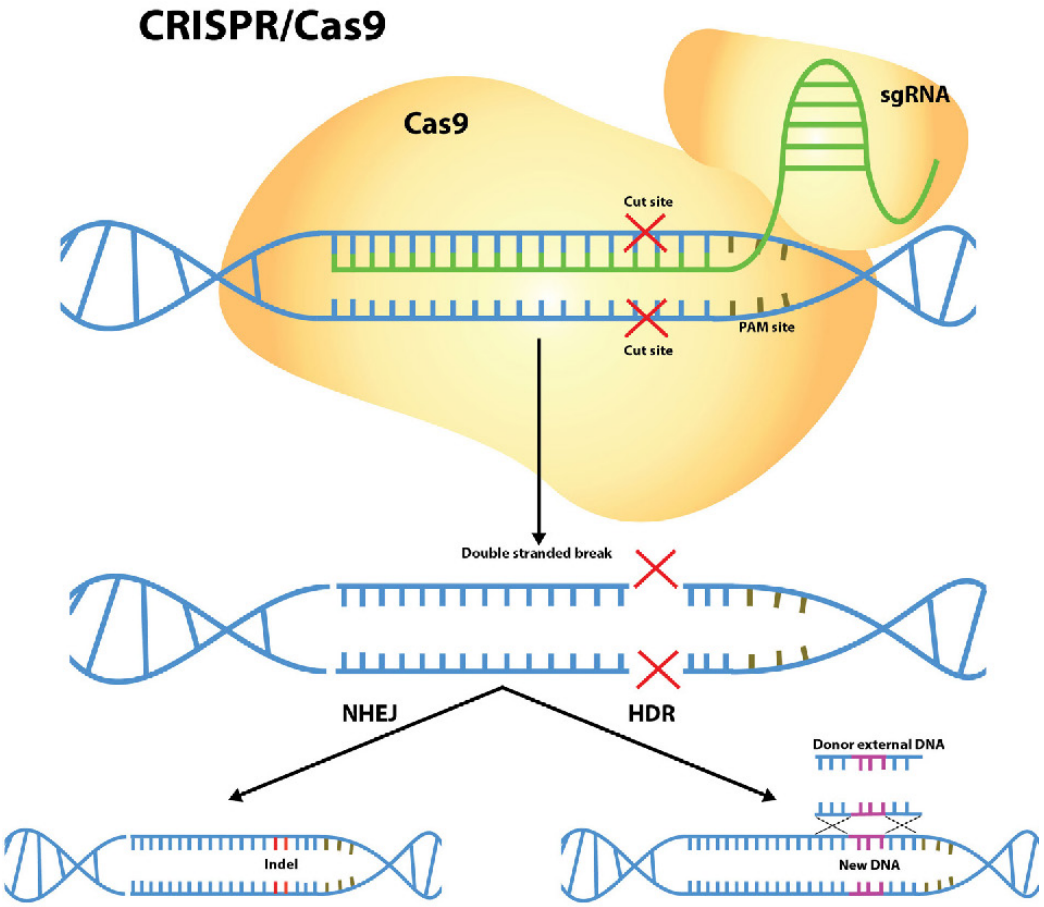

Figure 12 - Function of CRISPR/Cas9 in generating double-strand breaks in DNA and the reparation of these breaks Adapted from (Cribbs and Perera 2017).

The CRISPR/Cas9 system is continuously modified by scientists, leading to systems with altered properties and usage. One of many CRISPR/Cas9 system modifications is the inactivation of one of the two nuclease domains. The result is a Cas9 protein that is capable of single-strand breaks only (Cas9n). With this approach, two Cas9n proteins are used to generate a gene knockout, however, the specificity of this approach is increased 50- to 1,500-fold, as Cas9 proteins have to recognize more nucleotides. Nevertheless, there is a downside to this approach as the Cas9n protein has substantially lower efficiency compared to the wild-type Cas9 (Ran *et al.*, 2013).

4.3.2 CRISPR-TSKO system and polycistronic sgRNA

Another modification of the CRISPR/Cas9 system is the CRISPR-TSKO (CRISPR-Tissue-specific knockout). This system provides a solution for the generation of tissue-specific knockouts by using a tissue-specific promoter for Cas9 expression, combined with a ubiquitous promoter for the expression of gRNAs. It is built upon a modular cloning system, allowing for easy creation of custom promoters, fluorescent tags, linkers, gRNAs and Cas9 proteins. This is achieved by modules, designed for GoldenGate cloning (Engler, Kandzia and Marillonnet, 2008). It is imperative to realize that not all cloning systems are compatible, thus when the user wants to use another cloning system, the modules need to be adapted. The destination vector of this system enables direct cloning of one or two gRNAs. This can be increased to up to 12 sgRNAs by using a linker with AarI restriction sites instead of the unarmed sgRNA vector (Decaestecker *et al.*, 2019) - See Figure 13 for visual reference.

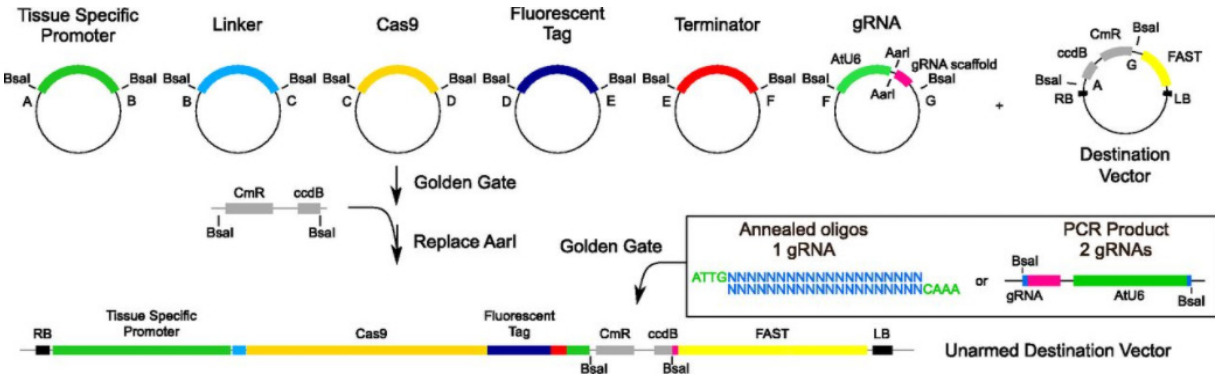

Figure 13 - The architecture of the CRISPR-TSKO cloning system. Adapted from (Decaestecker et al. 2019).

This approach was tested and experiments prove that this method is applicable for organ, tissue and cell line-specific knockout generation, providing an invaluable tool for gene function study in specific contexts (Decaestecker *et al.*, 2019). As the promoter used depends on the user, it can be used to generate tissue non-specific mutants too.

It is possible to produce multiple sgRNAs at the same time, using a polycistronic sequence. This sequence is based on the cleavage of tRNAs (transfer RNA) by cellular machinery (Xie, Minkenberg and Yang, 2015), namely RNAseP and RNAseZ that cleave tRNA regardless of the pre-tRNA sequence (Barbezier et al., 2009; Canino et al., 2009). The structure that allows this polycistronic transcription is composed of tRNA, followed by a sgRNA spacer with a sgRNA scaffold (referred to as gRNA). This is then repeated for every gRNA the user wants to add. The last gRNA is followed by a poly-A tail for transcription termination (Xie, Minkenberg and Yang, 2015). The described structure with the resulting sgRNAs can be seen in Figure 14 and a detail from the structure of the polycistronic sgRNA gene is in Figure 15. These two systems combined were chosen as the methods used for genetic manipulations in this thesis.

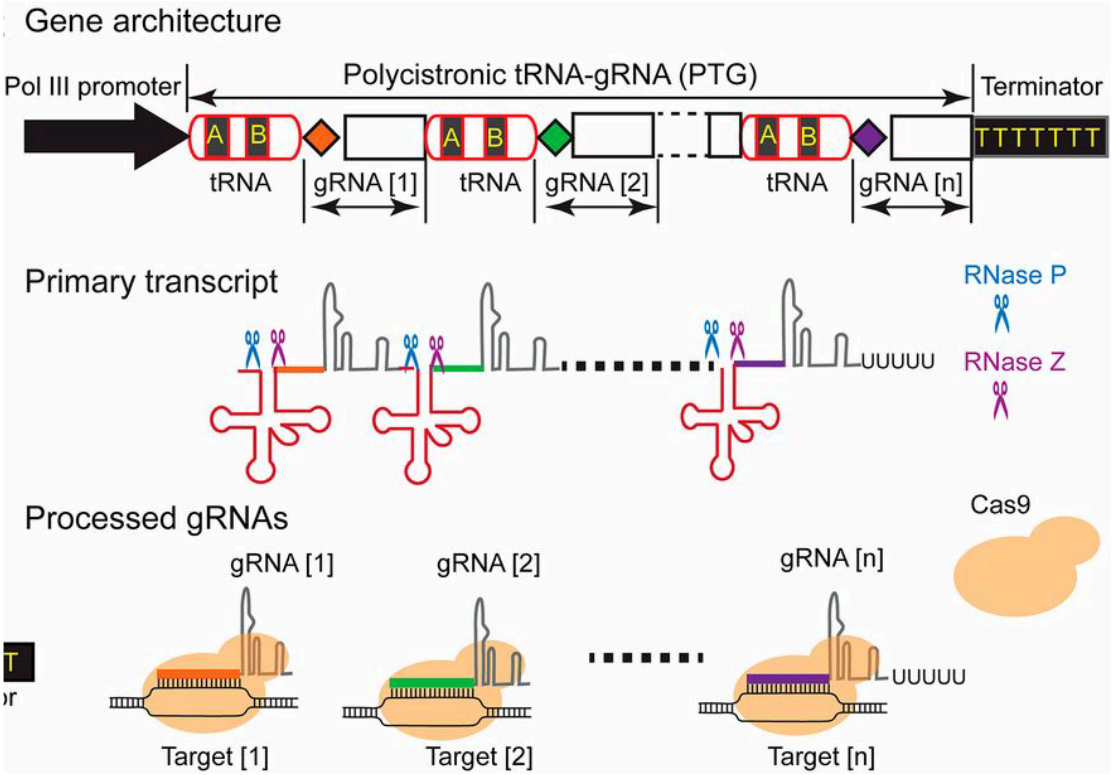

Figure 14 - sgRNA polycistronic gene architecture along with the resulting primary transcripts and sgRNA products Adapted from (Xie, Minkenberg, and Yang 2015).

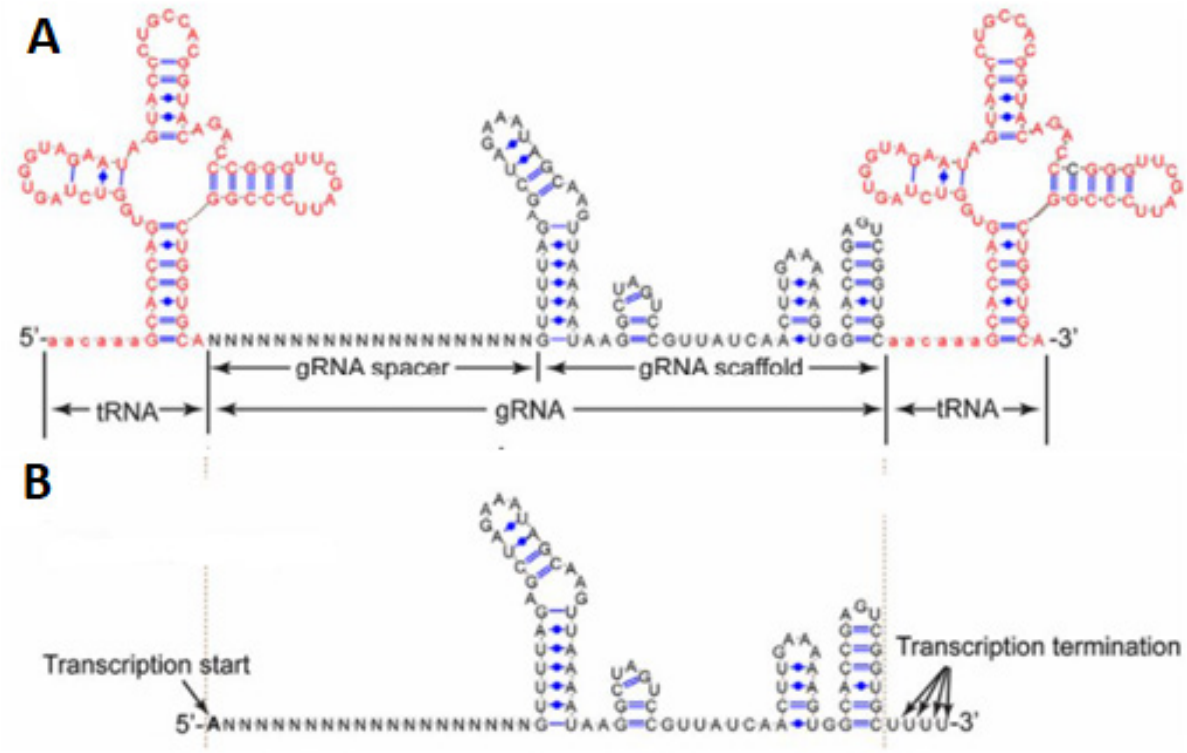

Figure 15 – Detail from the polycistronic sgRNA gene structure. Panel A shows the structure of all sgRNAs except the last one. Panel B depicts the last sgRNA with the transcription terminating end Adapted from (Xie, Minkenberg, and Yang 2015).

The use of the TSKO system will allow us to generate tissue-specific ADG1 and PGM *Arabidopsis* knockouts. As we have established that *adg1* and *pgm* mutants have pleiotropic phenotypes, this approach will allow us to impact only the cells that are expected to be involved in gravity perception. This will allow for a comparison of TSKO generated mutants with the lines of the original mutants, showing, whether the specific function of ADG1 and PGM in the tissues of the root cap results in a gravitropic response or if the genes need to function in the whole organism. The advantage of the *adg1* and *pgm* knockouts is that they allow for easy phenotype scoring by using Lugol staining as starch synthesis is expected to be impaired. The establishment of the TSKO methodology will allow generating gene knockouts not just in the cells of the columella, but in other tissues and the whole organism as well. The combined use of polycistronic gRNA expression with the Golden Braid system (Sarrion-Perdigones *et al.*, 2011) will allow the creation of a versatile tool for a wide range of applications in genome editing.

5. Methods and materials

5.1 Plant lines

In Table 1, you can find all used plant lines from other laboratories or created as a part of this thesis.

Line	Reference or preparation method
pHTR5:NLS-GFP-GUS	(Ingouff *et al.*, 2017)
pSMB::Cas9*GFP	Molecular cloning
pSMB::Cas9*PGM	Molecular cloning
pSMB::Cas9*ADG1	Molecular cloning
pUBI10::Cas9*AT5G14240	Molecular cloning

Table 1 - Plant lines used.

5.2 Growth conditions

Where not stated otherwise, seeds were stratified for two days at 4°C and were afterwards placed in a cultivation room with long-day conditions (16 hours light / 8 hours darkness, light intensity approximately 100 µmol * m^{-2} * sec^{-1} and temperature 21°C) on plates for 5 days. Plates contained the following: ½ Murashige Skoog salt mixture from Duchefa -2,15g/l; MES (MES*H_2O) – 0,5 g/l; pH 5,8; 1% plant agar from Duchefa; 1% sucrose.

After *in vitro* cultivations, plants, where appropriate, were transferred into Jiffy pellets and pots and then grown in a room with conditions as described above with an automatic water irrigation system.

5.3 Seed sterilization

The seeds used were sterilized using the chlorine vapour phase. The gas was made in a closed desiccation jar, containing tubes with *Arabidopsis thaliana* seeds, via the combination of 50 ml household bleach – Savo; and 1.5ml 37% HCl. The closed jar was placed into a fume hood and the seeds were being sterilized for approximately 4 hours. After this process, the tubes were closed, placed into a laminar flow box, and opened to dispose of any remaining chlorine gas.

5.4 Molecular cloning

Constructs containing a polycistronic CRISPR/Cas9 system were created by molecular GoldenBraid (Sarrion-Perdigones *et al.*, 2011) cloning using *Escherichia coli* TOP 10 and *Agrobacterium tumefaciens* GV3101 bacteria.

5.4.1 GoldenBraid modular cloning

The GoldenBraid (Sarrion-Perdigones *et al.*, 2011) cloning system is a modular system that uses type IIS restriction enzymes. The cleavage done by these enzymes remove their restriction sites and creates overhangs that serve as the basis for transcription unit assembly. Generally, parts can be created by PCR amplification with primers that have the specific BsmBI extension sites and amplify our templates of interest. The cloning design was carried out using the bioinformatics software Geneious Prime 2019_Full_Release('Geneious Prime', https://www.geneious.com). Multigenic DNA constructs were created using existing DNA parts from the GB 2.0 kit obtained from Diego Orzaez (Sarrion-Perdigones *et al.*, 2013 - Addgene kit # 1000000076, namely basic UPD, α and Ω plasmids). The units are designed from the smallest ones – GB cloning parts to the largest ones – Omega-level transcriptional units. After the creation of these units, plants can be transformed and then selected for further research purposes.

5.4.2 GoldenBraid cloning system level-0 part preparation

Parts that were used in the system were either obtained from the laboratory collection or prepared using the following protocol. Primers for PCR amplification and subsequent domestication were designed using the GB domesticator tool (*GoldenBraid domesticator*, https://gbcloning.upv.es/do/domestication/). The designed primers were tested *in silico* using Geneious Prime 2019_Full_Release ('Geneious Prime', https://www.geneious.com). The designed primers, alongside other components, were then used for PCR amplification of the desired DNA fragment. The PCR components and cycling conditions can be found in the tables below - Table 2 and Table 3.

PCR component	Concentration/volume
iProof buffer (Thermo Scientific)	4 µl
10µM dNTPs (Thermo Scientific)	0.4 µl
primer forward	c = 0.5 µM
primer reverse	c = 0.5 µM
DNA template	1 µl
iProof DNA polymerase (Thermo Scientific, 5U/µl)	0.1 µl
Milli-Q water	to final volume (20 µl)

Table 2 - PCR reaction components.

Step	Temperature (°C)	Time (s)	Repetitions
Initial denaturation	98	30	1
Denaturation	98	5	35
Annealing	60	15	
Extension	72	15	
Final Extension	72	300	1
Upkeep until product removed	16	∞	1

Table 3 - PCR reaction conditions.

After PCR, the DNA amplification was verified by the method of gel electrophoresis using (0,5 TAE buffer, 1.5% GelRed (GelRed® Nucleic Acid Gel Stain, Biotinum) 1% agarose (Agarose, universal, peqGOLD) at max 400mA, 80V for 20 minutes. After product verification, gel segments containing the DNA fragments were cut out and then the DNA was extracted using GeneJET Gel Extraction Kit (Thermo Scientific™) following the attached protocol (*Thermofisher GeneJET Gel Extraction Kit*, https://www.thermofisher.com/cz/en/home/technical-resources.html, *Thermofisher manuals*, https://www.thermofisher.com/cz/en/home/technical-resources.html). The concentration of the extracted DNA was measured using a nanodrop microvolume spectrometer.

The resulting DNA fragment was ligated with the pUPD2 vector (*Addgene - pUPD2*, https://www.addgene.org/68161). The protocol of the ligation reaction can be found in Table 4 below.

Reaction component	Total amount/volume
DNA fragment	40 ng
pUPD2 vector	75 ng
T4 ligase buffer (Promega, 10x concentrated)	1 µl
T4 DNA ligase (Promega, 3U/µl)	1 µl
BsmBI enzyme (Thermo Fischer, 10U/µl)	1 µl
Milli-Q water	to final volume (10 µl)

Table 4 - Components of the ligation reaction into pUPD2 vector.

For plasmid multiplication, all prepared plasmids were transformed into competent *E. coli* TOP10 strain bacteria by chemical transformation according to the appended Mix & Go protocol (*Mix & Go protocol for TOP 10 E. coli from Zymo Research*, https://files.zymoresearch.com/protocols/_t3001_t3002_mix_go_e._coli_transformation_kit_buffer_set.pdf). Plates contained 50 µl of 2% X-gal (5-Bromo-4chloro-3-indoxyl-beta-D-galactopyranoside from Biosynth) which was spread on the agar surface by a heat sterilized, cooled down glass rod. After the X-gal application, the suspensions of *E. coli* were spread by a glass rod

sterilized in the same manner. The plates were then transferred into a 37°C chamber for colonies to grow overnight.

Colony selection, based on the X-gal staining took place the next day. The selected colonies were then resuspended in 3ml of liquid LB medium with antibiotics - see Table 5 for reference. Bacteria were allowed to grow overnight in a 37°C chamber, placed on a shaker that gently mixed the suspension continuously. The following day plasmids were isolated from these bacteria suspensions using a GeneJet Plasmid Miniprep Kit from Thermo Scientific according to the attached protocol (*Thermofisher manuals*, https://www.thermofisher.com/cz/en/home/technical-resources.html). The isolation was followed by determining the concentration of obtained plasmids via nanodrop microvolume spectrometry. A restriction reaction - components in Table 6, with the duration of circa 1 hour at 37°C, followed by electrophoresis was used to verify the accuracy of our products. The plasmids were verified a second time using Sanger sequencing.

Vector	**Antibiotics**	**Concentration used**
Alpha	Kanamycin	50 µg/ml
pUPD2	Chloramphenicol	11 µg/ml
Omega	Spectinomycin	50 µg/ml

Table 5 - List of antibiotics used to select bacteria for transformation.

Component	**Total amount / volume**
DNA	1.5 µl of typical concentration (50-300 µg/mL)
Selected restriction enzyme	0.1 µl
Buffer for select restriction enzyme (10x concentrated, CutSmartR, BioLabs)	1 µl
Milli-Q water	to final volume (10 µl)

Table 6 - Restriction reaction components.

5.4.3 Preparation of Alpha-level transcriptional units

After all, parts have been prepared and verified, they were ligated into an Alpha-level transcriptional unit using GoldenBraid cloning - see Table 7.

Component	Total amount / volume
Promoter	75 ng
Terminator (optional)	75 ng
Prepared GB cloning compatible parts	75 ng/part
Alpha-level vector	75 ng
T4 DNA ligase	1 µl
T4 DNA ligase buffer	1 µl
BsaI enzyme	1 µl
Milli-Q water	To final volume (10 µl)

Table 7 – Alpha-level vector preparation mix components with corresponding amounts/volume.

After the transcriptional units have been prepared, alpha-level plasmids were multiplied by *E. coli* and subsequently purified and sequenced (process described in the previous chapter).

5.4.4 Preparation of Omega-level transcriptional units

To transform *Arabidopsis* plants, Omega-level constructs needed to be created from the alpha-level subunits. These were created via ligation of alpha subunits with the pDG3omega1 vector. The ligation components are listed in Table 8 with their respective amounts.

Component	Total amount / volume
Alpha-level transcriptional unit	75 ng/unit
pDG3omega1	75 ng
BsmBI enzyme (Thermo Fischer, 10U/µl)	1 µl
ligase buffer (10x concentration, Promega)	1 µl
T4 DNA ligase (Promega, 3U/µl)	1 µl
Milli-Q water	to 10 µl

Table 8 - Ligation components for omega-level vector synthesis.

The products of the ligation were multiplied and isolated from *E. coli* (as described in the previous chapters) and verified via Sanger sequencing.

5.5 Floral dip transformation of *Arabidopsis thaliana* plants

The floral dip was carried out on *Arabidopsis thaliana ecotype Col-0 (NASC ID: N70000)* plants. The procedure was based on (Clough and Bent, 1998). *Agrobacterium tumefaciens* cultures,

carrying the desired omega-level plasmid, were inoculated onto 1 ml of LB medium inside a 50 ml falcon tube and left for 6 hours to grow while on a shaker set on approximately 60 RPM at 28°C. After 6 hours, another 10 ml of LB media was added to the tube and left shaking overnight at the same settings.

The plants in the early flowering stage were prepared by cutting away all formed siliques and fertilized flowers, leaving only unfertilized flowers.

The day after, 40 ml of dip media (1 l H_2O, 100 g sucrose, 500 µl Silwet (AgroBio Opava) was added to the same tube and gently mixed with the culture. Prepared *Arabidopsis* flowers were dipped in the suspension for approximately 30 seconds. After dipping, the plants were attached to a stick and were placed in a dark and humid chamber for a day. The next day the plants were transferred to the cultivation room. After seed maturation, the seeds were harvested and selected.

5.6 Selection of transgenic plants

After sterilization, T1 seeds of plants containing vectors *pSMB::Cas9*ADG1*, *pSMB::Cas9*GFP* and *pSMB::Cas9*PGM* were grown for 5 days on vertical plates with a selection media containing ½ MS, 1% agar and Basta (glufosinate-ammonium, Cayman chemical, c = 15 µg/l) after 2 days of stratification. Viable, healthy-looking plants were then selected for microscopic analysis. Plants with the desired signal were then kept and transplanted into Jiffy pellets. These plants were transferred to the culture room and grown there. Once mature, seeds were harvested from these plants.

As of the line pUBI10::Cas9*AT5G14240, seeds were selected using a laser and light filter for mCherry/RFP (Red Fluorescent Protein) detection. Glowing seeds were selected and planted on vertical plates containing ½ MS, 1% agar media.

5.7 Lugol staining of lines *pSMB::Cas9*ADG1* and *pSMB::Cas9*PGM*

5-days old plants of *pSMB::Cas9*ADG1* and *pSMB::Cas9*PGM* were taken out of the vertical plates and placed for approximately 24 hours into 2% formaldehyde solution. After fixation, the plants were stained in Lugol solution for 1 minute and rinsed with distilled water. The plants were then transferred into a drop of distilled water on a microscope glass slide, covered and brought to the microscope for imaging.

5.8 Imaging

Lugol stained plants were imaged on an Olympus BX51 microscope equipped with an Apogee U4000 camera in brightfield. Low-resolution root gravitropism was observed using a scanner (Epson Perfection v700/v370) and controlled by an AutoIt script, set to image every 30 minutes for 4-24 hours, depending on the sample. The plants scanned were on their agar plates, placed on the scanning surface and covered by a piece of black fabric. High-resolution root gravitropism was imaged using a vertical spinning disc microscope – see Table 9 - Technical specifications of the spinning disc microscope. The mCherry fluorescent protein was excited using the 561 nm Laser while the green fluorescent protein (GFP) was excited using the 488 nm laser.

Spinning disc microscope	
Body	Carl Zeiss Axio Observer.7
Objectives	EC Plan-Neofluar 5X/0.16 M27 (FWD=18.5mm)
	Plant-Apochromat 10X/0.45 M27 (FWD=2.1mm)
	Plant-Apochromat 20X/0.8 M27 (FWD=0.55)
Confocal Unit	Spinning disk unit: Visiscope Confocal based on Yokogawa CSU-W1-T2 equipped with a VS-HOM1000 excitation light homogenizer
Detection	PRIME-95B Back-Illuminated Scientific CMOS Camera, 1200 x 1200 Pixel, 11 x 11 µm pixel size
Lasers	Laser 405 nm 150 mW
	Laser 488 nm 100 mW
	Laser 515 nm 100 mW
	Laser 561 nm 100 mW

Table 9 - Technical specifications of the spinning disc microscope.

5.9 Image analysis

The acquired images were analysed using the software ACORBA v.1.0 June 2021 (Serre and Fendrych, unpublished) to quantify the root bending dynamics and processed using Fiji (Schindelin *et al.*, 2012) for the analysis of expression patterns and preparation of figures.

5.10 DNA isolation

DNA was isolated from plants for genotyping using the following protocol:

Using a sterile Eppendorf tube, pinch out a disc from the leaf tissue into the tube (±20mg, 1cm^2). Put a stainless-steel ball into the tube, close it and freeze it in liquid nitrogen. After freezing, put the tube into the Retsch vibration mill and homogenize the sample for 30 seconds at 30 oscillations/second. Add 200 µl of extraction buffer – recipe found in Table 10, and vortex it for 5 seconds. Centrifuge the vortexed extract for 2 minutes at maximum speed. Immediately transfer the supernatant into a new Eppendorf tube, add 175 µl of isopropanol and mix thoroughly. Let the tube sit for 2 minutes at room temperature and then centrifuge it again for 4 minutes at maximum speed. Siphon the supernatant using a water vacuum pump and wash the pellet with 1 ml of 70% ethanol. Once again, transfer the tube into the centrifuge and run it for 5 minutes at maximum speed. Siphon the ethanol using a water vacuum pump and let the pellet dry for a few minutes. After there is no visible ethanol residue, dissolve the pellet in 5 µl 10 TE buffer and 45 µl sterile H_2O. The sample should be then stored at 4°C for a maximum of 1 month.

Chemical	Volume [ml]
200 mM Tris HCl - pH 7,5	20
250 mM NaCl	5
25 mM EDTA	5
0,5% SDS	5
H_2O	65

Table 10 - Extraction buffer components.

5.11 PCR genotyping

The PCR reaction components and cycling conditions used for genotyping the plant line *pUBI10::Cas9*AT5G14240* plants can be found in Table 11 and Table 12.

PCR component	Concentration/volume
10x DreamTaq polymerase buffer (Thermo Scientific)	2 µl
10µM dNTPs (Thermo Scientific)	0.4 µl
primer forward	c = 0.5 µM
primer reverse	c = 0.5 µM
DNA template	1 µl
DreamTaq DNA polymerase (Thermo Scientific, 5U/µl)	0.05 µl
Milli-Q water	to final volume (20 µl)

Table 11 - PCR reaction components used for the genotyping of plant line *pUBI10::Cas9*AT5G14240*.

Step	Temperature (°C)	Time (s)	Repetitions
Initial denaturation	95	30	1
Denaturation	95	5	35
Annealing	58	15	
Extension	72	15	
Final Extension	72	300	1
Upkeep until product removed	16	∞	1

Table 12 - PCR cycling conditions used for the genotyping of plant line *pUBI10::Cas9*AT5G14240*.

6. Results

6.1 Adapting the CRISPR/Cas9 TSKO system for GoldenBraid cloning

To make the CRISPR/Cas9 system versatile, a modular approach was chosen to enable both tissue-specific and non-specific mutant generation. As one of the goals of this diploma thesis is to explore if lowering the starch levels in the columella significantly affects the gravitropism of *Arabidopsis* roots, we have decided to target the genes ADG1 and PGM. We aimed to knock out these genes specifically in the columella in order to produce mutants that lack starch-filled statoliths but have an otherwise unimpaired starch synthesis. As a proof of principle, we have also established to make a mutant without tissue specificity and have selected the gene AT5G14240 for this purpose. Following this, we have re-designed the TSKO system for use in GoldenBraid cloning in the following way - omega vectors were constructed from five alpha-level subunits, namely Alpha1_1, Alpha1_2, Alpha1_3, Alpha1_4, Alpha2, each with a specific purpose. The Alpha1_1 subunit was designed to carry a promoter, the Cas9 protein with a fluorescent protein (mCherry) and a strong terminator. This subunit allows to target specific tissues or produce mutations throughout the whole plant by selecting a corresponding promoter. In our case, we used the SOMBRERO promoter for our tissue-specific lines – a transcriptional factor that is expressed in the root cap (Bennett *et al.*, 2010). The subunits Alpha1_2 and Alpha1_4 carry a P1- nuclear matrix attachment region which is expected to increase the activity of the insert while also reducing expression variance (Breyne *et al.*, 1992; Petersen *et al.*, 2002). The sequence of this matrix attachment region can be found in Supplement Table 1 The subunit Alpha1_3 carries a promoter active in the whole plant along with a polycistronic sequence that produces guide RNAs. These gRNAs guide and enable the Cas9 protein to induce site-specific double-strand breaks. The last subunit used – Alpha2 was used to provide a selection tool for transformed plants by carrying Basta resistance or mCherry tagged oleosin. An overview of specific Alpha-level parts used in the construction of created omega vectors can be found in Supplement Table 2. These alpha-subunits have regions labelled A1-C1. All regions have specific sequences on their borders. These provide a transcriptional unit map for use in GoldenBraid cloning – See Figure 16.

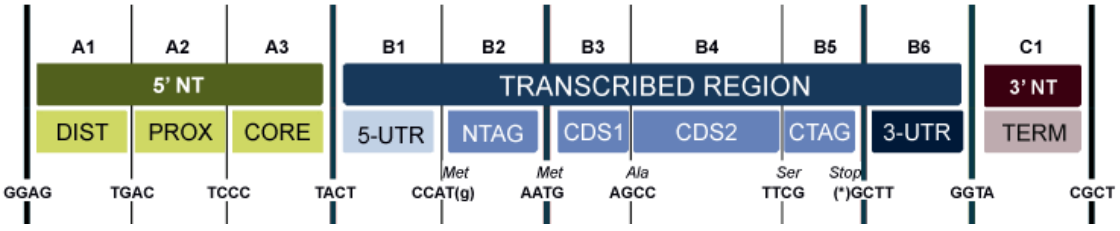

Figure 16 – Example map of GoldenBraid cloning units.

6.1.1 Alpha vector construction

6.1.1.1 Alpha1_1 vector construction for tissue-specific and non-specific Cas9 expression

The alpha 1_1 vector was designed to contain a promoter at sites A1-B2 that could be either tissue-specific or expressed throughout the whole plant. Following this promoter, the Cas9 protein for *Arabidopsis thaliana* was assigned to the B3-B4 sites. The Cas9 protein expresses along with a mCherry fluorescent protein (position B5) due to a 2A peptide (P2A) for ribosomal skipping, aiding Cas9 and mCherry expression. This provides a means to confirm the tissue-specific Cas9 expression by using fluorescence microscopy. At its end, the vector was designed to contain the Ubiquitin3 terminator on the B6-C1 position to terminate Cas9 and mCherry expression.

First of all, as we have received the sequence of Cas9 in three separate pieces, each containing a site for the enzyme BsaII. However, the last Cas9 part had to be domesticated for cloning into the B4 position, using the primers GB-AtCas9-F5 and GB-AtCas9-B4rev listed in Table 13.

Primer name	Primer sequence
GB-AtCas9-F5	GCGCCGTCTCGATAAGTTGATCAGGGAAGTGAA
GB-AtCas9-B4rev	GCGCCGTCTCGCTCACGAACCAACCTTCCTCTTCTTCTTAGG
GB2-2A-F	GCGCCGTCTCGCTCGTTCGGCTACCAACTTCAGCCTTTTG
GB2-eGFP_R2	GCGCCGTCTCGCTCAAAGCTCACTTGTACAGCTCGTCCA

Table 13 - Primers used for the domestication of level-0 components used in the construction of Alpha1_1 vector

We have used the present BsaII sites to connect the whole sequence of Cas9, using a ligation reaction (reaction in materials and methods). Following the reaction, we created a level-0 component, containing Cas9 in a pUPD2 vector in positions B3-B4, the method of which is described in the Materials and Methods section.

After the domestication of Cas9, I went on to clone and domesticate the 2A-mCherry which we have received from Dr Tomáš Moravec (Institute of Experimental Botany), into the B5 position using the primers GB2-2A-F and GB2-eGFP_R2 from Table 10 located above. After the domestication into the pUPD2 vector, the level-0 part was sent for sequencing, as seen in Figure 17.

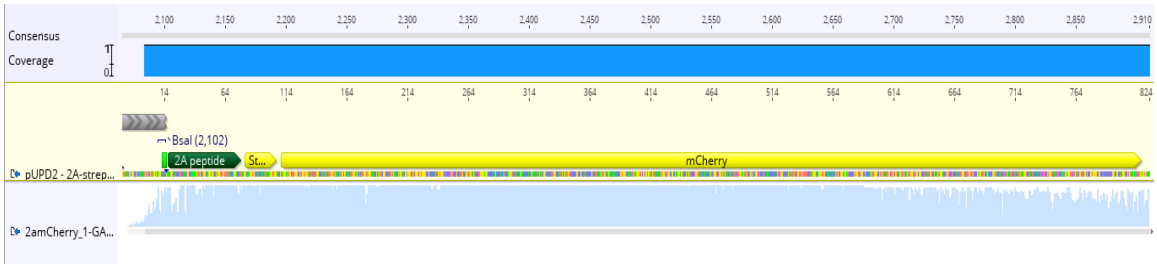

Figure 17 - Results of the sequencing of pUPD2 containing the 2A peptide and mCherry, visualised in Geneious.

For the promoter of the Alpha-level vector of tissue-specific mutants, we have used the plasmid pCK021*GB from MoClo Plant Parts II and Infrastructure Kit (https://www.addgene.org/kits/stuttmann-moclo-plant-infrastructure/#kit-contents). This plasmid contains the SOMBRERO promoter that facilitates the tissue-specific expression of Cas9 and mCherry. As for the tissue non-specific mutants, a plasmid containing the ubiquitin 10 promoter for *A. thaliana* was used that we had in the laboratory collection. The purpose of this promoter is to induce a stronger expression of Cas9 and mCherry, providing an enhanced number of mutants when compared to the Cauliflower Mosaic Virus 35S promoter that is commonly used for CRISPR/Cas9 (Castel *et al.*, 2019). These plasmids were ready to use for GoldenBraid cloning in the desired A1-B2 position. As the last part of the plasmid, the terminator, I have used another plasmid from the laboratory collection which contains the ubiquitin3 terminator for *A. thaliana* in the position B6-C1 for transcription termination. After all the subunits have been prepared, I have cloned them into the Alpha1_1 as seen in Figures 18 and 19, using the approach described in Methods and Materials.

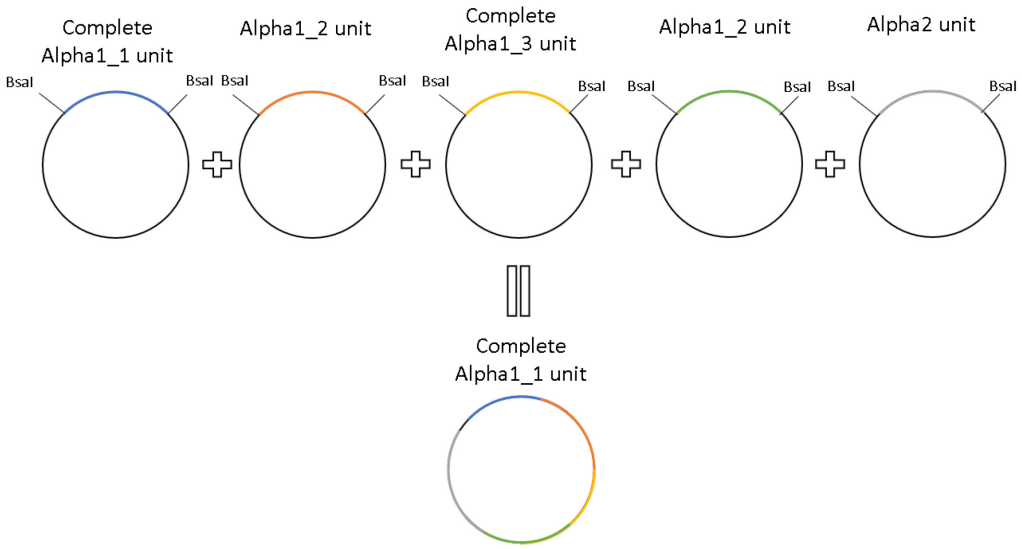

Figure 18 - Simplified visual representation of Alpha1_1 vector preparation.

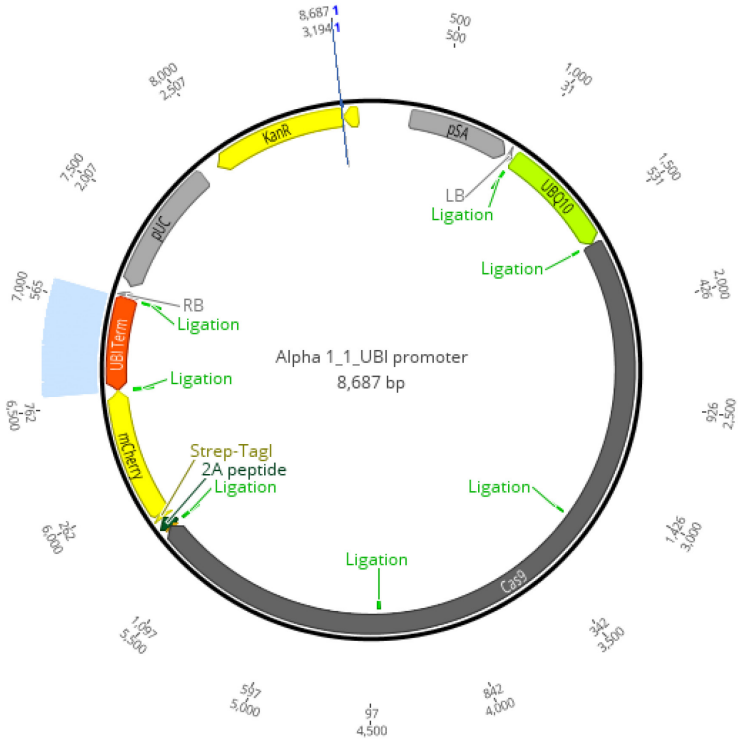

Figure 19 - Map of the Alpha1_1 vector used for the line *pUBI10::Cas9*AT5G14240*, containing the ubiquitin 10 promoter, Cas9, P2A peptide, mCherry, ubiquitin3 terminator and Alpha vector backbone sequences. Visualized in Geneious.

6.1.1.2 Polycistronic guide RNA system design and target selection

To increase the effectiveness and utility of the CRISPR/Cas9 system, we decided to include an option for the use of multiple gRNAs. In theory, the use of multiple gRNAs would not only allow for the targeting of multiple genes but also enable inducing multiple double-strand breaks in one gene, resulting in bigger deletions. These deletions make it possible to detect mutant specimens by using PCR and electrophoresis. To achieve the transcription of multiple gRNAs, we opted for using a single polycistronic gene, adapting a system designed by (Xie, Minkenberg and Yang, 2015). This system is based on a polycistronic gene that would use the tRNA processing apparatus already present in the cells. The whole premise of this system is using tRNAs, bordering gRNA sequences to ensure the correct cleavage of gRNA (gRNA spacer and gRNA scaffold). This is shown in Figure 20. The polycistronic gene is comprised of multiple tRNA-gRNA repetitions and ended with a poly-A sequence for transcription termination.

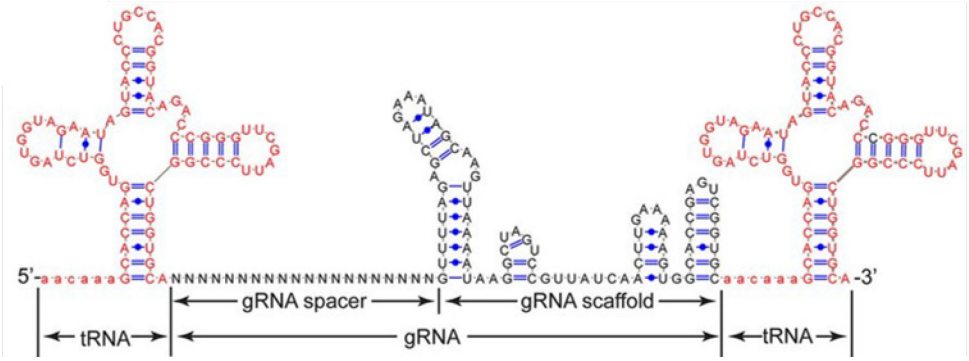

Figure 20 - Visual representation of a polycistron unit with parts that are cleaved by the cell machinery marked in red. Adapted from (Xie, Minkenberg and Yang, 2015).

The primers used were designed with the help of CRISPR-P 2.0 http://crispr.hzau.edu.cn/CRISPR2/) - see Figure 21, except for GFP targeting primers which were adapted to our system using primers from the paper of (Decaestecker *et al.*, 2019). The gRNA sequences were selected so that they have a high affinity to the target gene exon parts and a low number of off-target sites. In addition to the low number of off-target sites, the gRNAs should have low affinity to them and ideally, these sites were in intergenic or intron sections of the DNA. Two gRNAs were selected for each targeted gene, except for GFP, to create two double-strand breaks. Because of these 2 double-strand breaks, there is an increased chance of deletion mutations between the 2 gRNA binding sites which could cause loss of function mutations.

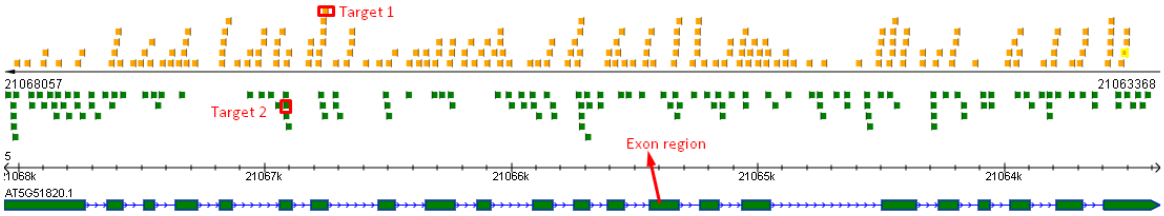

Figure 21 - gRNA selection in CRISPR-P 2.0.

The gRNA spacer sequences with their overhangs used for ligation and the respective primers used can be found in Supplement Tables 3-6. All the reaction parts of the gRNA synthesis are using the pGTR (*Addgene - pGTR plasmid sequence*, https://www.addgene.org/63143/sequences/) plasmid as the template for reactions. The whole process of guide RNA polycistronic gene construction and ligation into the Alpha1_3 vector can be seen in Figure 22.

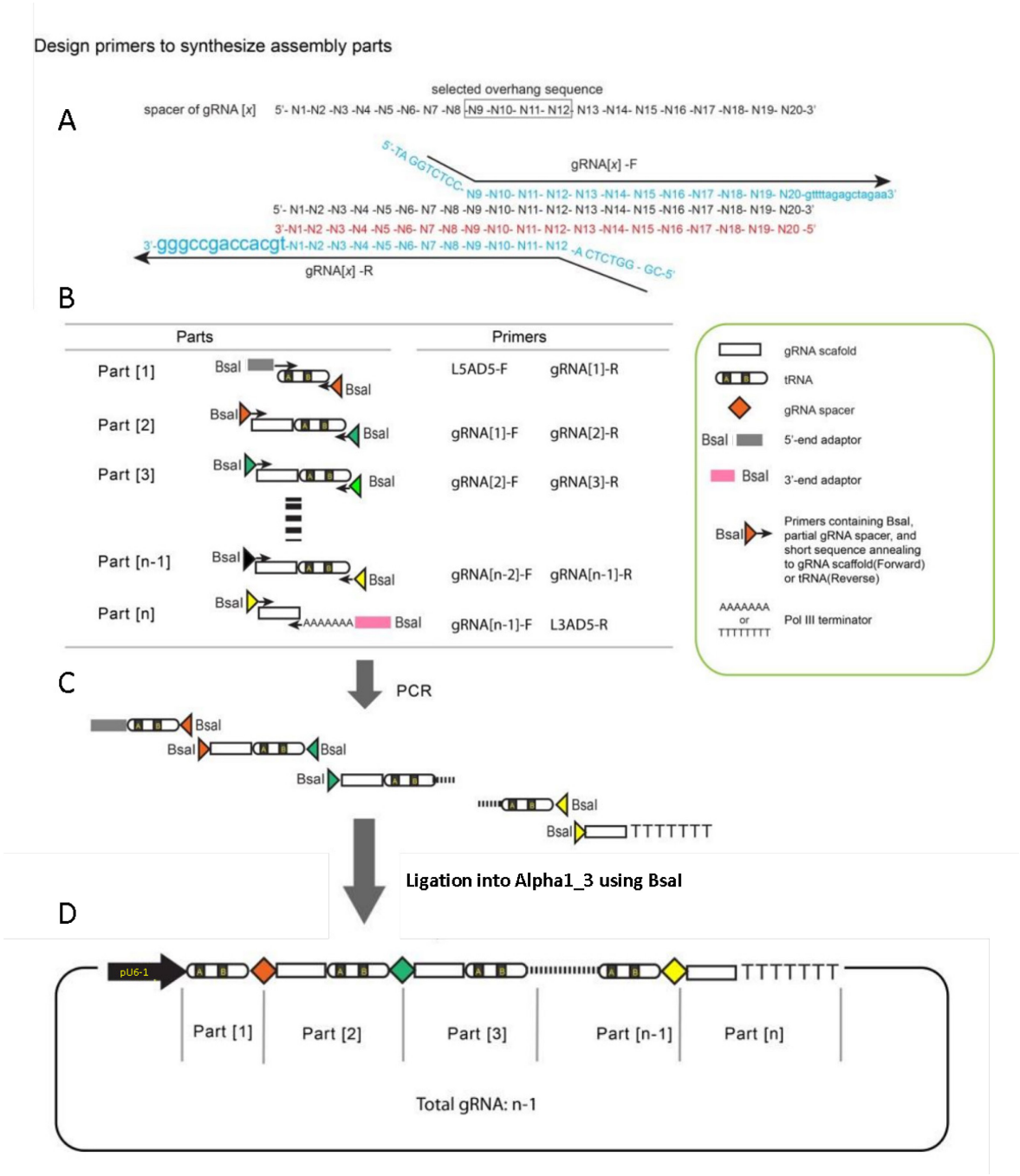

Figure 22 - Strategy for polycistronic gRNA gene design, part synthesis and assembly using GoldenBraid cloning. A) Schematic design of primers for gRNA spacer part with a 4 bp overhang, along with tRNA or gRNA sequences from the pGTR plasmid. In the case of the first and last part, these sequences are instead replaced with a 5'- or 3'- end respectively. B) Schematic of theoretical polycistronic gene parts created by the designed primers. C) Schematic of generated polycistronic gene parts and how they ligate with each other. D) A complete Alpha1_3 vector carrying a U6-1 promoter and the polycistronic gRNA gene with a terminator for polymerase III. Adapted from (Xie, Minkenberg and Yang, 2015).

The 5' overhang – ATTG is not an overhang used in GoldenBraid cloning, but it is there to pair with the overhang of the U6-1 promoter. The overhangs of the U6–1 promoter from plasmid pU6–1 (GB1204) (*Addgene - pU6-1 (GB1204)*, https://www.addgene.org/75405/) that are created

during GoldenBraid system cloning are 5' GGAG – which is a standard A1 site overhang; and 3' ATTG which as mentioned will ligate with the first part of the polycistronic gene for gRNA synthesis.

6.1.1.3 The construction of polycistronic gRNA gene carrying Alpha1_3 vector

We have designated the Alpha1_3 vector to carry the polycistronic gRNA gene with its promoter pU6-1. First of all, we have designed the gRNA polycistrons, as described in the chapter polycistronic guide RNA system design and target selection. Using the primers listed in Supplement Tables 3-6, we have made the gRNA polycistron subunits as seen in Figure 23.

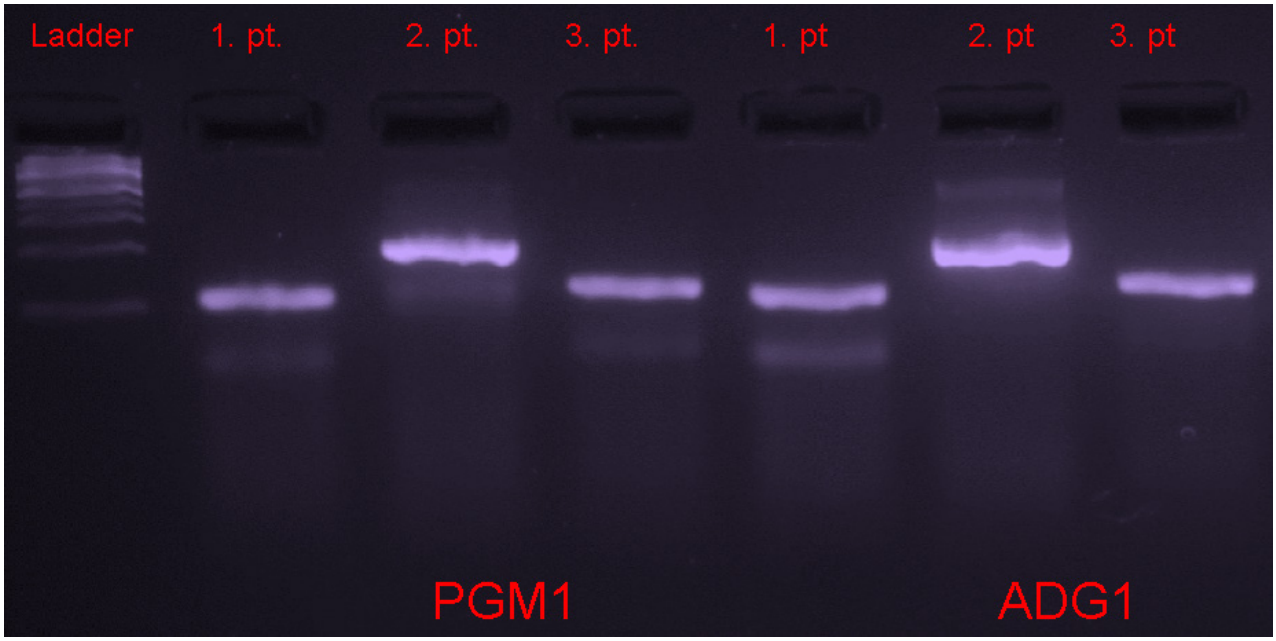

Figure 23 - Electrophoresis of synthesised subunits for lines *pSMB::Cas9*ADG1* and *pSMB::Cas9*PGM – 4% agarose gel.*

The polycistronic gRNA gene parts cover the GoldenBraid cloning regions B3 (part 1) to C1 (part 3; in the case of *pSMB::Cas9*GFP* part 2), occupying both the transcription and terminator regions as the sequences are designed to terminate by a polymerase III terminator. We had received a ready to use promoter - pU6-1 (*Addgene - pU6-1 (GB1204)*, https://www.addgene.org/75405/) in positions A1-B2 from the lab of doctor Lukáš Fischer (Charles University, Faculty of Science). Following this, we have created multiple alpha1_3 vectors, carrying different gRNA polycistronic sequences, depending on their specific target as previously seen in Figure 23. The list of these targets and gRNAs can be found in Supplement Tables 3-6. The polycistronic gRNA gene level-0 subunits were ligated into Alpha1_3 vector, along with the promoter of *A. thaliana* ubiquitin 3- see Figure 24.

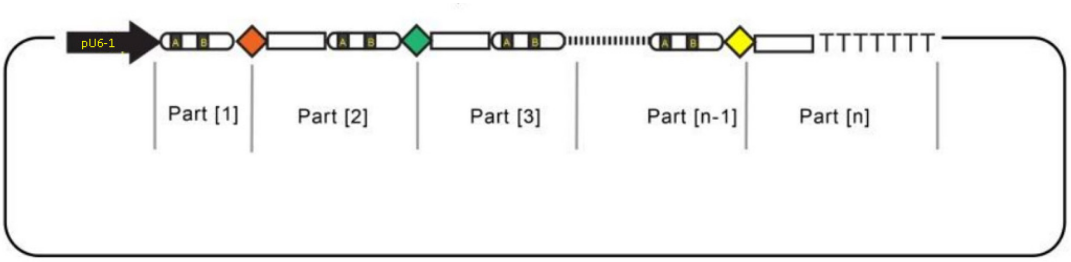

Figure 24 - Simplified visual representation of Alpha1_3 vector preparation. Adapted from (Xie, Minkenberg and Yang, 2015).

6.1.2 Omega vector construction

After all Alpha vectors were designed and constructed, final ligations into an omega vector took place – the ligation reaction protocol can be found in the Materials and Methods section. The differences in the omega vectors of tissue-specific and non-specific mutant plants are mainly in the Alpha1_1 and Alpha2 units. The omega vectors for tissue-specific mutants contain an Alpha1_1 unit with a mCherry and Cas9 protein that are expressed under the SOMBRERO promoter for specific localization of the expression into the root tip. Except for this unit, they contain an Alpha1_3 unit with a polycistronic gRNA gene for targeting specific genes (ADG1 or PGM) and an Alpha2 unit that contains Basta resistance for selection. This Basta resistance ensures, that only plants with an expressing omega vector are selected, increasing the chance that they express the Cas9 and gRNA polycistronic gene. These genes need to be expressed in all generations of tissue-specific mutants, as the mutations are not inherited due to their localization in the plant. On the other hand, the omega vectors for tissue non-specific mutants contain an Alpha1_1 unit with a mCherry and Cas9 protein, expressed under an ubiquitine10 promoter. This promoter is active throughout the whole plant. The Alpha2 unit of this vector contains mCherry tagged oleosin. This tagged oleosin ensures that only glowing seeds that most likely express Cas9 and the polycistronic gRNA gene are selected in T1. However, non-glowing seeds will be preferred for T2 - an active Cas9 with gRNAs is undesirable as they could cause additional mutations to the mutations the plants inherited from T1. The preparation of the omega vector via ligation reaction and an example of the final product can be seen in Figure 25 and Figure 26 respectively.

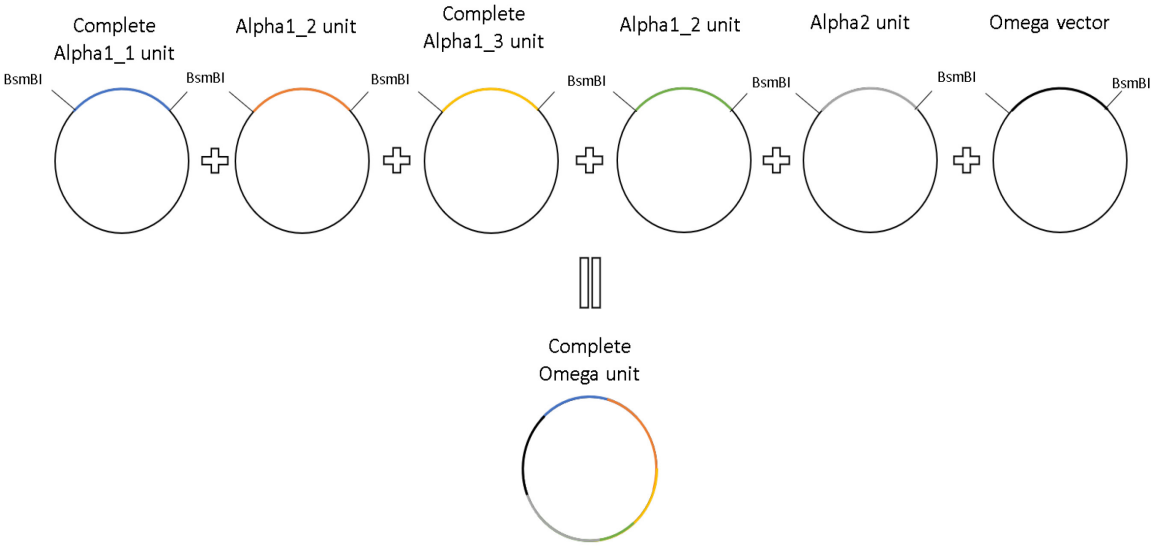

Figure 25 - Simplified visual representation of Omega vector preparation.

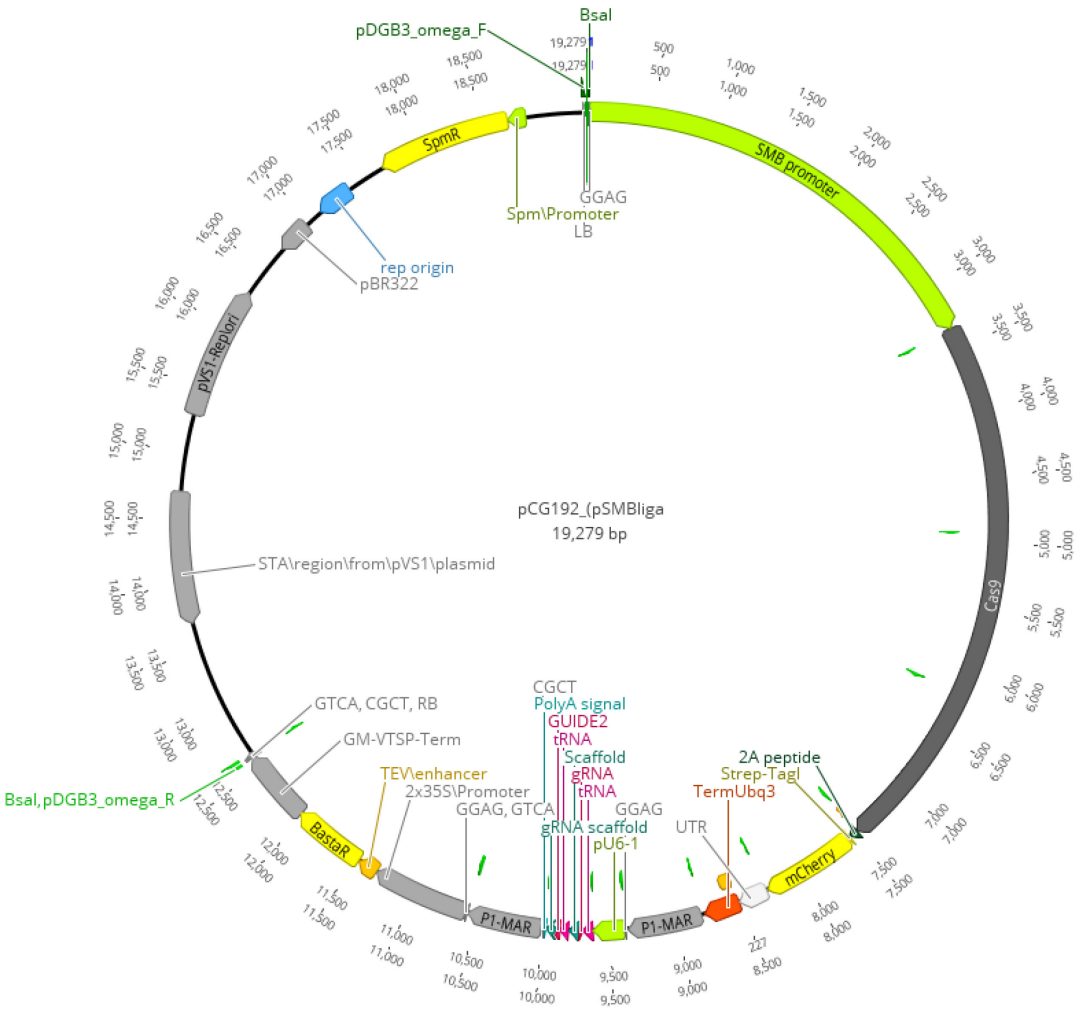

Figure 26 - Map of the Omega vector for the line *pSMB::Cas9*ADG1* visualized in Geneious.

6.2 Generation and selection of transgenic *Arabidopsis thaliana* lines

The omega vectors were designed with two main goals in mind – inducing a deletion in a specific gene – either plant-wide or in a specific tissue, and identification of these transgenic plants and the expression of the Cas9 protein. Transgenic *Arabidopsis t.* plants were prepared using the floral dip technique described in the Methods and Materials chapter. The T1 plants were then harvested and their seeds were selected based on their phenotype either under fluorescent light – case of transgenic line *pUBI10::Cas9*AT5G14240* or by selection based on the resistance to Basta - lines *pSMB::Cas9*ADG1, pSMB::Cas9*PGM* and *pSMB::Cas9*GFP* – See Figure 27.

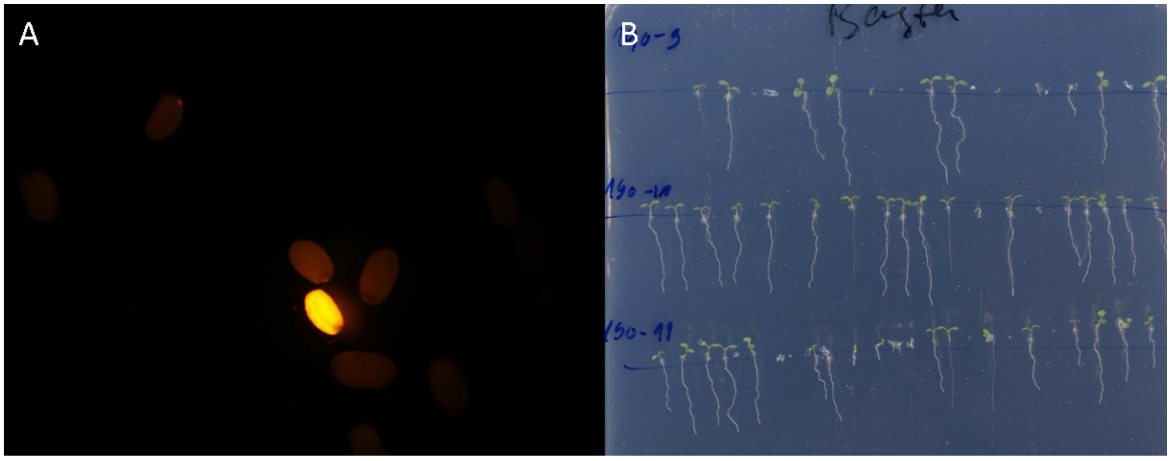

Figure 27 - Selection of transgenic lines: Picture A - Visual selection of glowing seeds of lines *pUBI10::Cas9*AT5G14240*. Picture B – Basta-mediated selection of lines *pSMB::Cas9*ADG1, pSMB::Cas9*PGM* and *pSMB::Cas9*GFP*.

6.3 Phenotype of tissue non-specific line *pUBI10::Cas9*AT5G14240*

The selected plants of the tissue non-specific line *pUBI10::Cas9*AT5G14240* were expected to carry a deletion in the targeted gene in all of their tissues, meaning the mutations that were induced are inheritable. In the T1 generation, the mutants of line *pUBI10::Cas9*AT5G14240* displayed several phenotypes, namely restricted growth of the whole plant, restricted growth of the primary root where lateral roots and adventitious roots take over and mutants where the primary root keeps growing but is strongly waving. Examples of restricted growth can be seen in Figure 28.

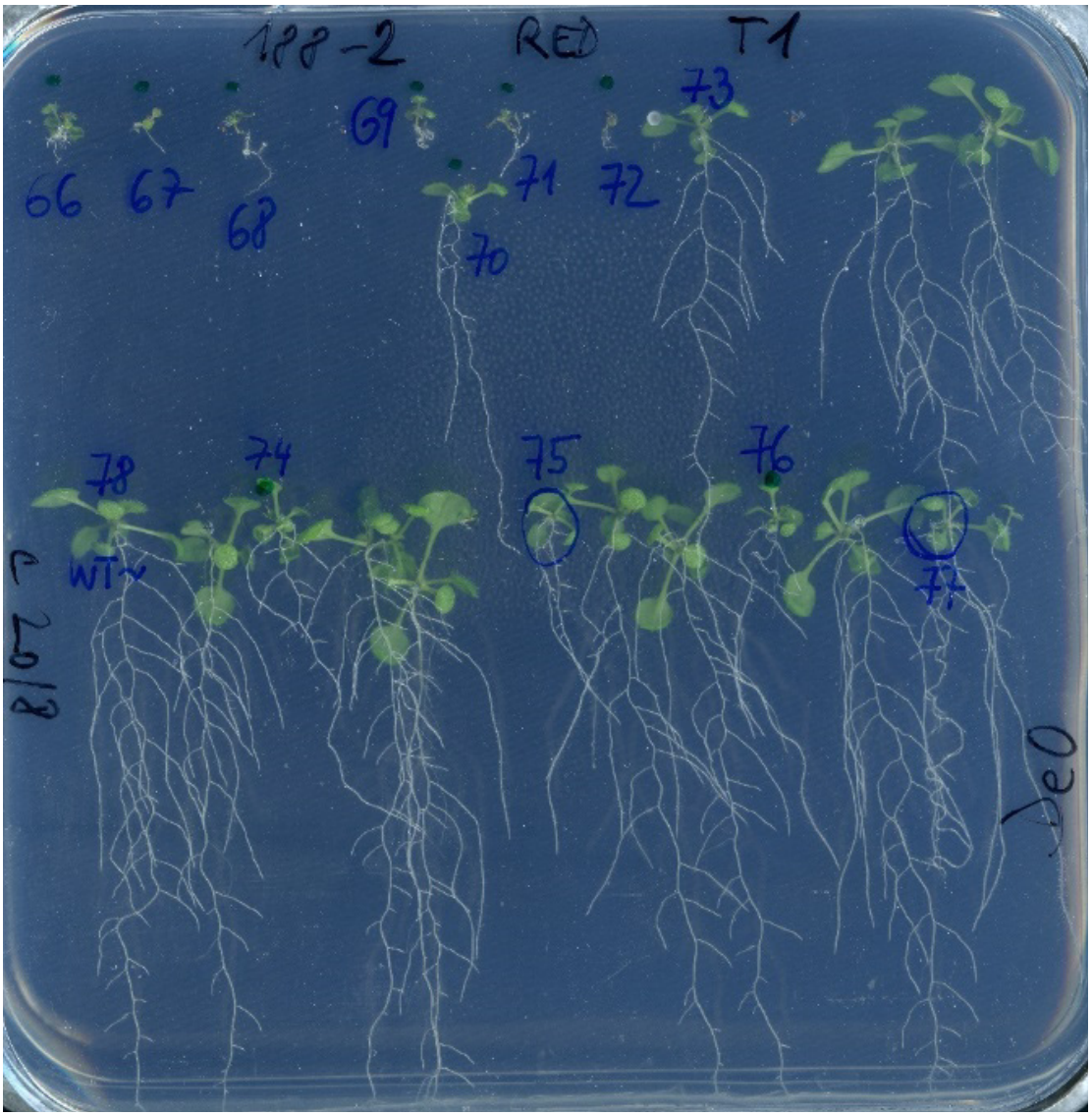

Figure 28 - Plants germinated from selected seeds of *pUBI10::Cas9*AT5G14240* line. Plants 66, 67, 68, 69, 71 and 72 with visible growth impairments.

The mutants were selected and their DNA was isolated according to the protocol in the Materials and Methods chapter, with the exception that the material was not the leaf of the plant, but the whole plant itself. Part of the collected material was used for a PCR reaction facilitated by

the primers At5gCRISPRcheck-F and At5gCRISPRcheck-R. A portion of the PCR product was sent for Sanger sequencing while the rest was used for deletion detection by electrophoresis. The sequence of the primer at5gCRISPR-Rseq that was used for Sanger sequencing, as well as the sequences of the two previously mentioned primers, can be found in Supplement Table 7. The results of these efforts can be seen in Figure 29. The presence of DNA fragments that are expected to be 619 bp long in the wells labelled 61, 62, 64, 66, 68 and 69 indicate that these tissues had cells carrying deletions in the amplified region. These PCR reaction products also contain a fragment that is expected to be 1358 bp long. The presence of this fragment indicates that the isolated DNA also originated from cells without deletions induced by CRISPR/Cas9, meaning, that the tissues were chimeric. This was later confirmed by the results of Sanger sequencing – the unclear readings after the sequence targeted by gRNA are caused by different genotypes present in the sample.

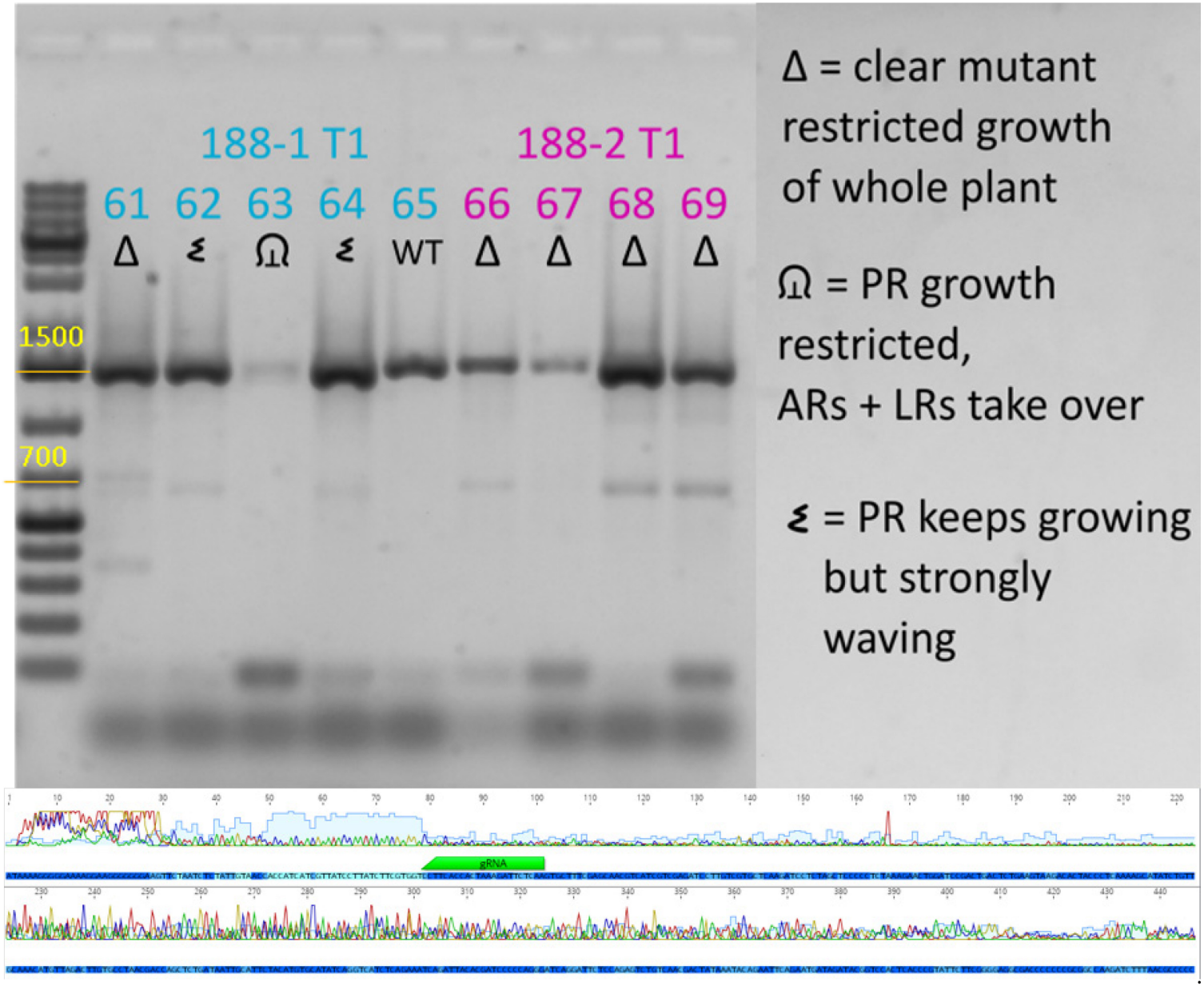

Figure 29

*Sequencing results and electrophoresis gel with marked symbol meanings of visibly impaired pUBI10::Cas9 *AT5G14240 plants.*

Expected fragments of 619 bp and 1358 bp length on the gel in case of successful deletions. Sequencing results visualized in Geneious.

6.4 Phenotypes of tissue-specific knockout lines *pSMB::Cas9*GFP, pSMB::Cas9*ADG1 and pSMB::Cas9*PGM*

In a similar manner to the previous line, the tissue-specific lines were expected to carry a deletion, induced by Cas9 and gRNA interactions with the DNA of the plants. However, the critical difference is that the lines *pSMB::Cas9*GFP*, *pSMB::Cas9*ADG1* and *pSMB::Cas9*PGM* were expected to carry targeted genes with deletions specifically in the columella cells of the root tip. In addition to these deletions, generated plant lines were expected to be Basta resistant as well as carry genes responsible for fluorescent tagging of cells with expected Cas9 expression.

The resulting T1 plants have generated fewer seeds than usual. Due to this lack of seeds, some of the T2 lines were not tested by chi-squared test for segregation ratios and as such are not listed in the segregation table - Table 14. The performed segregation analysis serves as a tool for easier attainment of homozygous lines in future generations.

Line	Surviving	Dying	Total	Expected number of insertions	p-value difference from Mendelian distribution
***pSMB::Cas9*PGM*-1**	34	7	41	Single insertion	0.2411285996
***pSMB::Cas9*PGM*-2**	33	8	41	Single insertion	0.4170770595
***pSMB::Cas9*PGM*-3**	29	12	41	Single insertion	0.5279301963
***pSMB::Cas9*PGM*-4**	18	15	33	n/a	n/a
***pSMB::Cas9*PGM*-5**	31	0	31	No insertions	n/a
***pSMB::Cas9*PGM*-6**	22	7	29	Single insertion	0.9146213879
***pSMB::Cas9*PGM*-8**	25	2	27	Double insertion	0.8037847063
***pSMB::Cas9*PGM*-9**	32	4	36	Double insertion	0.2282310395
***pSMB::Cas9*PGM*-10**	18	2	20	Double insertion	0.4884223166
***pSMB::Cas9*PGM*-11**	15	7	22	Single insertion	0.4601809354
***pSMB::Cas9*ADG1*-1**	23	12	35	Single insertion	0.2045587527
***pSMB::Cas9*ADG1*-2**	27	2	29	Double insertion	0.8856276131
***pSMB::Cas9*ADG1*-5**	23	2	25	Double insertion	0.7177418151
***pSMB::Cas9*ADG1*-6**	25	7	32	Single insertion	0.6830913983

Table 14 - Expected numbers of insertions of individual lines based on chi-square test and results of Basta selection. N/a = not applicable

The line *pSMB::Cas9*GFP* was used to verify the tissue-specific localization and activity of the Cas9 protein. The fluorescent mCherry protein and presumably the Cas9 protein was correctly localized in the root tip of the T1 and T2 generation of *pSMB::Cas9**GFP line, as can be seen in Figure 30. The dimmed GFP signal is the result of Cas9 activity as the gRNA in this line

was designed to induce a deletion in the gene necessary for GFP synthesis, while the red mCherry signal is the result of the Sombrero promoter-driven mCherry protein expression, signalling the tissue-specific localization of Cas9 co-expression due to the P2A ribosomal skipping peptide. Because of this, the intensity of mCherry fluorescence is expected to reflect the expression levels of Cas9 as in the case of (Decaestecker *et al.*, 2019).

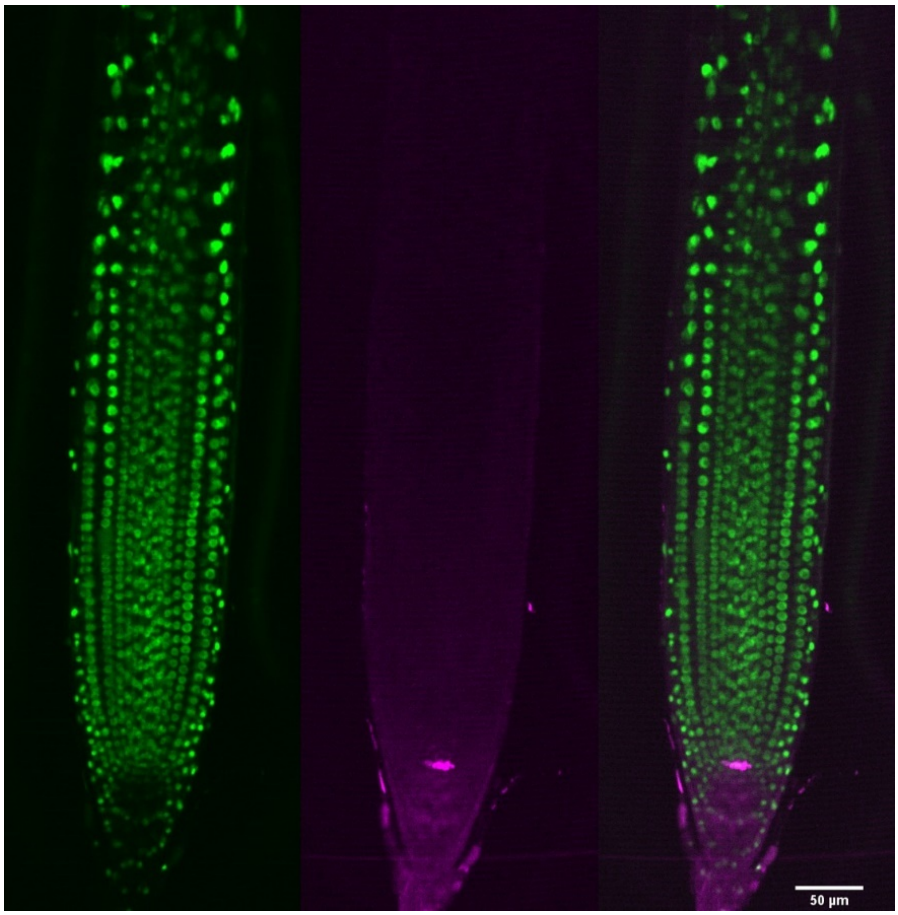

Figure 30 - From left to right: *pSMB::Cas9*GFP* line with excited GFP; *pSMB::Cas9*GFP* line with excited mCherry; composite image. Scale bar = 50 µm.

The remaining two lines displayed a similar pattern of fluorescence. You can see the fluorescence and bright-field images of lines *pSMB::Cas9*PGM* and *pSMB::Cas9*ADG1* in Figure 31 and Figure 32.

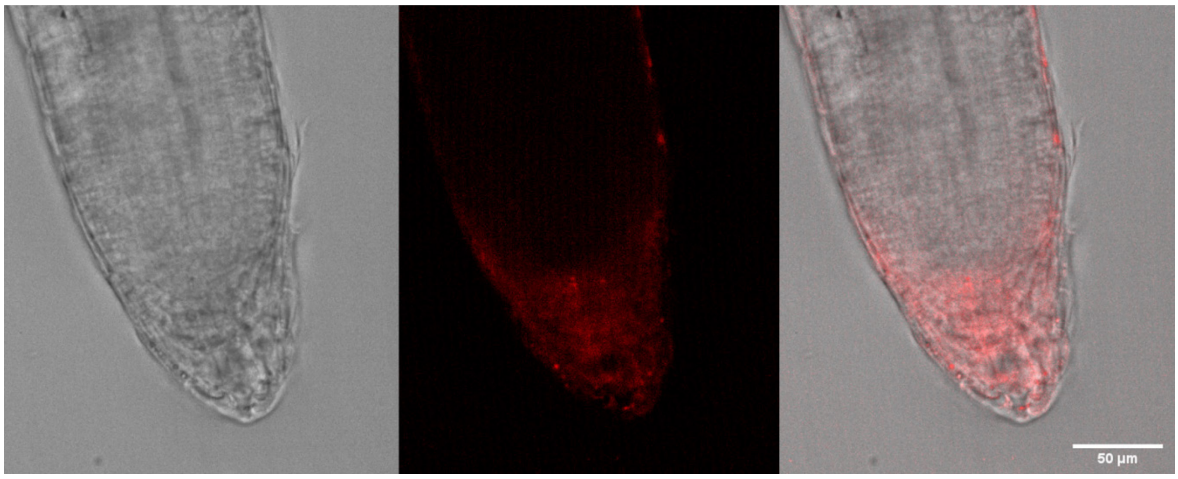

Figure 31 - From left to right: *pSMB::Cas9*PGM* line in brightfield; *pSMB::Cas9*PGM* line with excited mCherry; composite image. Scale bar = 50 µm.

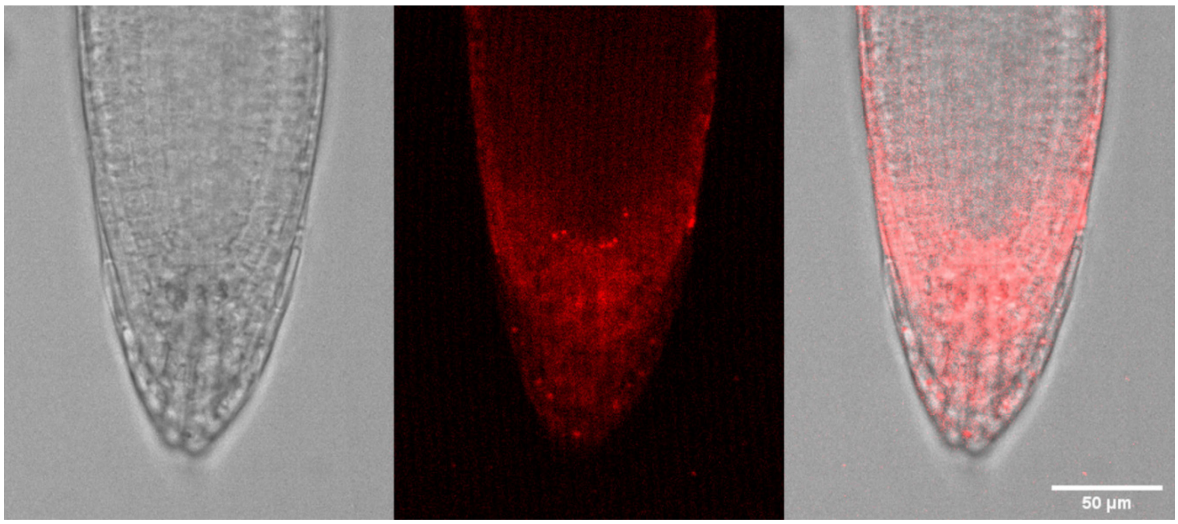

Figure 32 - From left to right*: pSMB::Cas9*ADG1* line in brightfield; *pSMB::Cas9*ADG1* line with excited mCherry; composite image. Scale bar = 50 µm.

6.5 Comparison of *pgm* and *adg1* insertion lines with CRISPR lines *pSMB::Cas9*PGM* and *pSMB::Cas9*ADG1* in terms of statolith content

After brightfield and fluorescence images of the lines were taken, we have stained the statoliths with the use of Lugol solution to visually assess starch levels in the columella. As a means of comparison of the tissue-specific CRISPR/Cas9 system effectiveness, we chose to compare the generated mutant phenotypes to the phenotypes of *pgm* and *adg1* insertional mutants and wild-type plants. These insertional mutants would also serve as an agravitropic reference for determining the

scope of effect columella-located starch has on gravitropic responses. Unfortunately, we were unable to obtain an *adg1* mutant line that was capable of germination. We have obtained *adg1* seeds from three different laboratories, however, all of them failed to germinate. To maximize our chances for seed germination, we have used not only ½ MS media that are commonly used in *A. thaliana.* cultivation but we have also tried media with added sucrose and with added gibberellic acid. As a consequence of this inability to germinate *adg1* plants, we only had *pgm* mutants for reference. In Figure 33, you can see a difference between the statoliths of the *pgm*, and wild-type lines.

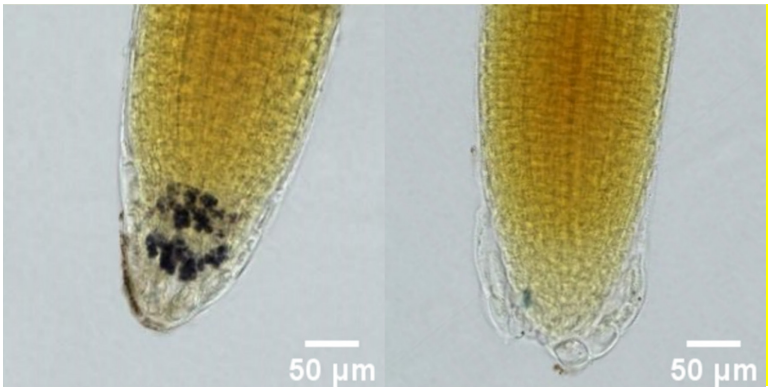

Figure 33 - From left to right: Wild-type plant with Lugol solution stained statoliths; *pgm* line with Lugol solution stained statoliths. Scale bar = 50 µm; brightfield

Even though the phenotype of *pgm* mutants was seemingly uniform – without visible starch granules, our lines *pSMB::Cas9*PGM* and *pSMB::Cas9*ADG1* showed high variability in columellar starch content from plant-to-plant. Some tissue-specific CRISPR/Cas9 plants had wild-type like levels of columella starch, however, there were also plants that visibly lacked the majority of starch, plants with one side of the columella seemingly starchless while the other side looked like that of a wild-type plant, plants with differing starch levels in different layers of the columella and other columella starch level variations. These phenotypes indicate different CRISPR/Cas9 efficiencies across the targeted tissue – where one columella cell could have its starch synthesis capabilities impaired, the sister cell could be unaffected. The frequency of mutant phenotypes was more common in the line *pSMB::Cas9*ADG1* than in the line *pSMB::Cas9*PGM*, implying differing efficiencies of the adapted system, depending on the gRNAs used. Examples of different phenotypes can be seen in Figure 34 and Figure 35.

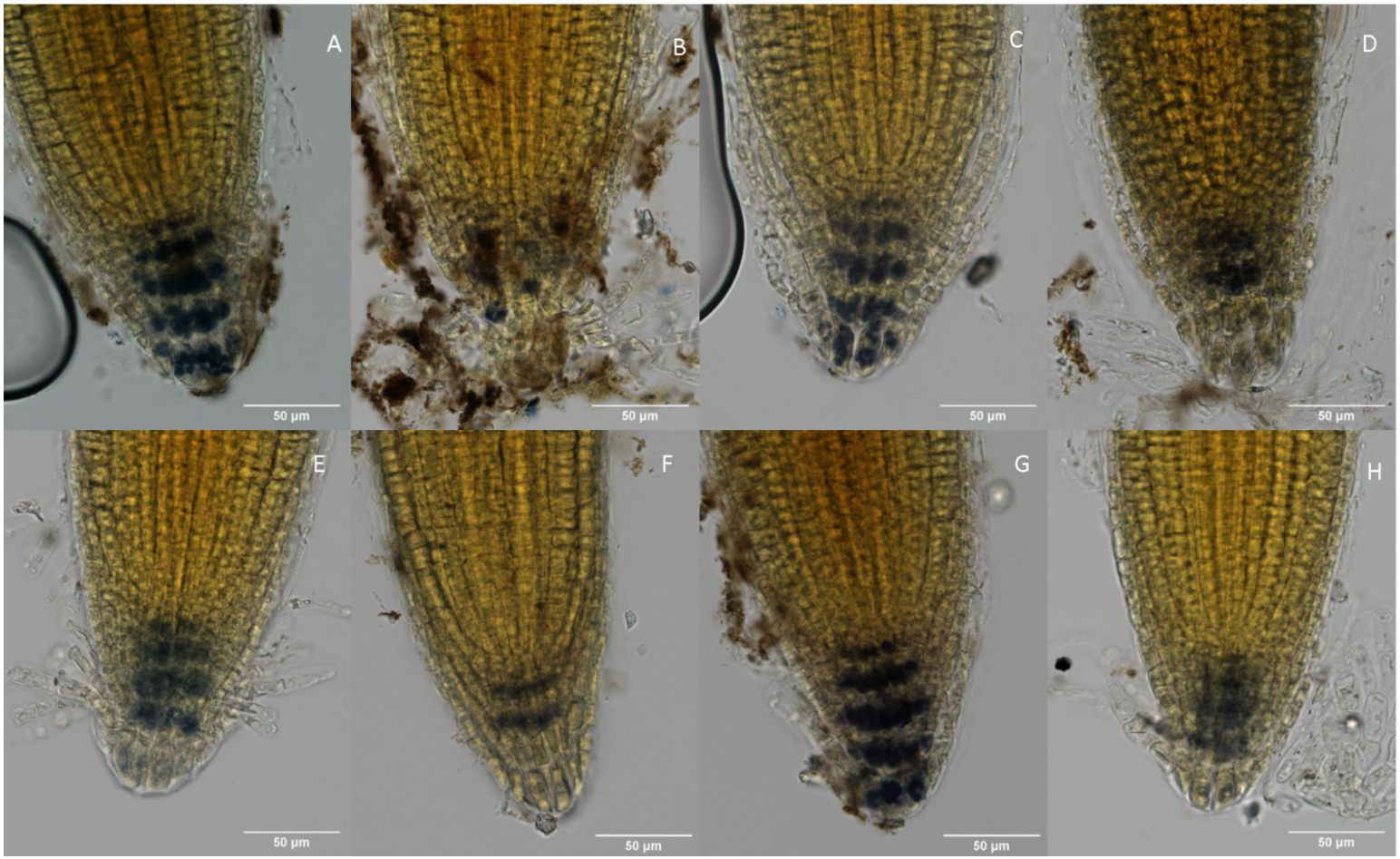

Figure 34

Picture A:
Wild-type plant with Lugol solution stained statoliths

Pictures B-H:
*pSMB::Cas9*PGM* line with Lugol solution stained statoliths. Scale bar = 50 µm.; brightfield

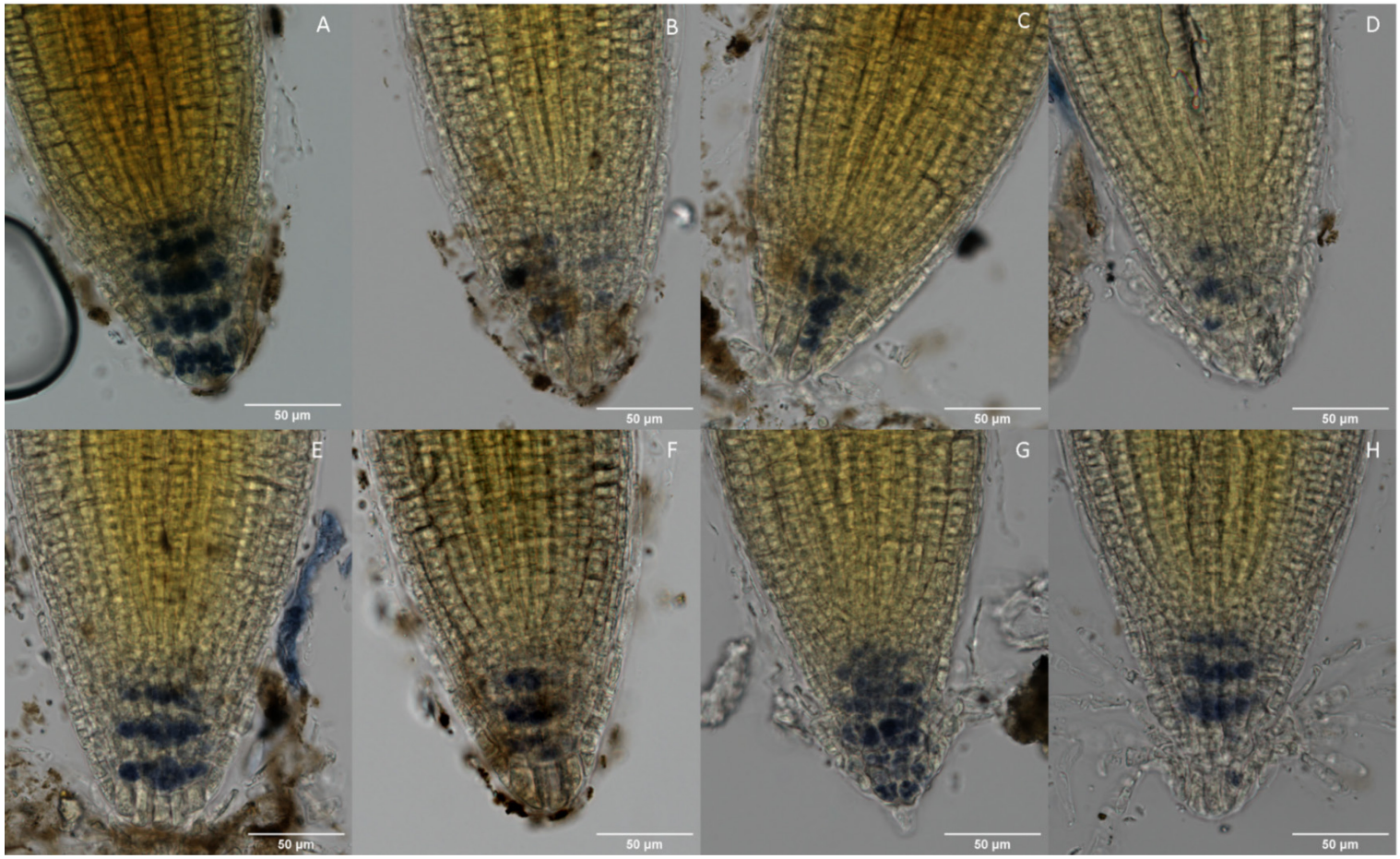

Figure 35

Picture A: Wild-type plant with Lugol solution stained statoliths

Pictures B-H: *pSMB::Cas9*ADG1* line with Lugol solution stained statoliths. Scale bar = 50 µm.; brightfield

6.6 Root gravitropism of *pgm, pSMB::Cas9*PGM* and *pSMB::Cas9*ADG1* mutants

After the visual comparison of the statolith content of root tips, we started measuring the response to gravity on both the microscope and scanner. These gravistimulation experiments were done both using our *pSMB::Cas9*PGM* and *pSMB::Cas9*ADG1* lines as well as the *pgm* insertion mutant line, using the same methods.

The low temporal resolution experiments that were conducted using a scanner revealed a similar gravitropic reaction in both *pSMB::Cas9*PGM* and *pSMB::Cas9*ADG1* lines compared to wild-type plants. The high-resolution experiments conducted on the microscope revealed that the insertional *pgm* mutants had diminished gravitropic reactions. When the last timepoints of gravitropism test data were statistically analyzed with non-parametric t-tests, *pgm* mutants showed a non-significant tendency (p - 0,063). When it comes to CRISPR/Cas9 generated mutants, the differences in gravitropic reactions of lines *pSMB::Cas9*PGM* and *pSMB::Cas9*ADG1* were deemed non-significant (*pSMB::Cas9*PGM* – p - 0,78 and *pSMB::Cas9*ADG1* – p - 0,81) – boxplots in Figure 37. Although the non-parametric t-test did not show significant differences between wild-type plants and the tissue-specific mutant gravitropism, a high degree of variance between the bending angles of individual *pSMB::Cas9*PGM* plants can be observed. The results of gravistimulation experiments can be found in the graphs and boxplots on the next pages - Figure 36 and Figure 37.

Only *pgm* and CRISPR/Cas9 generated mutants are compared to wild-type plants, as we have been unable to germinate seeds of *adg1* mutants.

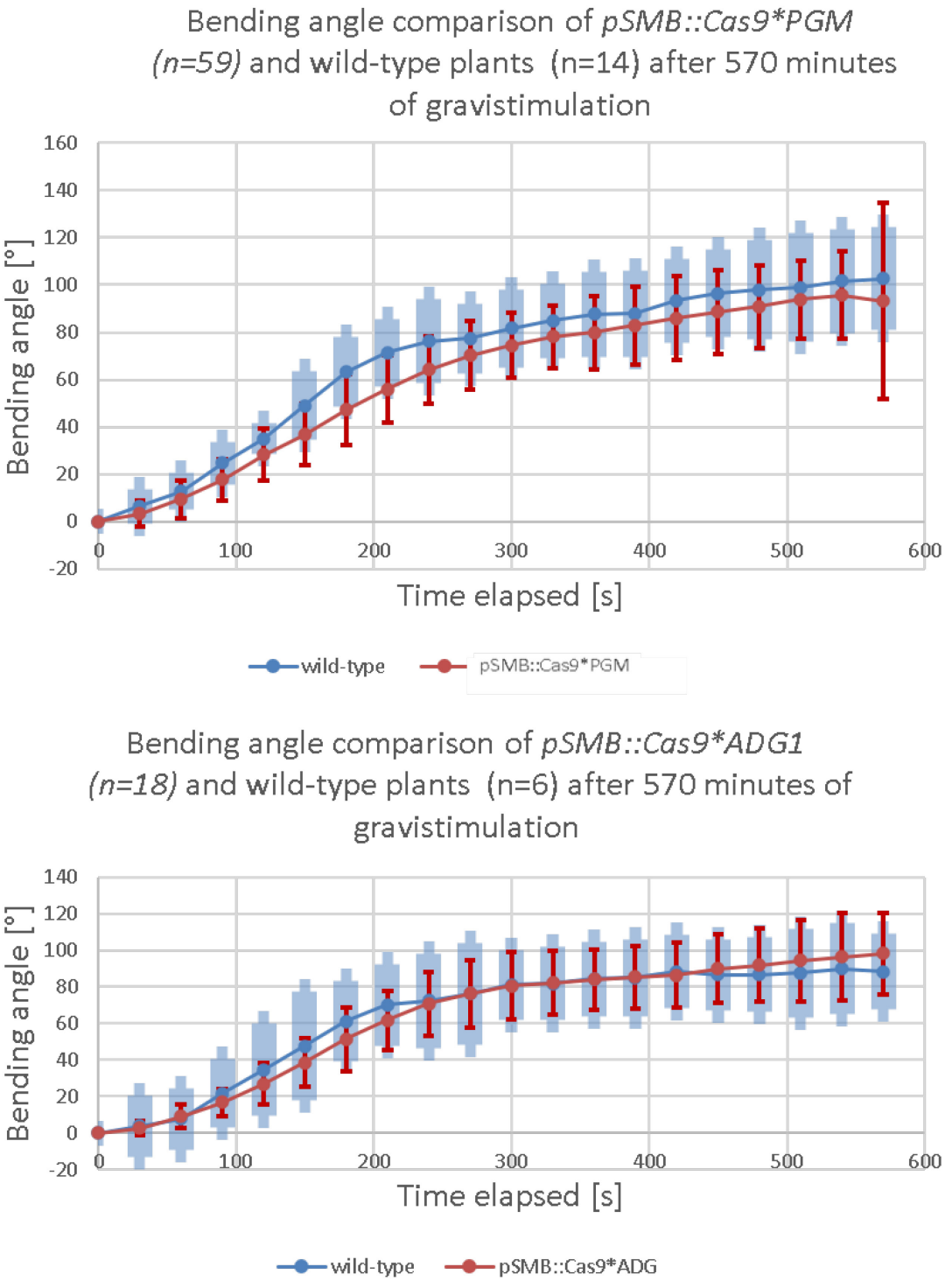

Figure 36 - Graphs of bending angle comparisons of *pSMB::Cas9*PGM and pSMB::Cas9*ADG1* lines in low temporal resolution with data from the scanner.

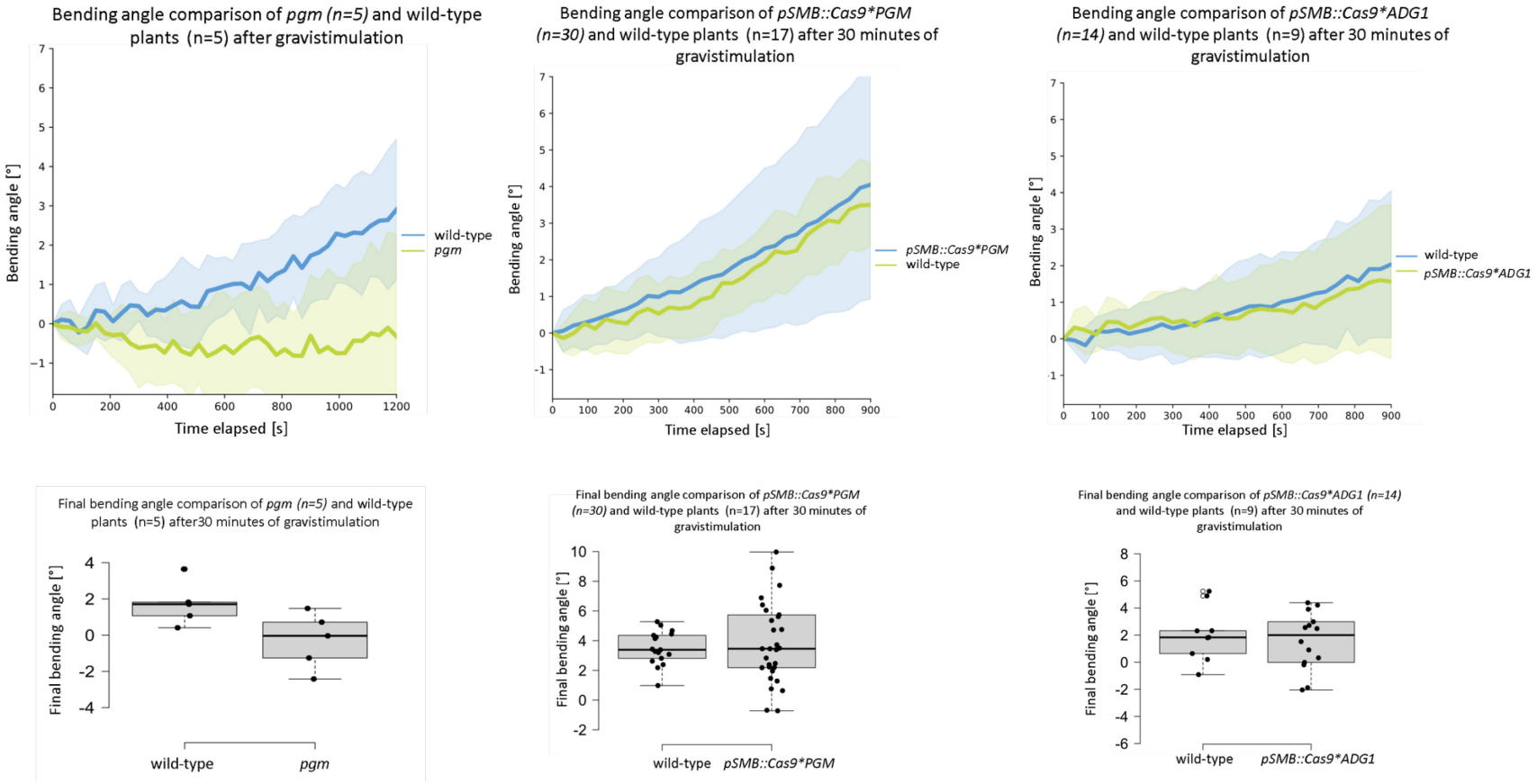

Figure 37 - Graphs of bending angle comparisons of tissue-specific lines in high temporal resolution with data from the microscope. The final bending angle was tested, using a non-parametric t-test resulting in the following p- values *pgm* – p= 0,063*; pgm, pSMB::Cas9*PGM* – p= 0,78; *pSMB::Cas9*ADG1* – p= 0,81.

6.7 Future experiments

The results of gravitropic experiments require further experimentation to provide clear results that might lead to the confirmation or rejection of the hypothesis on statolith role in plant gravitropism. First of all, to be able to correctly make a comparison of insertion and tissue-specific lines, a homozygous mutant line must be generated. Following this, a generation of at least one homozygous T3 or T4 line from all the different CRISPR/Cas9 generated lines must also be produced, if possible - the mutation could be lethal.

Once the homozygous lines are obtained, the localization of mCherry fluorescence should be investigated to confirm the tissue specific expression of the transgenic system. This should be done in the whole plant, not just the primary root. If the homozygous line generation is successful and the mCherry protein localizes correctly, the DNA of mutant root tips should be extracted and verified whether the predicted deletions occur. The off-target sites of gRNAs should also be sequenced to confirm that the phenotype is not a result of other, unintended mutations.

After mutation specificity is confirmed, a verification of root tip starch synthesis via Lugol solution staining should be carried out and compared with the *adg1* and *pgm* mutants, as well as wild-type plants. Following this, starch presence in other tissues should be investigated, as well as both the high- and low-resolution gravitropism experiments are to be performed. These will provide the means to compare and evaluate the magnitude of the response to gravistimulation of homozygous transgenic lines. This could provide insight, whether statoliths play as big of a role in plant gravitropism as previously believed, or starch itself is the key component in understanding plant gravity sensing.

Other future experiments could include observation and comparison of secondary and higher degree root formation and gravistimulation response, hormonal complementation of possible agravitropic phenotype, testing of root phototropism if the phenotype would be agravitropic in the *pSMB::Cas9*PGM* and/or *pSMB::Cas9*ADG1* mutants.

In the case that the adapted CRISPR/Cas9 system fails to produce tissue-specific mutants with high mutation rates and low chimerism even after a homozygous line is attained, experiments with different gRNAs and/or promoters could provide the means to achieve the desired results.

7. Discussion

As to our knowledge, this is the first work, where statolith starch was specifically targeted to exclude any possible effects of starch deficiency in the rest of the plant on root gravitropic bending. This distinct feature was achieved by the modification of a new CRISPR/Cas9 system combining approaches from (Xie, Minkenberg and Yang, 2015) and (Decaestecker *et al.*, 2019).

7.1 Adaptation of the TSKO and gRNA polycistronic system for use with GoldenBraid

The first goal of this diploma thesis was to adapt the tissue-specific knockout system along with the use of polycistronic gRNA for GoldenBraid system cloning. The final design is based on the TSKO system of (Decaestecker *et al.*, 2019) serving as a backbone, combined with the polycistronic gRNA expression designed by (Xie, Minkenberg and Yang, 2015) with the GoldenBraid modular system of (Sarrion-Perdigones *et al.*, 2011). Thanks to this, the system can be fully modified to the needs of the user by changing parts of the system with ease, using enzymes for GoldenBraid cloning (Sarrion-Perdigones *et al.*, 2011).

This design led to successful constructions of multiple omega vectors. Using these vectors, we were able to transform *A. thaliana* plants and generate mutants – both tissue-specific and non-specific. This allows for studies of tissue-specific mutations that would prove fatal if induced in the whole plant or could provide insight into protein function in different tissues.

Compared to the original TSKO system (Decaestecker *et al.*, 2019), the adapted system enables multiple targeted DNA double-strand breaks in specific tissues thanks to the polycistronic gRNA gene. Multiple genes can be targeted due to the generation of multiple gRNAs (Xie, Minkenberg and Yang, 2015), compared to the one or two inserted gRNAs from the original TSKO system.

7.2 *Arabidopsis* transformation and creation of CRISPR/Cas9 mutants

In order to insert the successfully constructed Omega vectors into wild-type plants, the transformation of *Agrobacterium tumefaciens*, its multiplication and the subsequent floral dip of Col-0 plants was carried out. This floral dip proved to be successful as transformed plant flowers produced seeds that were either Basta resistant (tissue-specific mutants) or contained mCherry (tissue non-specific mutants). The T1 generation plants produced a reduced number of seeds, resulting in a lower number of available T2 generation plants for experiments. As this happened with tissue-specific mutants (as none of the non-specific mutants were in cultivation) and none of the CRISPR/Cas9 targeted genes are listed as affecting seed yield in comparative studies

conducted on *Arabidopsis* (Van Daele *et al.*, 2012), we hypothesize that this was caused by external factors. This hypothesis is supported by the fact, that during the cultivation of the T1 generation plants, a drought period caused by a malfunction of the cultivation room (effect on seed yield known from experiments on *Brassica napus* (Hatzig *et al.*, 2018)), followed by an infestation of fungus gnats (*Sciaridae*) took place. We cannot rule out the possibility that this was caused by our CRISPR/Cas9 system, as we do possess data that would confirm or deny this hypothesis.

7.3 Tissue-specificity of the adapted CRISPR/Cas9 system

The plants that passed the selection process had to have the specificity of Cas9 expression sites confirmed. This was done visually by the observation of root tip localized mCherry fluorescence in tissue-specific mutants. Cas9 and mCherry were expected to be expressed in the root cap of tissue-specific mutants due to the specific expression of the SMB promoter in the root tip (Willemsen *et al.*, 2008). The inspection of the selected plants confirmed this presumed localization. Except for the columella tissue, mCherry fluorescence was also present in the lateral root cap, however, this expression localization had no other observed effects in *pSMB::Cas9*ADG1* and *pSMB::Cas9*PGM* mutants, due to the lack of starch granules in the tissue.

Undoubtedly, the specificity of the Cas9 expression in our tissue-specific mutants will have to be verified by fluorescence microscopy of whole plants, not only the root itself. In addition to this, genotyping the target gene in the whole plant except the root tip could further aid the investigation of the adapted CRISPR/Cas9 system tissue-specificity.

7.4 Mutagenesis caused by the adapted CRISPR/Cas9 system in lines *pSMB::Cas9*GFP*, *pSMB::Cas9*ADG1* and *pSMB::Cas9*PGM*

Other than Cas9 localization, the effects of Cas9-induced mutagenesis by double-strand breaks were also investigated. The expression and activity of Cas9 were expected to cause a diminished presence of GFP in the line *pSMB::Cas9*GFP* (Figure 30), as demonstrated with the original TSKO system (Decaestecker *et al.*, 2019). Nevertheless, we did not carry out enough observation repetitions to be able to verify the functionality of our system in *pSMB::Cas9*GFP* mutants with certainty.

The T1 and T2 generations of the remaining tissue-specific mutants - *pSMB::Cas9*PGM* and *pSMB::Cas9*ADG1* showed predominantly chimeric phenotypes and some normal starch

accumulation in the roots, unlike in the case of (Decaestecker *et al.*, 2019) where the majority of pSMB expressed Cas9 tissue-specific T1 mutants showed loss of target protein expression and some were chimeric. Currently, Cas9 generated chimeric phenotypes present a challenge that is not limited only to the TSKO system (Jang *et al.*, 2016; Charrier *et al.*, 2019). Because mutations caused by the repair of DNA double-strand breaks are non-random and are usually short insertions or deletions (Allen *et al.*, 2019; Decaestecker *et al.*, 2019; Zhang *et al.*, 2020), it is likely that the observed low effect on phenotypes of individual mutant lines, as well as the differences in their occurrence rates, are gRNA sequence dependent. We hypothesize that the high rate of chimeric phenotypes could be shifted to a more uniform mutant phenotype by changing the gRNA sequences used.

7.5 Mutagenesis caused by the adapted CRISPR/Cas9 system in the line *pUBI10::Cas9*AT5G14240*

The adapted system was also used to produce mutations in the AT5G14240 gene that were not specific to a tissue. The approach has proven to be functional with several T1 plants containing mutations confirmed both by sequencing and PCR.

The *pUBI10::Cas9*AT5G14240* plants display a strong mutant phenotype. These plants are visibly impaired, having phenotypes of restricted growth, restricted growth of the primary root and strongly waving primary roots. The sequencing results suggest that mutants are chimeric, just like the tissue-specific mutants. Due to the non-specificity of affected tissues, this issue should be resolved by the T2 generation plants, where each line should have only 1 type of cell as they would contain the mutations carried by the gametes. Selection for non-glowing seeds would provide a means to select plants that are not expressing Cas9. The selected plants would then not generate mutations *de novo*, as is typical for the TSKO system (Decaestecker *et al.*, 2019). Although this would resolve the issue of chimeric plants, the mutants themselves would be most likely heterozygous and in need of at least one further generation to be homozygous with no chimerism. To reduce the chimerism of the T1 generation plants with targets without tissue specificity, a regeneration step could be added as in the case of (Malabarba *et al.*, 2021).

The mutagenesis caused by Cas9 throughout the whole plant was attained by using the *UBI10* promoter, in contrast to the tissue-specific *SMB* promoter. Although the Egg cell-specific *EC1.2* and Cauliflower Mosaic Virus 35S promoter are commonly used promoters for transgene expression that is active in most tissues (Sunilkumar *et al.*, 2002; Wang *et al.*, 2015), we have decided on the use of the *UBI10* promoter. The reasoning behind this decision is that *UBI10* was

found to be more effective in *Arabidopsis* compared to *35S* (Castel *et al.*, 2019; Wolabu *et al.*, 2020) and *EC1.2* use resulted in lower (Wolabu *et al.*, 2020) or in some cases only slightly increased mutation rates compared to *UBI10* (Castel *et al.*, 2019).

7.6 Comparison of responses to the vector of gravity in wild-type plants, *pgm* insertion mutants and tissue-specific CRISPR induced *pgm* and *adg1* mutants

There have been multiple works that both support and dismiss the role of statoliths in plant gravitropism (Vitha, Zhao and Sack, 2000; Fitzelle and Kiss, 2001; Bai and Wolverton, 2011; Edelmann, 2018). These studies measured changes in root bending angle periodically in intervals upwards of 20 minutes. A temporal resolution like this is not sufficient, as pH changes of root cap apoplast occur within 2 minutes after gravistimulation and by 10 minutes growth-related pH changes are detectable in the cell walls of the elongation zone (Fasano *et al.*, 2001). Redistribution of auxin also occurs within 5 minutes after gravistimulation in the root tip (Band *et al.*, 2012). Because of these rapid changes, we have decided to perform high-resolution experiments on gravitropism in addition to the low-resolution ones. The results of high-resolution experiments suggest that *pgm* insertional mutants might have reduced sensitivity to gravity (p=0,063). This trend of reduced sensitivity starts to appear within those 20 minutes after gravistimulation, confirming a need for the high temporal resolution used. This is further supported by the statolith sedimentation time, which occurs about 3.5 minutes after 90° reorientation (Leitz, Kang and Schoenwaelder, 2009).

The very nature of the high-resolution experiment might have influenced the obtained data as the stage of the microscope moved every 30 seconds. This in turn may have influenced the wild-type plants, under the assumption that the *pgm* mutants would be insensitive to this movement as they lack starch. Considering this fact, further testing with bigger time windows between stage movements is required. An additional influence on the significance of our results could be the fact, that these mutants do not lack starch completely, as noted by (Harrison, Hedley and Wang, 1998).

As of *pSMB::Cas9*PGM* and *pSMB::Cas9*ADG1*, our experiments show no significant differences from wild-type plants. Nonetheless, the differences between individual mutant plants used for high-resolution experiments appear to be substantial, both in their starch content and their response to gravity. The low-resolution experiments seem to indicate a slower rate of root bending after a ± 65° change has been attained. To confirm this, further measurements and analysis are needed, however, this would correspond with the rapid reduction of auxin asymmetry observer by (Band *et al.*, 2012). These results probably arose from the chimeric nature of Cas9 generated

tissue-specific mutants. To maximize the exactness of our research data, we suggest separating plants according to their fluorescence and statolith content, preferably measuring the response of plants with no visible statoliths. Due to large differences between individual plants and their responses, we cannot unambiguously interpret the results of experiments done on the lines *pSMB::Cas9*PGM* and *pSMB::Cas9*ADG1*.

From our point of view, the available literature as well as the results of our experiments, as inconclusive as they may be, suggest that starch in statoliths plays a crucial role in graviperception and the following formation of auxin gradient in the roots.

7.7 Work limitations

The experiments carried out in this thesis have several limitations, influencing the scope and quality. The first limitation – the number of available seeds arose most probably from technical difficulties and pests in the grow rooms, limiting some plant lines and excluding them from gravitropic experiments.

The gravitropic experiments, especially the high-resolution ones, are limited by the capacity of the containers used to hold the plants, as well as the time it takes to conduct them. The chamber used for the gravity-sensing experiments on the microscope can hold a maximum of about 8 plants at a time, limiting the number of specimens that can be analysed at a given time window. The experiment also cannot be carried out completely without the influence of the stage movement as the microscope would be able only to capture one plant.

Furthermore, the chimeric nature of the tissue-specific mutant plants strongly influences their phenotype, resulting in a wide range of behaviour. This could be lessened by selection based on either fluorescence or statolith content, however, it cannot be fully negated as far as we are aware.

7.8 Summary

In conclusion, tissue non-specific and specific mutants were generated by adapting and using CRISPR/Cas9 technology. These have been confirmed by the observation of phenotypes, as well as sequencing of the tissue non-specific mutants. The T1 generation of both of the mutant types has proven to be chimeric. The insertional *pgm* mutants show a nearly-significant response difference to the gravity vector compared to the wild-type plants, however, their CRISPR/Cas9 tissue-specific variant did not show this difference, most probably due to its chimerism. Future steps should include sorting the tissue-specific mutants by fluorescence levels and/or statolith

content to limit the influence of differing degrees of starch content. As for the non-specific mutants, homozygous mutants need to be obtained to determine the mutant phenotype and possible gene function.

8. Conclusion and future perspectives

The primary aims of this thesis were to adopt and utilize a modular CRISPR-Cas9 TSKO system to study the effects of diminished starch levels in the root tip on gravity perception.

With this goal in mind, this system was created and adopted for use with the GoldenBraid cloning system. The designed TSKO system works as intended as can be seen from both the sequencing of tissue non-specific mutants and the phenotype of the tissue-specific mutants. As we have observed, the expression of Cas9 under the promoter SMB is localized to the root tip as predicted. The DNA of the tissues was not sequenced and should be done in future experiments to confirm the effects of localized Cas9 expression and whether they align with our predictions. Despite this, we consider the GoldenBraid adaptation of the TSKO system with the use of gRNA polycistron a success The effects of Cas9 on the DNA are not inherited by progenitors of the mother plant in the tissue-specific mutants and need to be re-induced by Cas9. As a consequence, the resulting phenotype is chimeric. We theorize, that the effect of Cas9 could be strengthened by attaining homozygosity from the perspective of our insert.

The second generation of transformants was used for gravity response experiments as well as determining the number of insertions in the parent plants. The gravity perception experiments did not yield any significant results however, some differences may be observed in the graphs. Regardless of our insignificant outcome in gravity sensing of CRISPR/Cas9 induced *pgm* and *adg1* mutants, we recommend carrying out the same experiments in further generations, especially those that have become homozygous in our insert. This suggestion is based on the significant difference of *pgm* insertion mutants compared to Col plants as well as the theorised effect mentioned above.

Further experiments are recommended to determine the importance of starch granules on gravity perception, including observation of gravity vector perception of homozygous insert lines in their roots, observation and comparison of secondary and higher degree root formation and gravistimulation response, hormonal complementation and other experiments depending on the outcome of the previous ones.

Ultimately, this diploma thesis resulted in the adoption of a valuable tool for genetic manipulation into a specific cloning system with the option to target multiple genes as well as specify the target tissue and tried to shed some light on the significance of statoliths for root gravity perception.

9. Bibliography

Addgene - pGTR plasmid sequence (Accessed 08.07.2021). Available at: https://www.addgene.org/63143/sequences/.

Addgene - pU6-1 (GB1204) (Accessed 13.04.2021). Available at: https://www.addgene.org/75405/.

Addgene - pUPD2 (Accessed 04.07.2021). Available at: https://www.addgene.org/68161.

Allen, F. *et al.* (2019) 'Predicting the mutations generated by repair of Cas9-induced double-strand breaks', *Nature Biotechnology*, 37(1), pp. 64–82. doi: 10.1038/nbt.4317.

Ashraf, A. *et al.* (2019) 'Evolution of Deeper Rooting 1-like homoeologs in wheat entails the C-terminus mutations as well as gain and loss of auxin response elements', *PLoS ONE*, 14(4), p. e0214145. doi: 10.1371/journal.pone.0214145.

Bai, H. and Wolverton, C. (2011) 'Gravitropism in lateral roots of *Arabidopsis* pgm-1 mutants is indistinguishable from that of wild-type', *Plant Signaling and Behavior*, 6(10), pp. 1423–1424. doi: 10.4161/psb.6.10.16963.

Band, L. R. *et al.* (2012) 'Root gravitropism is regulated by a transient lateral auxin gradient controlled by a tipping-point mechanism', *Proceedings of the National Academy of Sciences of the United States of America*, 109(12), pp. 4668–4673. doi: 10.1073/pnas.1201498109.

Barbezier, N. *et al.* (2009) 'Processing of a dicistronic tRNA-snoRNA precursor: Combined analysis in vitro and in vivo reveals alternate pathways and coupling to assembly of snoRNP', *Plant Physiology*, 150(3), pp. 1598–1610. doi: 10.1104/pp.109.137968.

Barlow, P. W. (1974) 'Recovery of geotropism after removal of the root cap', *Journal of Experimental Botany*, 25(6), pp. 1137–1146. doi: 10.1093/jxb/25.6.1137.

Barlow, P. W. and Rathfelder, E. L. (1985) 'Distribution and redistribution of extension growth along vertical and horizontal gravireacting maize roots', *Planta*, 165(1), pp. 134–141. doi: 10.1007/BF00392222.

Barrangou, R. *et al.* (2007) 'CRISPR provides acquired resistance against viruses in prokaryotes', *Science*, 315(5819), pp. 1709–1712. doi: 10.1126/science.1138140.

Bates, G. W. and Goldsmith, M. H. M. (1983) ‘Rapid response of the plasma-membrane potential in oat coleoptiles to auxin and other weak acids’, *Planta*, 159(3), pp. 231–237. doi: 10.1007/BF00397530.

Bennett, T. *et al.* (2010) ‘SOMBRERO, BEARSKIN1, and BEARSKIN2 regulate root cap maturation in *Arabidopsis’*, *Plant Cell*, 22(3), pp. 640–654. doi: 10.1105/tpc.109.072272.

Bérut, A. *et al.* (2018) ‘Gravisensors in plant cells behave like an active granular liquid’, *Proceedings of the National Academy of Sciences of the United States of America*. 2018/04/30. National Academy of Sciences, 115(20), pp. 5123–5128. doi: 10.1073/pnas.1801895115.

BioInfo (2016) *Crispr-P 2.0*, *National Key Laboratory of Crop Genetic Improvement and Center for Bioinformatics*. Available at: http://crispr.hzau.edu.cn/cgi-bin/CRISPR2/CRISPR.

Birnbaum, K. *et al.* (2003) ‘A Gene Expression Map of the *Arabidopsis* Root’, *Science*, 302(5652), pp. 1956–1960. doi: 10.1126/science.1090022.

Björkman, T. (1992) ‘Perception of gravity by plants’, *Advances in Space Research*, 12(1), pp. 195–201. doi: 10.1016/0273-1177(92)90283-4.

Blancaflor, E. B., Fasano, J. M. and Gilroy, S. (1998) ‘Mapping the functional roles of cap cells in the response of *Arabidopsis* primary roots to gravity’, *Plant Physiology*, 116(1), pp. 213–222. doi: 10.1104/pp.116.1.213.

Blancaflor, E. B. and Masson, P. H. (2003) ‘Plant Gravitropism. Unraveling the Ups and Downs of a Complex Process’, *Plant Physiology*, 133(4), pp. 1677–1690. doi: 10.1104/pp.103.032169.

Bolotin, A. *et al.* (2005) ‘Clustered regularly interspaced short palindrome repeats (CRISPRs) have spacers of extrachromosomal origin’, *Microbiology*, 151(8), pp. 2551–2561. doi: 10.1099/mic.0.28048-0.

Boonsirichai, K. *et al.* (2003) ‘Altered Response to Gravity Is a Peripheral Membrane Protein That Modulates Gravity-Induced Cytoplasmic Alkalinization and Lateral Auxin Transport in Plant Statocytes’, *Plant Cell*, 15(11), pp. 2612–2625. doi: 10.1105/tpc.015560.

Boutté, Y., Ikeda, Y. and Grebe, M. (2007) ‘Mechanisms of auxin-dependent cell and tissue polarity’, *Current Opinion in Plant Biology*, 10(6), pp. 616–623. doi: 10.1016/j.pbi.2007.07.008.

Brady, S. M. *et al.* (2007) 'A high-resolution root spatiotemporal map reveals dominant expression patterns', *Science*, 318(5851), pp. 801–806. doi: 10.1126/science.1146265.

Braun, M. and Limbach, C. (2006) 'Rhizoids and protonemata of characean algae: Model cells for research on polarized growth and plant gravity sensing', *Protoplasma*, 229(2–4), pp. 133–142. doi: 10.1007/s00709-006-0208-9.

Brauner, K. *et al.* (2014) 'Exaggerated root respiration accounts for growth retardation in a starchless mutant of *Arabidopsis thaliana'*, *Plant Journal*, 79(1), pp. 82–91. doi: 10.1111/tpj.12555.

Breyne, P. *et al.* (1992) 'Characterization of a plant scaffold attachment region in a DNA fragment that normalizes transgene expression in tobacco', *Plant Cell*, 4(4), pp. 463–471. doi: 10.1105/tpc.4.4.463.

Briggs, G. C., Mouchel, C. F. and Hardtke, C. S. (2006) 'Characterization of the plant-specific BREVIS RADIX gene family reveals limited genetic redundancy despite high sequence conservation', *Plant Physiology*, 140(4), pp. 1306–1316. doi: 10.1104/pp.105.075382.

Brumos, J., Alonso, J. M. and Stepanova, A. N. (2014) 'Genetic aspects of auxin biosynthesis and its regulation', *Physiologia Plantarum*, 151(1), pp. 3–12. doi: 10.1111/ppl.12098.

Canino, G. *et al.* (2009) '*Arabidopsis* encodes four tRNase Z enzymes', *Plant Physiology*, 150(3), pp. 1494–1502. doi: 10.1104/pp.109.137950.

Caspar, T., Huber, S. C. and Somerville, C. (1985) ' Alterations in Growth, Photosynthesis, and Respiration in a Starchless Mutant of *Arabidopsis thaliana* (L.) Deficient in Chloroplast Phosphoglucomutase Activity ', *Plant Physiology*, 79(1), pp. 11–17. doi: 10.1104/pp.79.1.11.

Castel, B. *et al.* (2019) 'Optimization of T-DNA architecture for Cas9-mediated mutagenesis in *Arabidopsis'*, *PLoS ONE*, 14(1), p. e0204778. doi: 10.1371/journal.pone.0204778.

Charrier, A. *et al.* (2019) 'Efficient targeted mutagenesis in apple and first time edition of pear using the CRISPR-Cas9 system', *Frontiers in Plant Science*, 10, p. 40. doi: 10.3389/fpls.2019.00040.

Chauvet, H. *et al.* (2016) 'Inclination not force is sensed by plants during shoot gravitropism', *Scientific Reports*, 6, p. 35431. doi: 10.1038/srep35431.

Cholodny, N. (1927) ‘Wuchshormone und Tropismen bei den Pflanzen.’, *Biologisches Zentralblatt*, 475(1), pp. 604–629. Available at: http://ci.nii.ac.jp/naid/10007185046/en/ (Accessed: 19 July 2021).

Clavauda, C. *et al.* (2017) ‘Revealing the frictional transition in shear-thickening suspensions’, *Proceedings of the National Academy of Sciences of the United States of America*, 114(20), pp. 5147–5152. doi: 10.1073/pnas.1703926114.

Clough, S. J. and Bent, A. F. (1998) ‘Floral dip: A simplified method for Agrobacterium-mediated transformation of *Arabidopsis thaliana*’, *Plant Journal*, 16(6), pp. 735–743. doi: 10.1046/j.1365-313X.1998.00343.x.

Correa-Aragunde, N. *et al.* (2016) ‘The Auxin-Nitric Oxide Highway: A Right Direction in Determining the Plant Root System’, in, pp. 117–136. doi: 10.1007/978-3-319-40713-5_6.

Courrech du Pont, S. *et al.* (2003) ‘Granular Avalanches in Fluids’, *Physical Review Letters*, 90(4), p. 4. doi: 10.1103/PhysRevLett.90.044301.

Cribbs, A. P. and Perera, S. M. W. (2017) ‘Science and bioethics of CRISPR-CAS9 gene editing: An analysis towards separating facts and fiction’, *Yale Journal of Biology and Medicine*, 90(4), pp. 625–634.

Van Daele, I. *et al.* (2012) ‘A comparative study of seed yield parameters in *Arabidopsis thaliana* mutants and transgenics’, *Plant Biotechnology Journal*, 10(4), pp. 488–500. doi: 10.1111/j.1467-7652.2012.00687.x.

Darwin, C. (2014) *The origin of species by means of natural selection, or, The preservation of favoured races in the struggle for life.*, *The origin of species by means of natural selection, or, The preservation of favoured races in the struggle for life* London : John Murray, 1859. doi: 10.5962/bhl.title.87916.

Darwin, C. and Darwin, F. (2009) *The power of movement in plants*, *The Power of Movement in Plants*. London :John Murray,. doi: 10.1017/CBO9780511693670.

Decaestecker, W. *et al.* (2019) ‘CRISPR-Tsko: A technique for efficient mutagenesis in specific cell types, tissues, or organs in *Arabidopsis’*, *Plant Cell*, 31(12), pp. 2868–2887. doi: 10.1105/tpc.19.00454.

Dharmasiri, N., Dharmasiri, S. and Estelle, M. (2005) 'The F-box protein TIR1 is an auxin receptor', *Nature*, 435(7041), pp. 441–445. doi: 10.1038/nature03543.

Dhonukshe, P. *et al.* (2007) 'Clathrin-Mediated Constitutive Endocytosis of PIN Auxin Efflux Carriers in *Arabidopsis'*, *Current Biology*, 17(6), pp. 520–527. doi: 10.1016/j.cub.2007.01.052.

Dindas, J. *et al.* (2018) 'AUX1-mediated root hair auxin influx governs SCFTIR1/AFB-type Ca2+ signaling', *Nature Communications*, 9(1), p. 1174. doi: 10.1038/s41467-018-03582-5.

Dindas, J. *et al.* (2020) 'Pitfalls in auxin pharmacology', *New Phytologist*, 227(2), pp. 286–292. doi: 10.1111/nph.16491.

Dolan, L. *et al.* (1993) 'Cellular organisation of the *Arabidopsis thaliana* root', *Development*, 119(1), pp. 71–84. doi: 10.1242/dev.119.1.71.

Dubey, S. M. *et al.* (2021) 'No time for transcription—rapid Auxin responses in plants', *Cold Spring Harbor Perspectives in Medicine*, 11(7), p. a039891. doi: 10.1101/cshperspect.a039891.

Edelmann, H. G. (2018) 'Graviperception in maize plants: is amyloplast sedimentation a red herring?', *Protoplasma*, 255(6), pp. 1877–1881. doi: 10.1007/s00709-018-1272-7.

Engelsdorf, T. *et al.* (2013) 'Reduced carbohydrate availability enhances the susceptibility of *Arabidopsis* toward Colletotrichum higginsianum', *Plant Physiology*, 162(1), pp. 225–238. doi: 10.1104/pp.112.209676.

Engelsdorf, T. *et al.* (2017) 'Cell wall composition and penetration resistance against the fungal pathogen Colletotrichum higginsianum are affected by impaired starch turnover in *Arabidopsis* mutants', *Journal of Experimental Botany*, 68(3), pp. 701–713. doi: 10.1093/jxb/erw434.

Engler, C., Kandzia, R. and Marillonnet, S. (2008) 'A one pot, one step, precision cloning method with high throughput capability', *PLoS ONE*, 3(11), p. e3647. doi: 10.1371/journal.pone.0003647.

Fasano, J. M. *et al.* (2001) 'Changes in root cap pH are required for the gravity response of the *Arabidopsis* root', *Plant Cell*, 13(4), pp. 907–921. doi: 10.1105/tpc.13.4.907.

Felle, H., Peters, W. and Palme, K. (1991) 'The electrical response of maize to auxins', *BBA - Biomembranes*, 1064(2), pp. 199–204. doi: 10.1016/0005-2736(91)90302-O.

Fendrych, M. *et al.* (2018) ‘Rapid and reversible root growth inhibition by TIR1 auxin signalling’, *Nature Plants*, 4(7), pp. 453–459. doi: 10.1038/s41477-018-0190-1.

Firn, R. and Digby, J. (1977) ‘The Role of the Peripheral Cell Layers in the Geotropic Curvature of Sunflower Hypocotyls: a New Model of Shoot Geotropism’, *Functional Plant Biology*, 4(3), p. 337. doi: 10.1071/pp9770337.

Fitzelle, K. J. and Kiss, J. Z. (2001) Restoration of gravitropic sensitivity in starch-deficient mutants of *Arabidopsis* by hypergravity, *Journal of Experimental Botany*. doi: 10.1093/jxb/52.355.265.

Friml, Jiří *et al.* (2002) ‘AtPIN4 mediates sink-driven auxin gradients and root patterning in *Arabidopsis*’, *Cell*, 108(5), pp. 661–673. doi: 10.1016/S0092-8674(02)00656-6.

Friml, Jlří *et al.* (2002) ‘Lateral relocation of auxin efflux regulator PIN3 mediates tropism in *Arabidopsis*’, *Nature*, 415(6873), pp. 806–809. doi: 10.1038/415806a.

Friml, J. *et al.* (2003) ‘Efflux-dependent auxin gradients establish the apical-basal axis of *Arabidopsis’*, *Nature*, 426(6963), pp. 147–153. doi: 10.1038/nature02085.

Furutani, M. *et al.* (2020) ‘Polar recruitment of RLD by LAZY1-like protein during gravity signaling in root branch angle control’, *Nature Communications*, 11(1), p. 76. doi: 10.1038/s41467-019-13729-7.

Gälweiler, L. *et al.* (1998) ‘Regulation of polar auxin transport by AtPIN1 in *Arabidopsis* vascular tissue’, *Science*, 282(5397), pp. 2226–2230. doi: 10.1126/science.282.5397.2226.

Garneau, J. E. *et al.* (2010) ‘The CRISPR/cas bacterial immune system cleaves bacteriophage and plasmid DNA’, *Nature*, 468(7320), pp. 67–71. doi: 10.1038/nature09523.

Ge, L. and Chen, R. (2016) ‘Negative gravitropism in plant roots’, *Nature Plants*, 2(11), p. 16155. doi: 10.1038/nplants.2016.155.

Ge, L. and Chen, R. (2019) ‘Negative gravitropic response of roots directs auxin flow to control root gravitropism’, *Plant Cell and Environment*, 42(8), pp. 2372–2383. doi: 10.1111/pce.13559.

Geldner, N. *et al.* (2001) ‘Auxin transport inhibitors block PIN1 cycling and vesicle trafficking’, *Nature*, 413(6854), pp. 425–428. doi: 10.1038/35096571.

GoldenBraid domesticator (Accessed 10.04.2021). Available at: https://gbcloning.upv.es/do/domestication/.

Gray, W. M. *et al.* (2001) 'Auxin regulates SCFTIR1-dependent degradation of AUX/IAA proteins', *Nature*, 414(6861), pp. 271–276. doi: 10.1038/35104500.

Gupta, D. *et al.* (2019) 'CRISPR-Cas9 system: A new-fangled dawn in gene editing', *Life Sciences*, 232, p. 116636. doi: 10.1016/j.lfs.2019.116636.

Haberlandt, G. (1902) 'Über die Perception des geotropischen Reizes', *Ber.dt.bot.Ges*, 18(6), pp. 261–72. doi: https://doi.org/10.1111/j.1438-8677.1900.tb04908.x.

Harrison, C. J., Hedley, C. L. and Wang, T. L. (1998) 'Evidence that the rug3 locus of pea (Pisum sativum L.) encodes plastidial phosphoglucomutase confirms that the imported substrate for starch synthesis in pea amyloplasts is glucose-6-phosphate', *Plant Journa*, 13(6), pp. 753–762. doi: 10.1046/j.1365-313X.1998.00077.x.

Hatzig, S. V. *et al.* (2018) 'Drought stress has transgenerational effects on seeds and seedlings in winter oilseed rape (Brassica napus L.)', *BMC Plant Biology*, 18(1), p. 297. doi: 10.1186/s12870-018-1531-y.

Hayashi, K. I. *et al.* (2012) 'Rational design of an auxin antagonist of the SCF TIR1 auxin receptor complex', *ACS Chemical Biology*, 7(3), pp. 590–598. doi: 10.1021/cb200404c.

Hou, G. *et al.* (2004) 'The promotion of gravitropism in *Arabidopsis* roots upon actin disruption is coupled with the extended alkalinization of the columella cytoplasm and a persistent lateral auxin gradient', *Plant Journal*, 39(1), pp. 113–125. doi: 10.1111/j.1365-313X.2004.02114.x.

Iglesias, A. A. and Preiss, J. (1992) 'Bacterial glycogen and plant starch biosynthesis', *Biochemical Education*, 20(4), pp. 196–203. doi: 10.1016/0307-4412(92)90191-N.

Ingouff, M. *et al.* (2017) 'Live-cell analysis of DNA methylation during sexual reproduction in *Arabidopsis* reveals context and sex-specific dynamics controlled by noncanonical RdDM', *Genes and Development*, 31(1), pp. 72–83. doi: 10.1101/gad.289397.116.

Ishino, Y. *et al.* (1987) 'Nucleotide sequence of the iap gene, responsible for alkaline phosphatase isoenzyme conversion in Escherichia coli, and identification of the gene product', *Journal of Bacteriology*, 169(12), pp. 5429–5433. doi: 10.1128/jb.169.12.5429-5433.1987.

Ishino, Y., Krupovic, M. and Forterre, P. (2018) 'History of CRISPR-Cas from encounter with a mysterious repeated sequence to genome editing technology', *Journal of Bacteriology*, 200(7), p. JB.00580-17. doi: 10.1128/JB.00580-17.

Jang, G. *et al.* (2016) 'Genetic chimerism of CRISPR/Cas9-mediated rice mutants', *Plant Biotechnology Reports*, 10(6), pp. 425–435. doi: 10.1007/s11816-016-0414-7.

Jansen, R. *et al.* (2002) 'Identification of genes that are associated with DNA repeats in prokaryotes', *Molecular Microbiology*, 43(6), pp. 1565–1575. doi: 10.1046/j.1365-2958.2002.02839.x.

Jiang, K. *et al.* (2016) 'Salt stress affects the redox status of *Arabidopsis* root meristems', *Frontiers in Plant Science*, 7(FEB2016). doi: 10.3389/fpls.2016.00081.

Jinek, M. *et al.* (2012) 'A programmable dual-RNA-guided DNA endonuclease in adaptive bacterial immunity', *Science*, 337(6096), pp. 816–821. doi: 10.1126/science.1225829.

Jones, J. W. and Adair, C. R. (1938) 'A "lazy" mutation in rice', *Journal of Heredity*, 29(8), pp. 315–318. doi: 10.1093/oxfordjournals.jhered.a104527.

Kepinski, S. and Leyser, O. (2005) 'The *Arabidopsis* F-box protein TIR1 is an auxin receptor', *Nature*, 435(7041), pp. 446–451. doi: 10.1038/nature03542.

Kiss, J. Z., Wright, J. B. and Caspar, T. (1996) 'Gravitropism in roots of intermediate-starch mutants of *Arabidopsis'*, *Physiologia Plantarum*, 97(2), pp. 237–244. doi: 10.1034/j.1399-3054.1996.970205.x.

Kleine-Vehn, J. *et al.* (2010) 'Gravity-induced PIN transcytosis for polarization of auxin fluxes in gravity-sensing root cells', *Proceedings of the National Academy of Sciences of the United States of America*, 107(51), pp. 22344–22349. doi: 10.1073/pnas.1013145107.

Knight, T. A. (1806) 'V. On the direction of the radicle and germen during the vegetation of seeds. By Thomas Andrew Knight, Esq. F. R. S. In a letter to the Right Hon. Sir Joseph Banks, K. B. P. R. S', *Philosophical Transactions of the Royal Society of London*, 96, pp. 99–108. doi: 10.1098/rstl.1806.0006.

Křeček, P. *et al.* (2009) 'The PIN-FORMED (PIN) protein family of auxin transporters', *Genome Biology*, 10(12), p. 249. doi: 10.1186/gb-2009-10-12-249.

Leitz, G., Kang, B. H. and Schoenwaelder, M. E. A. (2009) 'Statolith sedimentation kinetics and force transduction to the cortical endoplasmic reticulum in gravity-sensing *Arabidopsis* columella cells', *Plant Cell*, 21(3), pp. 843–860. doi: 10.1105/tpc.108.065052.

Limbach, C. *et al.* (2005) 'How to activate a plant gravireceptor. Early mechanisms of gravity sensing studied in characean rhizoids during parabolic flights', *Plant Physiology*, 139(2), pp. 1030–1040. doi: 10.1104/pp.105.068106.

Lin, T.-P. *et al.* (1988) ' Isolation and Characterization of a Starchless Mutant of *Arabidopsis thaliana* (L.) Heynh Lacking ADPglucose Pyrophosphorylase Activity ', *Plant Physiology*, 86(4), pp. 1131–1135. doi: 10.1104/pp.86.4.1131.

Luschnig, C. *et al.* (1998) 'EIR1, a root-specific protein involved in auxin transport, is required for gravitropism in *Arabidopsis thaliana*', *Genes and Development*, 12(14), pp. 2175–2187. doi: 10.1101/gad.12.14.2175.

Makarova, K. S. *et al.* (2015) 'An updated evolutionary classification of CRISPR-Cas systems', *Nature Reviews Microbiology*, 13(11), pp. 722–736. doi: 10.1038/nrmicro3569.

Malabarba, J. *et al.* (2021) 'New strategies to overcome present CRISPR/CAS9 limitations in apple and pear: Efficient dechimerization and base editing', *International Journal of Molecular Sciences*, 22(1), pp. 1–20. doi: 10.3390/ijms22010319.

Marchant, A. *et al.* (1999) 'AUX1 regulates root gravitropism in *Arabidopsis* by facilitating auxin uptake within root apical tissues', *EMBO Journal*, Ltd, 18(8), pp. 2066–2073. doi: 10.1093/emboj/18.8.2066.

Marraffini, L. A. and Sontheimer, E. J. (2008) 'CRISPR interference limits horizontal gene transfer in staphylococci by targeting DNA', *Science*, 322(5909), pp. 1843–1845. doi: 10.1126/science.1165771.

Milo, R. *et al.* (2009) 'BioNumbers The database of key numbers in molecular and cell biology', *Nucleic Acids Research*, 38(SUPPL.1), pp. D750-3. doi: 10.1093/nar/gkp889.

Mix & Go protocol for TOP 10 E. coli from Zymo Research (Accessed 04.07.2021). Available at: https://files.zymoresearch.com/protocols/_t3001_t3002_mix_go_e._coli_transformation_kit_buffer_set.pdf.

Mojica, F. J. M. *et al.* (2005) 'Intervening sequences of regularly spaced prokaryotic repeats derive from foreign genetic elements', *Journal of Molecular Evolution*, 60(2), pp. 174–182. doi: 10.1007/s00239-004-0046-3.

Monshausen, G. B. *et al.* (2011) 'Dynamics of auxin-dependent Ca 2+ and pH signaling in root growth revealed by integrating high-resolution imaging with automated computer vision-based analysis', *Plant Journal*, 65(2), pp. 309–318. doi: 10.1111/j.1365-313X.2010.04423.x.

Müller, A. *et al.* (1998) 'AtPIN2 defines a locus of *Arabidopsis* for root gravitropism control', *EMBO Journal*, 17(23), pp. 6903–6911. doi: 10.1093/emboj/17.23.6903.

Müller, A., Hillebrand, H. and Weiler, E. W. (1998) 'Indole-3-acetic acid is synthesized from L-tryptophan in roots of *Arabidopsis thaliana*', *Planta*, 206(3), pp. 362–369. doi: 10.1007/s004250050411.

Nawy, T. *et al.* (2005) 'Transcriptional profile of the *Arabidopsis* root quiescent center', *Plant Cell*, 17(7), pp. 1908–1925. doi: 10.1105/tpc.105.031724.

Nazarian-Firouzabadi, F. and Visser, R. G. F. (2017) 'Potato starch synthases: Functions and relationships', *Biochemistry and Biophysics Reports*, 10, pp. 7–16. doi: 10.1016/j.bbrep.2017.02.004.

Němec, B. (1900) 'Über die Art der Wahrnehmung des Schwerkraftreizes bei den Pflanzen', *Ber. Dtsch. Bot. Ges*. John Wiley & Sons, Ltd, 18(6), pp. 241–245. doi: https://doi.org/10.1111/j.1438-8677.1900.tb04905.x.

Nishimasu, H. *et al.* (2014) 'Crystal structure of Cas9 in complex with guide RNA and target DNA', *Cell*, 156(5), pp. 935–949. doi: 10.1016/j.cell.2014.02.001.

Noh, B., Murphy, A. S. and Spalding, E. P. (2001) ' Multidrug Resistance –like Genes of *Arabidopsis* Required for Auxin Transport and Auxin-Mediated Development ', *The Plant Cell*, 13(11), pp. 2441–2454. doi: 10.1105/tpc.010350.

Okada, K. *et al.* (1991) 'Requirement of the Auxin Polar Transport System in Early Stages of *Arabidopsis* Floral Bud Formation.', *The Plant Cell*, 3(7), pp. 677–684. doi: 10.1105/tpc.3.7.677.

Overbeek, J. Van (1936) '"Lazy," an a-geotropic form of maize: " gravitational indifference" rather than structural weakness accounts for prostrate growth-habit of this form', *Journal of Heredity*, 27(3), pp. 93–96. doi: 10.1093/oxfordjournals.jhered.a104191.

Paponov, I. A. *et al.* (2019) 'Auxin-induced plasma membrane depolarization is regulated by AUXIN transport and not by AUXIN BINDING PROTEIN1', *Frontiers in Plant Science*. Frontiers Media S.A., 9, p. 1953. doi: 10.3389/fpls.2018.01953.

Perbal, G. (1999) 'Gravisensing in roots', *Advances in Space Research*, 24(6), pp. 723–729. doi: 10.1016/S0273-1177(99)00405-6.

Periappuram, C. *et al.* (2000) 'The plastidic phosphoglucomutase from *Arabidopsis*. A reversible enzyme reaction with an important role in metabolic control', *Plant Physiology*, 122(4), pp. 1193–1199. doi: 10.1104/pp.122.4.1193.

Petersen, K. *et al.* (2002) 'Matrix attachment regions (MARs) enhance transformation frequencies and reduce variance of transgene expression in barley', *Plant Molecular Biology*, 49(1), pp. 45–58. doi: 10.1023/A:1014464127973.

Petrášek, J. *et al.* (2006) 'PIN proteins perform a rate-limiting function in cellular auxin efflux', *Science*, 312(5775), pp. 914–918. doi: 10.1126/science.1123542.

Pickard, B. G. and Thimann, K. V. (1966) *Geotropic response of wheat coleoptiles in absence of amyloplast starch.*, *The Journal of general physiology*. doi: 10.1085/jgp.49.5.1065.

Pouliquen, O. *et al.* (2017) 'A new scenario for gravity detection in plants: The position sensor hypothesis', *Physical Biology*, 14(3), p. 35005. doi: 10.1088/1478-3975/aa6876.

Pourcel, C., Salvignol, G. and Vergnaud, G. (2005) 'CRISPR elements in Yersinia pestis acquire new repeats by preferential uptake of bacteriophage DNA, and provide additional tools for evolutionary studies', *Microbiology*, 151(3), pp. 653–663. doi: 10.1099/mic.0.27437-0.

Preiss, J. (1982) 'Biosynthesis of Starch and Its Regulation', in Loewus, F. A. and Tanner, W. (eds) *Plant Carbohydrates*, pp. 397–417. doi: 10.1007/978-3-642-68275-9_10.

Prigge, M. J. *et al.* (2020) 'Genetic analysis of the *Arabidopsis* TIR1/AFB auxin receptors reveals both overlapping and specialized functions', *eLife*, 9, p. e54740. doi: 10.7554/eLife.54740.

Qfix (2012) ‘Geneious Prime’, pp. 1–148. Available at: https://www.geneious.com.

Ramírez-Sánchez, O. *et al.* (2016) ‘Plant Proteins Are Smaller Because They Are Encoded by Fewer Exons than Animal Proteins’, *Genomics, Proteomics and Bioinformatics*, 14(6), pp. 357–370. doi: 10.1016/j.gpb.2016.06.003.

Ran, F. A. *et al.* (2013) ‘XDouble nicking by RNA-guided CRISPR cas9 for enhanced genome editing specificity’, *Cell*, 154(6), pp. 1380–1389. doi: 10.1016/j.cell.2013.08.021.

Retzer, K. *et al.* (2019) ‘Brassinosteroid signaling delimits root gravitropism via sorting of the *Arabidopsis* PIN2 auxin transporter’, *Nature Communications*, 10(1), p. 5516. doi: 10.1038/s41467-019-13543-1.

Richter, P., Strauch, S. M. and Lebert, M. (2019) ‘Disproval of the Starch-Amyloplast Hypothesis?’, *Trends in Plant Science*, 24(4), pp. 291–293. doi: 10.1016/j.tplants.2019.02.008.

Robert, H. S. and Offringa, R. (2008) ‘Regulation of auxin transport polarity by AGC kinases’, *Current Opinion in Plant Biology*, 11(5), pp. 495–502. doi: 10.1016/j.pbi.2008.06.004.

Ruegger, M. *et al.* (1998) ‘The TIR1 protein of *Arabidopsis* functions in auxin response and is related to human SKP2 and yeast Grr1p’, *Genes and Development*, 12(2), pp. 198–207. doi: 10.1101/gad.12.2.198.

Sabater, M. and Rubery, P. H. (1987) ‘Auxin carriers in Cucurbita vesicles - I. Imposed perturbations of transmembrane pH and electrical potential gradients characterised by radioactive probes’, *Planta*, 171(4), pp. 501–506. doi: 10.1007/BF00392298.

Sarrion-Perdigones, A. *et al.* (2011) ‘GoldenBraid: An iterative cloning system for standardized assembly of reusable genetic modules’, *PLoS ONE*, 6(7), p. e21622. doi: 10.1371/journal.pone.0021622.

Sarrion-Perdigones, A. *et al.* (2013) ‘Goldenbraid 2.0: A comprehensive DNA assembly framework for plant synthetic biology’, *Plant Physiology*, 162(3), pp. 1618–1631. doi: 10.1104/pp.113.217661.

Sato, E. M. *et al.* (2015) ‘New insights into root gravitropic signalling’, *Journal of Experimental Botany*, 66(8), pp. 2155–2165. doi: 10.1093/jxb/eru515.

Schindelin, J. *et al.* (2012) 'Fiji: An open-source platform for biological-image analysis', *Nature Methods*, 9(7), pp. 676–682. doi: 10.1038/nmeth.2019.

Senn, A. P. and Goldsmith, M. H. M. (1988) ' Regulation of Electrogenic Proton Pumping by Auxin and Fusicoccin as Related to the Growth of Avena Coleoptiles ', *Plant Physiology*, 88(1), pp. 131–138. doi: 10.1104/pp.88.1.131.

Serre, N. B. C. *et al.* (2021) 'AFB1 controls rapid auxin signalling through membrane depolarization in *Arabidopsis thaliana* root', *Nature Plants*, 7(9), pp. 1229–1238. doi: 10.1038/s41477-021-00969-z.

Serre, N. B. and Fendrych, M. (Unpublished) 'ACORBA: Automated workflow to calculate root tip angle over time', *Unpublished*.

Shachar, B. L. (1967) *Studies on the root cap and its significance in graviperception*. University of London, Thesis

Shih, H. W. *et al.* (2015) 'The cyclic nucleotide-gated channel CNGC14 regulates root gravitropism in *Arabidopsis thaliana*', *Current Biology*, 25(23), pp. 3119–3125. doi: 10.1016/j.cub.2015.10.025.

Singh, M., Gupta, A. and Laxmi, A. (2017) 'Striking the right chord: Signaling enigma during root gravitropism', *Frontiers in Plant Science*, 8. doi: 10.3389/fpls.2017.01304.

Skowyra, D. *et al.* (1997) 'F-box proteins are receptors that recruit phosphorylated substrates to the SCF ubiquitin-ligase complex', *Cell*, 91(2), pp. 209–219. doi: 10.1016/S0092-8674(00)80403-1.

Staves, M. P. (1997) *Cytoplasmic streaming and gravity sensing in Chara internodal cells*, *Planta*. doi: 10.1007/pl00008119.

Stitt, M. and Zeeman, S. C. (2012) 'Starch turnover: Pathways, regulation and role in growth', *Current Opinion in Plant Biology*, 15(3), pp. 282–292. doi: 10.1016/j.pbi.2012.03.016.

Sunilkumar, G. *et al.* (2002) 'Developmental and tissue-specific expression of CaMV 35S promoter in cotton as revealed by GFP', *Plant Molecular Biology*, 50(3), pp. 463–479. doi: 10.1023/A:1019832123444.

Swarup, R. *et al.* (2001) 'Localization of the auxin permease AUX1 suggests two functionally distinct hormone transport pathways operate in the *Arabidopsis* root apex', *Genes and Development*, 15(20), pp. 2648–2653. doi: 10.1101/gad.210501.

Swarup, R. *et al.* (2005) 'Root gravitropism requires lateral root cap and epidermal cells for transport and response to a mobile auxin signal', *Nature Cell Biology*, 7(11), pp. 1057–1065. doi: 10.1038/ncb1316.

Tan, X. *et al.* (2007) 'Mechanism of auxin perception by the TIR1 ubiquitin ligase', *Nature*. England, 446(7136), pp. 640–645. doi: 10.1038/nature05731.

Tanaka, A. *et al.* (2002) 'Positional effect of cell inactivation on root gravitropism using heavy-ion microbeams', *Journal of Experimental Botany*, 53(369), pp. 683–687. doi: 10.1093/jexbot/53.369.683.

Taniguchi, M. *et al.* (2017) 'The *Arabidopsis* LAZY1 family plays a key role in gravity signaling within statocytes and in branch angle control of roots and shoots', *Plant Cell*, 29(8), pp. 1984–1999. doi: 10.1105/tpc.16.00575.

The Nobel Prize (2020) 'Press Release: The Nobel Prize in Chemistry 2020', *Nobel Prize Outreach*, pp. 1–4. Available at: https://www.nobelprize.org/prizes/chemistry/2020/press-release/%0Ahttp://www.nobelprize.org/nobel_prizes/chemistry/laureates/2007/press.html (Accessed: 11 September 2021).

Thermofisher GeneJET Gel Extraction Kit (Accessed 10.04.2021). Available at: https://www.thermofisher.com/cz/en/home/technical-resources.html.

Thermofisher manuals (Accessed 10.04.2021). Available at: https://www.thermofisher.com/search/results?docTypes=Manuals&persona=DocSupport&linkIn=true.

Toyota, M. and Gilroy, S. (2013) 'Gravitropism and mechanical signaling in plants', *American Journal of Botany*, 100(1), pp. 111–125. doi: 10.3732/ajb.1200408.

Tsugeki, R. and Fedoroff, N. V. (1999) 'Genetic ablation of root cap cells in *Arabidopsis'*, *Proceedings of the National Academy of Sciences of the United States of America*, 96(22), pp. 12941–12946. doi: 10.1073/pnas.96.22.12941.

Utsuno, K. *et al.* (1998) 'AGR, an Agravitropic locus of *Arabidopsis thaliana*, encodes a novel membrane-protein family member', *Plant and Cell Physiology*, 39(10), pp. 1111–1118. doi: 10.1093/oxfordjournals.pcp.a029310.

Vanneste, S. and Friml, J. (2009) 'Auxin: A Trigger for Change in Plant Development', *Cell*. United States, 136(6), pp. 1005–1016. doi: 10.1016/j.cell.2009.03.001.

Vitha, S., Zhao, L. and Sack, F. D. (2000) 'Interaction of root gravitropism and phototropism in *Arabidopsis* wild-type and starchless mutants', *Plant Physiology*, 122(2), pp. 453–461. doi: 10.1104/pp.122.2.453.

Wang, S. M. *et al.* (1998) 'Characterization of ADG1, an *Arabidopsis* locus encoding for ADPG pyrophosphorylase small subunit, demonstrates that the presence of the small subunit is required for large subunit stability', *Plant Journal*, 13(1), pp. 63–70. doi: 10.1046/j.1365-313X.1998.00009.x.

Wang, Z. P. *et al.* (2015) 'Egg cell-specific promoter-controlled CRISPR/Cas9 efficiently generates homozygous mutants for multiple target genes in *Arabidopsis* in a single generation', *Genome Biology*, 16(1), p. 144. doi: 10.1186/s13059-015-0715-0.

Wayne, R., Staves, M. P. and Leopold, A. C. (1990) 'Gravity-dependent polarity of cytoplasmic streaming in Nitellopsis', *Protoplasma*, 155(1–3), pp. 43–57. doi: 10.1007/BF01322614.

Weijers, D. *et al.* (2005) 'Developmental specificity of auxin response by pairs of ARF and Aux/IAA transcriptional regulators', *EMBO Journal*, 24(10), pp. 1874–1885. doi: 10.1038/sj.emboj.7600659.

Went, F. (1926) 'On growth-accelerating substances in the coleoptile of Avena sativa', *Proceedings of the Koninklijke Nederlandse Akademie van Wetenschappen*, 30(1925), pp. 10–19. Available at: http://ci.nii.ac.jp/naid/10021910846/en/ (Accessed: 19 July 2021).

Willemsen, V. *et al.* (2008) 'The NAC Domain Transcription Factors FEZ and SOMBRERO Control the Orientation of Cell Division Plane in *Arabidopsis* Root Stem Cells', *Developmental Cell*, 15(6), pp. 913–922. doi: 10.1016/j.devcel.2008.09.019.

Wisniewska, J. *et al.* (2006) 'Polar PIN localization directs auxin flow in plants', *Science*, 312(5775), p. 883. doi: 10.1126/science.1121356.

Wolabu, T. W. *et al.* (2020) 'Improving the genome editing efficiency of CRISPR/Cas9 in *Arabidopsis* and Medicago truncatula', *Planta*, 252(2), p. 15. doi: 10.1007/s00425-020-03415-0.

Wolverton, C., Ishikawa, H. and Evans, M. L. (2002) 'The kinetics of root gravitropism: Dual motors and sensors', *Journal of Plant Growth Regulation*, 21(2), pp. 102–112. doi: 10.1007/s003440010053.

Xie, K., Minkenberg, B. and Yang, Y. (2015) 'Boosting CRISPR/Cas9 multiplex editing capability with the endogenous tRNA-processing system', *Proceedings of the National Academy of Sciences of the United States of America*, 112(11), pp. 3570–3575. doi: 10.1073/pnas.1420294112.

Yang, Y. *et al.* (2006) 'High-Affinity Auxin Transport by the AUX1 Influx Carrier Protein', *Current Biology*, 16(11), pp. 1123–1127. doi: 10.1016/j.cub.2006.04.029.

Yoder, T. L. *et al.* (2001) 'Amyloplast sedimentation dynamics in maize columella cells support a new model for the gravity-sensing apparatus of roots', *Plant Physiology*, 125(2), pp. 1045–1060. doi: 10.1104/pp.125.2.1045.

Yoshihara, T., Spalding, E. P. and Iino, M. (2013) 'AtLAZY1 is a signaling component required for gravitropism of the *Arabidopsis thaliana* inflorescence', *Plant Journal*, 74(2), pp. 267–279. doi: 10.1111/tpj.12118.

Zeeman, S. C., Kossmann, J. and Smith, A. M. (2010) 'Starch: Its metabolism, evolution, and biotechnological modification in plants', *Annual Review of Plant Biology*, 61, pp. 209–234. doi: 10.1146/annurev-arplant-042809-112301.

Zhang, H. and McCarty, N. (2017) 'CRISPR Editing in Biological and Biomedical Investigation', *Journal of Cellular Biochemistry*, 118(12), pp. 4152–4162. doi: 10.1002/jcb.26111.

Zhang, N. *et al.* (2020) 'Generation and Molecular Characterization of CRISPR/Cas9-Induced Mutations in 63 Immunity-Associated Genes in Tomato Reveals Specificity and a Range of Gene Modifications', *Frontiers in Plant Science*, 11, p. 10. doi: 10.3389/fpls.2020.00010.

Zhang, Y. *et al.* (2019) 'Auxin-mediated statolith production for root gravitropism', *New Phytologist*, 224(2), pp. 761–774. doi: 10.1111/nph.15932.

10. Supplement

P1-Mattrix attachment region sequence
TATATTGAGATATTAGTGTATAATATAATTTCCGCACTCTCTTTTAAATTAATAATACAAGATTTAGAAAAA ATGAACTTTAATTTTGAGATATTAGTGTGTAATTCTCAGTAGAGAATTTCCTAAGTTCACCCAAAAGTATA TCATTTTCCTCTTAAGAAAATACAAACACTACCTAATTTTATCCCCTATAAATATCTAAAAATTTGCATCTCA TAAAATTTACCAATTATTTATTTTTTAAGATATTTTACTAATTATCTATAACTATTAATAATCAAAATTATTTC ATTGATGTACATATTTCAATAGATAATTTACCCCTTAATCACTTAATAAATTTTAAATTTTCATTATTTTTAT ATAATTTATAGTCTTTTTTATTAACTATATTTAAATTTTATTTTTTATTATTAAAAAAATTTAGAGAGACACA TTTTTCCCTAATTAGTCATATATAAGAAAAATAACATTTGGGTAAAATGTGAGAGCCCAAACGCAATTCGT GTTGGGCCTAAAGGGCCCACGAAGTAGATACTAAAGGATGCCCTCATCGATGAA

Supplement Table 1 - Sequence of the P1-Matrix attachment region used in Alpha1_2 and Alpha1_4 subunits.

Omega vector	Component	Total amount / volume
pSMB::Cas9*PGM ***pSMB::Cas9*GFP*** ***pSMB::Cas9*ADG1***	pDG1alfa1_1 (SMB promoter with Cas9-AA-mCherry)	75 ng
	pDG1alfa1_3 with desired gRNA and U6-1	75 ng
	pDG3omega1	75 ng
	pDG1alfa1_2 with MAR	75 ng
	pDG1alfa1_4 with MAR	75 ng
	pDG1alpha2 vector with Basta resistance	75 ng
	BsmBI enzyme (Thermo Fischer, 10U/µl)	1 µl
	ligase buffer (10x concentration, Promega)	1 µl
	T4 DNA ligase (Promega, 3U/µl)	1 µl
	Milli-Q water	to 10 µl
pUBI10::Cas9*AT5G14240	pDG1alfa1_1 (UBI promoter with Cas9-AA-mCherry)	75 ng
	pDG1alfa1_3 with desired gRNA and U6-1	75 ng
	pDG3omega1	75 ng

	pDG1alfa1_2 with MAR	75 ng
	pDG1alfa1_4 with MAR	75 ng
	pDG1alpha2 vector with oleosin-mCherry	75 ng
	BsmBI enzyme (Thermo Fischer, 10U/µl)	1 µl
	ligase buffer (10x concentration, Promega)	1 µl
	T4 DNA ligase (Promega, 3U/µl)	1 µl
	Milli-Q water	to 10 µl

Supplement Table 2 - Omega vector ligation reaction components and their used amount/volume.

Target - PGM: AT5G51820			
gRNA sequence 1	GGTGGACCTGAATATGACTGGGG		
gRNA sequence 2	GATTACAGCGGAAACCGCTGGGG		
Primers 5' -> 3'			
PGM_g1_F	TAGGTCTCCTGAATATGACTGGTTTTAGAGCTAGAA		
PGM_g1_R	ATGGTCTCA*ATTCAGGTCCACC*TGCACCAGCCGGGAA		
PGM_g2_F	TAGGTCTCCCGGAAACCGCTGGTTTTAGAGCTAGAA		
PGM_g2_R	CGGGTCTCATCCGCTGTAATCTGCACCAGCCGGG		
L5AD5-F	TAGGTCTCCATTGACAAAGCACCAGTGG		
L3AD5-R	TAGGTCTCCAGCGAAAAAAAAAAGCACCGACTCG		
Reaction			
	Primers used	**5‘overhang**	**3‘overhang**
Part1	L5AD5-F + PGM_g1_R	ATTG	TTCA
Part2	PGM_g1_F + PGM_g2_R	TGAA	TCCG
Part3	PGM_g2_F + L3AD5-R	CGGA	CGCT

Supplement Table 3 - gRNA sequences used for the Alpha1_3 subunit of the *pSMB::Cas9*PGM* line along with primers used for the synthesys of polycistronic gRNA gene parts and overhangs used for ligation.

Target - GFP			
gRNA sequence	GATGCCGCACGTCACGAAGT		
Primers 5' -> 3'			
TSKO_GFP_g_F	TAGGTCTCCACGTCACGAAGTGTTTTAGAGCTAGAA		
TSKO_GFP_g_R	ATGGTCTCAACGTGCGGCATCTGCACCAGCCGGGAA		
L5AD5-F	TAGGTCTCCATTGACAAAGCACCAGTGG		
L3AD5-R	TAGGTCTCCAGCGAAAAAAAAAAGCACCGACTCG		
Reaction			
	Primers used	**5‘overhang**	**3‘overhang**
Part1	L5AD5-F + TSKO_GFP_g_R	ATTG	ACGT
Part2	TSKO_GFP_g_F + L3AD5-R	ACGT	CGCT

Supplement Table 4 - gRNA sequences used for the Alpha1_3 subunit of the *pSMB::Cas9*GFP* line along with primers used for the synthesys of polycistronic gRNA gene parts and overhangs used for ligation.

Target - ADG1: AT5G48300			
gRNA sequence 1	GCATCAAGCATCTTAGACGGTGG		
gRNA sequence 2	GCGAAAGGAAGTGTACCCATAGG		
Primers 5' -> 3'			
ADG_g3_F	TAGGTCTCCCATCTTAGACGGGTTTTAGAGCTAGAA		
ADG_g3_R	ATGGTCTCAGATGCTTGATGCTGCACCAGCCGGGAA		
ADG_g8_F	TAGGTCTCCAAGTGTACCCATGTTTTAGAGCTAGAA		
ADG_g8_R	ATGGTCTCAACTTCCTTTCGCTGCACCAGCCGGGAA		
L5AD5-F	TAGGTCTCCATTGACAAAGCACCAGTGG		
L3AD5-R	TAGGTCTCCAGCGAAAAAAAAAAGCACCGACTCG		
Reaction			
	Primers used	**5‘overhang**	**3‘overhang**
Part1	L5AD5-F + ADG_g3_R	ATTG	GATG
Part2	ADG_g3_F + ADG_g8_R	CATC	ACTT
Part3	ADG_g8_F + L3AD5-R	AAGT	CGCT

Supplement Table 5 - gRNA sequences used for the Alpha1_3 subunit of the *pSMB::Cas9*GFP* line along with primers used for the synthesis of polycistronic gRNA gene parts and overhangs used for ligation.

Target - AT5G14240			
gRNA sequence 1	GAGGTTGTCTGAGCTAAGAGAGG		
gRNA sequence 2	GTTCATAGAACGAGTGGTGAAGG		
Primers 5' -> 3'			
At5g14240_g11_F	TAGGTCTCCCTGAGCTAAGAGGTTTTAGAGCTAGAA		
At5g14240_g11_R	ATGGTCTCATCAGACAACCTCTGCACCAGCCGGGAA		
At5g14240_g46_F	TAGGTCTCCAACGAGTGGTGAGTTTTAGAGCTAGAA		
At5g14240_g46_R	ATGGTCTCACGTTCTATGAACTGCACCAGCCGGGAA		
L5AD5-F	TAGGTCTCCATTGACAAAGCACCAGTGG		
L3AD5-R	TA GGTCTCCAGCGAAAAAAAAAAGCACCGACTCG		
Reaction			
	Primers used	5‘overhang	3‘overhang
Part1	L5AD5-F + At5g14240_g11_R	ATTG	TCAG
Part2	At5g14240_g11_F + At5g14240_g46_R	CTGA	CGTT
Part3	At5g14240_g46_F + L3AD5-R	AACG	CGCT

Supplement Table 6 - gRNA sequences used for the Alpha1_3 subunit of the *pUBI10::Cas9*AT5G14240* line along with primers used for the synthesis of polycistronic gRNA gene parts and overhangs used for ligation.

Primer	**Primer sequence**
At5gCRISPRcheck-F	AGAGGAGGAGCTTGAGGATCTT
At5gCRISPRchech-R	GGTCGTGATTTTAAGCCGTACA
at5gCRISPR-Rseq	GGTCAGTGGTTGAGTTGTTCG

Supplement Table 7 - Primers used for PCR genotyping and sequencing of *pUBI10::Cas9*AT5G14240* line with their respective sequences.